

**Aus der Klinik und Poliklinik für Neurologie  
der Universität Würzburg**

**Direktor: Professor Dr. med. Jens Volkmann**

**Of cells and enzymes:**

**How dermal fibroblasts can impact pain in Fabry Disease**

**and**

**Why looking at the 3D-structure of  $\alpha$ -Galactosidase A may be worthwhile for clinical  
management of Fabry patients**

**Über Zellen und Enzyme:**

**Wie Hautfibroblasten Schmerz bei Morbus Fabry beeinflussen können**

**und**

**Warum sich die Betrachtung der 3D-Struktur der  $\alpha$ -Galaktosidase A für die klinische  
Versorgung von Fabry Patienten lohnt**

**Inauguraldissertation**

**zur Erlangung der Doktorwürde der**

**Medizinischen Fakultät**

**der**

**Julius-Maximilians-Universität Würzburg**

**vorgelegt von**

**Vanessa Christine Hochheimer**

**aus Dettelbach**

**Würzburg, August 2021**

**Referentin:** Prof. Dr. Nurcan Üçeyler

**Korreferent bzw. Korreferentin:** Prof. Dr. Christoph Wanner

**Dekan:** Prof. Dr. Matthias Frosch

**Tag der mündlichen Prüfung:** 02.12.2022

**Die Promovendin ist Ärztin.**

## Table of contents

|         |  |        |
|---------|--|--------|
| 1       | Annotation concerning the structure of this thesis .....     | - 1 -  |
| 2       | Introduction .....   | - 1 -  |
| 2.1     | General theoretical background: Fabry disease .....          | - 1 -  |
| 2.1.1   | Definition and pathophysiological background.....            | - 1 -  |
| 2.1.2   | Epidemiology .....   | - 2 -  |
| 2.1.3   | Genetic basis .....  | - 2 -  |
| 2.1.4   | Symptoms and disease process .....                           | - 3 -  |
| 2.1.5   | Diagnostics .....  | - 7 -  |
| 2.1.6   | Therapy .....  | - 9 -  |
| 2.1.7   | Challenges in FD .....                                       | - 11 - |
| 2.2     | Theoretical background for Study I .....                     | - 13 - |
| 2.2.1   | Involvement of the peripheral nervous system .....           | - 13 - |
| 2.2.1.1 | Clinical presentation .....                                  | - 13 - |
| 2.2.1.2 | Pathophysiology of FD-associated pain .....                  | - 14 - |
| 2.2.2   | Cutaneous nociception .....                                  | - 15 - |
| 2.2.2.1 | Relevant structures and processes .....                      | - 15 - |
| 2.2.2.2 | Role of dermal fibroblasts .....                             | - 16 - |
| 2.2.2.3 | Ion channels in dermal fibroblasts .....                     | - 17 - |
| 2.2.3   | Aims of Study I.....   | - 18 - |
| 2.3     | Theoretical background of Study II.....                      | - 19 - |
| 2.3.1   | 3D-structure defects in enzymes .....                        | - 19 - |
| 2.3.1.1 | 3D-structure of enzymes .....                                | - 19 - |
| 2.3.1.2 | Impact of 3D-structure defects of enzymes in hereditary..... | - 19 - |
|         | Diseases.....  | - 19 - |
| 2.3.1.3 | 3D-structure of $\alpha$ -GalA and its defects in FD .....   | - 20 - |

|           |   |        |
|-----------|---|--------|
| 2.3.2     | Aims of Study II.....   | - 22 - |
| 3         | Materials and Methods.....                                      | - 23 - |
| 3.1       | Study I.....  | - 23 - |
| 3.1.1     | Study cohort.....   | - 23 - |
| 3.1.1.1   | FD patient cohort.....  | - 23 - |
| 3.1.1.2   | Control cohort.....   | - 23 - |
| 3.1.1.3   | Subgroups in the study cohort.....                              | - 23 - |
| 3.1.2     | FD mutation analysis: classical and non-classical mutations.... | - 24 - |
| 3.1.3     | Clinical phenotyping.....                                       | - 25 - |
| 3.1.3.1   | Neurological assessment .....                                   | - 25 - |
| 3.1.3.1.1 | Medical history and neurological examination .....              | - 25 - |
| 3.1.3.1.2 | Würzburg Fabry Pain Questionnaire .....                         | - 25 - |
| 3.1.3.1.3 | Quantitative sensory testing (QST).....                         | - 25 - |
| 3.1.3.1.4 | Nerve conduction studies .....                                  | - 26 - |
| 3.1.3.1.5 | Diagnosis of small fiber neuropathy (SFN) .....                 | - 26 - |
| 3.1.3.2   | Assessment of cardiomyopathy.....                               | - 26 - |
| 3.1.3.3   | Assessment of nephropathy .....                                 | - 26 - |
| 3.1.4     | Skin sample acquisition .....                                   | - 27 - |
| 3.1.4.1   | Skin biopsy .....   | - 27 - |
| 3.1.4.2   | Determination of IENFD .....                                    | - 27 - |
| 3.1.4.3   | Primary fibroblast culture.....                                 | - 28 - |
| 3.1.5.    | Cell culture experiments .....                                  | - 28 - |
| 3.1.5.1   | Analysis of Gb3 deposits in fibroblasts.....                    | - 28 - |
| 3.1.5.1.1 | Immunocytochemistry for Gb3.....                                | - 28 - |
| 3.1.5.1.2 | Determination of Gb3 load.....                                  | - 29 - |
| 3.1.5.2   | Incubation experiments .....                                    | - 29 - |

|           |  |        |
|-----------|--|--------|
| 3.1.5.3   | Patch-clamp analysis.....  | - 30 - |
| 3.1.5.4   | Gene expression analysis .....                                       | - 32 - |
| 3.1.5.4.1 | mRNA extraction .....  | - 32 - |
| 3.1.5.4.2 | Reverse transcription PCR .....                                      | - 32 - |
| 3.1.5.4.3 | qRT-PCR.....   | - 32 - |
| 3.1.5.5   | Protein expression analysis.....                                     | - 33 - |
| 3.1.5.5.1 | ELISA .....  | - 33 - |
| 3.1.5.5.2 | Western Blot analysis .....  | - 34 - |
| 3.1.6     | Statistical analysis and figure preparation .....                    | - 35 - |
| 3.2       | Study II.....  | - 35 - |
| 3.2.1     | Study cohort.....  | - 35 - |
| 3.2.2     | Subgroups in the study cohort.....                                   | - 35 - |
| 3.2.2     | FD mutation analysis .....   | - 36 - |
| 3.2.2.1   | Distinction between classical and non-classical mutations....        | - 36 - |
| 3.2.2.2   | Distinction by AAE location in the $\alpha$ -GalA 3D-structure ..... | - 37 - |
| 3.2.3     | Clinical phenotyping.....  | - 37 - |
| 3.2.3.1   | Neurological assessment .....  | - 37 - |
| 3.2.3.2   | Assessment for cardiomyopathy .....                                  | - 37 - |
| 3.2.3.3   | Assessment for nephropathy.....                                      | - 38 - |
| 3.2.4     | FD-related laboratory tests .....                                    | - 39 - |
| 3.2.5     | Statistical analysis and figure preparation .....                    | - 39 - |
| 4         | Results .....  | - 40 - |
| 4.1       | Study I.....   | - 40 - |
| 4.1.1     | Epidemiology .....   | - 40 - |
| 4.1.2     | Characterization of the FD patient cohort .....                      | - 40 - |
| 4.1.2.1   | Genetic findings.....  | - 40 - |

|   |        |
|---|--------|
| 4.1.2.2 Clinical findings .....   | - 41 - |
| 4.1.2.2.1 All main organ manifestations in FD .....   | - 41 - |
| 4.1.2.2.2 FD-associated pain.....   | - 42 - |
| 4.1.3 Gb3 load analysis .....   | - 44 - |
| 4.1.3.1 Median Gb3 load and median number of swollen cells in<br>fibroblasts of FD patients and healthy controls .....          | - 44 - |
| 4.1.3.2 Median Gb3 load and median amount of swollen cells in<br>fibroblasts of different FD subgroups .....                    | - 45 - |
| 4.1.3.3 Median Gb3 load at different ERT-biopsy intervals .....   | - 46 - |
| 4.1.3.4 Median Gb3 load in two consecutive biopsies of two male FD<br>patients .....  | - 47 - |
| 4.1.4 Patch-clamp analysis.....   | - 48 - |
| 4.1.4.1 Description of the measured current .....   | - 48 - |
| 4.1.4.2 Functional difference of K <sub>Ca</sub> 1.1 between FD and healthy<br>control fibroblasts .....                        | - 50 - |
| 4.1.5 Gene and protein expression of K <sub>Ca</sub> 1.1 in fibroblasts of FD patients<br>and healthy controls .....            | - 51 - |
| 4.1.6 Gene expression of various cytokines and chemokines in<br>fibroblasts of FD patients and healthy controls.....            | - 52 - |
| 4.1.7 Analysis of pNF- $\kappa$ B p65 in fibroblasts of FD patients and healthy<br>controls pre- and post-TNF stimulation ..... | - 54 - |
| 4.2 Study II .....  | - 56 - |
| 4.2.1 Epidemiology .....  | - 56 - |
| 4.2.2 Genetic characterization of the study cohort.....   | - 56 - |
| 4.2.2.1 Frequency of classical and non-classical mutations in the study<br>cohort - separated by sex .....                      | - 56 - |
| 4.2.2.2 AAE location types in $\alpha$ -GalA 3D-structure.....  | - 56 - |

|           |  |        |
|-----------|--|--------|
| 4.2.2.2.1 | Frequency of AAE location types as wells as the frequency of each individual mutation.....                 | - 56 - |
| 4.2.2.2.2 | Illustration of AAEs in the $\alpha$ -GalA 3D-structure.....   | - 59 - |
| 4.2.2.2.3 | Frequency of classical and non-classical mutations in the study cohort separated by AAE location type..... | - 60 - |
| 4.2.3     | Clinical characterization of patient subgroups .....   | - 61 - |
| 4.2.3.1   | Clinical characterization of male FD patients.....   | - 61 - |
| 4.2.3.1.1 | Clinical characterization of male patients younger than 35 years ('<35y-group').....                       | - 61 - |
| 4.2.3.1.2 | Clinical characterization of male patients between 35 and 55 years ('35-55y-group').....                   | - 63 - |
| 4.2.3.1.3 | Clinical characterization of male patients older than 55 years ('>55y-group').....                         | - 65 - |
| 4.2.3.1.4 | Clinical characterization of all male patients.....  | - 67 - |
| 4.2.3.2   | Clinical characterization of female FD patients.....   | - 69 - |
| 4.2.3.2.1 | Clinical characterization of female patients younger than 35 years (<35y-group).....                       | - 69 - |
| 4.2.3.2.2 | Clinical characterization of female patients between 35 and 55 years ('35-55y-group').....                 | - 71 - |
| 4.2.3.2.3 | Clinical characterization of female patients older than 55 years ('>55y-group').....                       | - 73 - |
| 4.2.3.2.4 | Clinical characterzation of all female patients.....   | - 75 - |
| 4.2.4     | $\alpha$ -GalA activity and plasma lyso-Gb3 levels.....  | - 77 - |
| 5         | Discussion.....  | - 78 - |
| 5.1       | Study I.....   | - 78 - |
| 5.2       | Study II.....  | - 85 - |
| 5.3       | Limitations and strengths .....  | - 89 - |
| 5.3.1     | Study I .....  | - 89 - |

|       |                               |        |
|-------|-------------------------------|--------|
| 5.3.2 | Study II .....                | - 90 - |
| 5.4.  | Overall conclusion .....      | - 91 - |
| 6     | Summary/Zusammenfassung ..... | - 92 - |
| 6.1   | English Summary .....         | - 92 - |
| 6.2   | Deutsche Zusammenfassung..... | - 94 - |
| 7     | Bibliography .....            | - 96 - |

Parts of the presented data have been published in:

**Rickert, V.**, Kramer, D., Schubert, A.-L., Sommer, C., Wischmeyer, E., Üçeyler, N. (2020). Globotriaosylceramide-induced reduction of Kca1.1 channel activity and activation of Notch1 signaling pathway in skin fibroblasts of male Fabry patients with pain. *Exp Neurol*, 324, 113-134.  
doi:10.1016/j.expneurol.2019.113134

**Rickert, V.**, Wagenhäuser, L., Nordbeck, P., Wanner, C., Sommer, C., Rost, S., Üçeyler, N. (2020). Stratification of Fabry mutations in clinical practice: a closer look at  $\alpha$ -galactosidase A-3D structure. *J Int Med*, 288(5), 593-604.  
doi:10.1111/joim.13125

Some parts of this thesis include partially adapted content from the sources listed above.



## **1 Annotation concerning the structure of this thesis**

This thesis comprises the work of two different studies on Fabry disease. The first one (in the following referred to as “Study I”) is an experimental study including skin samples of patients with Fabry disease (FD) and healthy controls. In the course of this study, the idea behind the second, clinical study (including only patients with Fabry disease; in the following referred to as “Study II”) was developed, comparing clinical and laboratory parameters of different Fabry disease subgroups. For better comprehension, introduction (partially), methods, results, and discussion (partially) of this thesis are divided according to the respective Study I and Study II.

## **2 Introduction**

### **2.1 General theoretical background: Fabry disease**

#### **2.1.1 Definition and pathophysiological background**

Fabry disease (OMIM 301500) is one of approximately 50 inborn lysosomal storage diseases (LSD) – more precisely, a glycosphingolipidosis – resulting from mutations in the gene encoding the hydrolyzing enzyme  $\alpha$ -galactosidase A ( $\alpha$ -GalA). Unlike most LSDs that are passed on autosomal-recessively, FD is inherited in an X-chromosomal manner (Boustany, 2013) leading to severe disease manifestation especially in men. As mutated  $\alpha$ -GalA can only limitedly or not at all hydrolyze the terminal  $\alpha$ -galactosyl moieties from glycosphingolipids for degradation, substrates such as globotriaosylceramide (Gb3) and its derivatives (e.g. the deacylated form lyso-Gb3) accumulate excessively in a variety of body tissues and fluids including kidneys, heart, nervous and vascular

system, and blood plasma. Substrate accumulation induces cellular dysfunction, cell death, and eventually organ failure reducing life expectancy (Ferreira et al., 2017; Sueoka et al., 2015).

### **2.1.2 Epidemiology**

Albeit a rare disease, FD is pan-ethnic and occurs worldwide. It is estimated that between 1:40000 and 1:117000 people carry  $\alpha$ -GalA mutations (Meikle et al., 1999), with a high variety between countries. Since many studies are based solely on affected patients, the actual prevalence is probably higher. (Germain, 2010). Therefore, a growing number of newborn screenings has been performed over the past years, revealing that up to 1 out of 1250 newborns carries an  $\alpha$ -GalA variant, mostly of yet unknown significance (Hwu et al., 2009; Lin et al., 2009; Van der Tol et al., 2014).

### **2.1.3 Genetic basis**

FD results from mutations in the gene encoding the enzyme  $\alpha$ -GalA, which is located on the X-chromosome's long arm of, in the Xq22.1 region, and consists of 12436 base pairs (Kornreich et al., 1989), of which 1393 are arranged in seven exons and are thus protein-encoding. FD mutations have been found in all exons and parts of the introns. While point mutations such as missense and nonsense mutations induce exchange of a single amino acid in  $\alpha$ -GalA or creation of a stop codon, larger gene rearrangements such as deletions, insertions, duplications or splice site mutations lead to a grossly altered polypeptide sequence (Bishop et al., 1988; Garman et al., 2004a). Over 1000 different mutations have been described so far (<http://fabry-database.org/mutants/>), most of which are private, i.e. merely occur in a single family. When mutations are found in several unrelated families, they usually form 'mutation hot spots' such as CpG nucleotides. Of all types, missense

mutations build the majority (approx. 60%), while the other mutation types are found less frequently (Cooper et al., 1988; Pastores et al., 2002). Although less suggested by the X-linked mode of inheritance, up to 91% of heterozygous women have subjective or objective disease manifestations (Street et al., 2006; Wang et al., 2007). The pathophysiological basis is not yet fully understood, some studies support the concept of skewed X-inactivation (Dobrovolny et al., 2005; Maier et al., 2006; Redonnet-Vernhet et al., 1996), while others ascribe less importance to this theory (Elstein et al., 2012; Juchniewicz et al., 2018).

#### **2.1.4 Symptoms and disease process**

As most LSDs, FD may present with a wide clinical variability. Disease severity depends i.a. on the underlying mutation since the different mutations impair  $\alpha$ -GalA activity to a variable extent (Nagueh, 2014). Based on residual  $\alpha$ -GalA activity and clinical presentation, two different phenotypes can be differentiated: the classical and the non-classical or late-onset phenotype. Especially men with a classical phenotype have no or very low residual  $\alpha$ -GalA activity, while those with non-classical phenotype and generally women show less of it (Rozenfeld, 2009).  $\alpha$ -GalA activity determines substrate accumulation and thus, drives disease severity and progression (Ferreira and Gahl, 2017). In general, men are affected earlier and often more severely than women, due to the X-linked type of inheritance (Germain, 2010). Disease severity among women varies between asymptomatic courses, also in classical phenotypes, and full disease expression (Wang et al., 2007; Whybra et al., 2001). As demonstrated in Fig. 1, disease severity and progression differs between patients with classical and non-classical phenotypes.

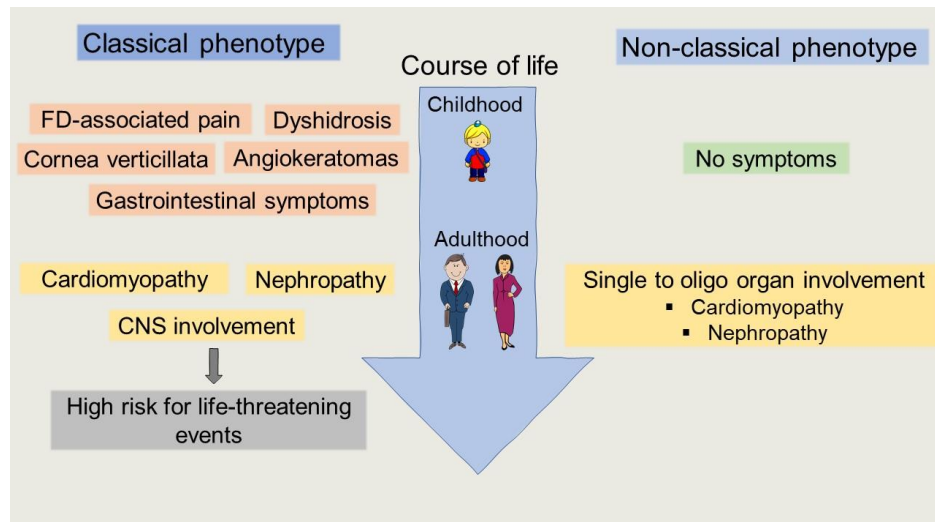


**Figure 1. Disease process in classical and non-classical FD phenotype**

In patients with a classical phenotype, symptom onset is in childhood. Patients report neuropathic pain, dyshidrosis, and gastrointestinal symptoms such as diarrhea or abdominal pain and cornea verticillata. Also angiokeratomas can typically be found already. As adults, patients suffer from a multi-organ involvement with high risk for life-threatening events. In contrast, in patients with non-classical phenotype, disease manifestation does not start before adulthood and is typically limited to a single or few organs such as heart or kidney. Abbreviations: CNS=central nervous system; FD=Fabry disease. Content adapted from *Germain, 2010*.

In many cases of classical FD, symptom onset is in childhood, more precisely at a mean of six years in boys and nine years in girls (Ellaway, 2016) starting with an involvement of the nervous system, presenting with FD-associated pain. Pediatric patients additionally report dyshidrosis with heat intolerance and gastrointestinal problems such as abdominal pain or diarrhea. Also, cornea verticillata and angiokeratomas can be found already in children (Hopkin et al., 2008; Zarate et al., 2008). Early-onset symptoms usually remain present in adulthood, while more organ systems are affected and organ damage increases due to progressive substrate accumulation. Likely because of higher residual  $\alpha$ -GalA activity and thus slower substrate accumulation, patients with non-classical FD develop symptoms up to four to six decades later in life, and report limited spread of disease, usually of one or few inner organs (Desnick, 2018; Germain, 2010). Major inner organs that may be severely affected are the heart

and kidneys, usually starting in adulthood. Cardiac abnormalities such as arrhythmias or left ventricular hypertrophy can result in need for organ transplantation due to heart failure and even sudden cardiac death if not prevented with an implantable cardiac device or pacemaker (Shah et al., 2005; Weidemann et al., 2016). Also, renal impairment inducing albuminuria and reduction of glomerular filtration rate (GFR), often begins in young adulthood and can result in end-stage renal failure with obligation to renal replacement therapy, e.g. via hemodialysis or transplant (Waldek et al., 2014; Wanner et al., 2010). Cerebral strokes and transient ischemic attacks are also more frequent among FD patients than in the general population (Grewal, 1994; Rolfs et al., 2013). Additionally, Gb3 can also harm smaller organs such as the inner ears, inducing tinnitus or hearing loss. All these processes sooner or later give rise to a number of restrictions in everyday life. It is therefore not surprising that many FD patients suffer from depression and experience limited quality of life (Arends et al., 2015; Cole et al., 2007). Life-threatening events usually occur between 40 and 50 years of age, and mean life expectancy is reduced to 58 years in males and 75 years in females (Waldek et al., 2009). The main causes of death among FD patients are cardiovascular events (36%), infections, e.g. following hemodialysis (15%), and renal failure (9%) (Mehta et al., 2009). For the convenience of the clinical reader, Table 1 provides an overview of all main typical symptoms and live-threatening events in FD.

**Table 1. List of typical symptoms and life-threatening events in FD**

| <b>Organ system</b>           | <b>Symptoms</b>   | <b>Life-threatening events</b>   |
|-------------------------------|---|--|
| <b>Nervous system</b>         | FD-associated pain<br>SFN<br>Anhidrosis or hypohidrosis   | Cerebral stroke<br>TIA   |
| <b>Heart</b>                  | Left ventricular hypertrophy<br>Arrhythmia (e.g. impaired heart variability)<br>Angina and dyspnea<br>Heart failure | Myocardial infarction<br>ICD- or pacemaker-obligatory arrhythmias<br>Atrial fibrillation<br>Cardiac decompensation |
| <b>Kidneys</b>                | Reduction of GFR (<60 ml/min/1.72m <sup>2</sup> )<br>Albuminuria<br>Proteinuria                                     | RRT- obligatory renal failure  |
| <b>Gastrointestinal tract</b> | Nausea and vomiting<br>Diarrhea<br>Postprandial pain  |  |
| <b>Skin</b>                   | Angiokeratomas  |  |
| <b>Ears</b>                   | Tinnitus<br>Hearing loss  |  |
| <b>Eyes</b>                   | Cornea verticillata   |  |
| <b>Others</b>                 | Chronic fatigue<br>Depression<br>Chronic cough and wheezing<br>Difficulty gaining weight<br>Vitamin D deficiency    |  |

Abbreviations: FD=Fabry disease; GFR=glomerular filtration rate; ICD=implantable cardiac device; RRT=renal replacement therapy; SFN=small fiber neuropathy; TIA=transient ischemic attack

## 2.1.5 Diagnostics

Due to its rarity and wide clinical variability, FD is often missed or remains unrecognized for over a decade. Despite the long time since the first description and FD experts' efforts to spread information and guidelines to the medical and general community, this delay in diagnosis has not improved since about the year 2000 (Reisin et al., 2017). Fig. 2 shows the diagnostic sequence in FD.

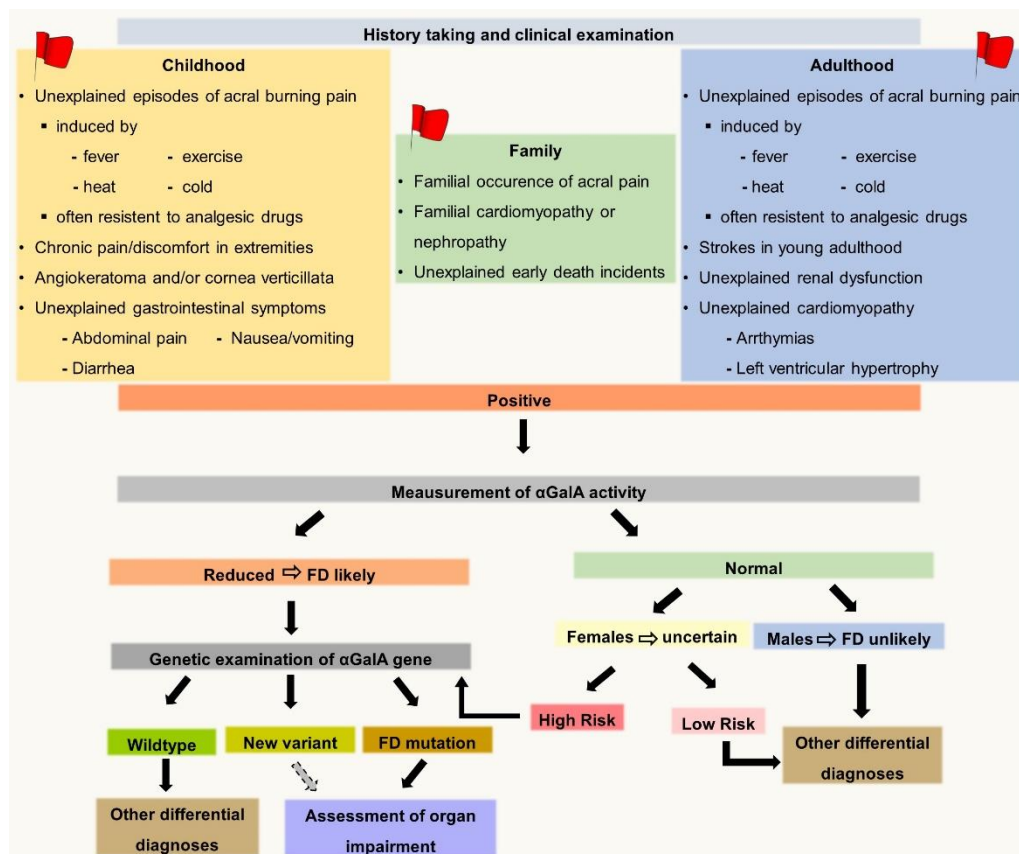


**Figure 2. Diagnostics in FD**

Red flags in medical history and clinical examination can hint towards FD and, if positive, are followed by biochemical investigations including measurement of  $\alpha$ -GalA activity and genetic testing of the  $\alpha$ -GalA gene to exclude or confirm FD. If a FD mutation or a new variant in  $\alpha$ -GalA gene is found, physical and instrument-based examination by a multi-disciplinary team is performed to evaluate disease severity and detect organ impairment. If FD is not present, other differential diagnoses need to be considered. Abbreviations:  $\alpha$ -GalA= $\alpha$ -Galactosidase A; FD=Fabry disease. Content adapted from Desnick et al. 2003 and Üçeyler and Sommer, 2013.

Several red flags hinting towards FD can be detected by thorough medical history taking and clinical examination. If present, biochemical investigations and/or genetic testing of the  $\alpha$ -GalA gene are crucial to exclude or confirm FD. If a FD mutation or a new variant in the  $\alpha$ -GalA gene is found, physical and instrument-based examination by a multi-disciplinary team is performed to evaluate disease severity and detect organ impairment (see Table 2) (Tuttolomondo et al., 2013; Üçeyler et al., 2013b).

**Table 2. Multi-disciplinary examination in FD**

| <b>Medical specialty</b> | <b>Specific examinations</b>   |
|--------------------------|--|
| <b>Neurologist</b>       | Nerve conduction studies<br>QST<br>Skin biopsy<br>Extra- and transcranial duplex sonography<br>Cranial MRI   |
| <b>Cardiologist</b>      | (exercise) ECG<br>Cardiac MRI<br>Echocardiography  |
| <b>Nephrologist</b>      | Determination of <ul style="list-style-type: none"> <li>• Serum creatinin</li> <li>• Creatinin clearance</li> <li>• Protein excretion</li> <li>• GFR</li> </ul> Kidney biopsy (if appropriate) |
| <b>ENT physician</b>     | Tone audiometry<br>Caloric tests   |
| <b>Ophthalmologist</b>   | Slit lamp examination  |
| <b>Dermatologist</b>     | Screening for angiokeratomas, teleangiectasia and lymphoedema  |

Abbreviations: ECG=Electrocardiogram; ENT=Ears, nose and throat; FD=Fabry disease; GFR=Glomerular filtration rate; MRI=Magnetic resonance imaging; QST=Quantitative sensory testing. Content adapted from Üçeyler and Sommer, 2013.



Also, a family screening should be considered to identify other family members with FD. After baseline assessment, regular follow-up investigations each or every two to five years are essential to monitor disease process and reevaluate therapeutic options, also for asymptomatic patients (Desnick et al., 2003).

### 2.1.6 Therapy

FD therapy requires interdisciplinary collaboration and should ideally be managed by specialized centers. Though therapeutic aims should be determined individually for each patient, the key therapeutic aims are:

- reduction of symptom severity
- prevention of disease process/organ manifestation
- improvement of quality of life and organ manifestation as well as
- normalization of life expectancy (Mehta et al., 2010).

Treatment of FD includes specific therapeutic approaches as well as symptomatic therapy. Table 3 gives an overview of current and possibly emerging FD-specific therapy options.

**Table 3. FD-specific therapy forms and their current status**

| Therapy                                     | Current status                              |
|---|---|
| <b>Agalsidase <math>\alpha/\beta</math></b> | Approved for treatment in the EU since 2001 |
| <b>Migalastat</b>                           | Approved for treatment in the EU since 2016 |
| <b>Lucerastat</b>                           | Phase 3 trial                               |
| <b>AVR-RD-01 gene therapy</b>               | Phase 1/2 trial                             |

Abbreviation: FD=Fabry disease.

Since the underlying pathophysiology of FD is deficient activity of the enzyme  $\alpha$ -GalA, it seems natural that one therapeutic approach is the enzyme replacement therapy (ERT). Approved for treatment in the EU in 2001, it was the first and up until 2016 the only FD-specific therapy, available via two different compounds: agalsidase  $\alpha$  (Replagal®) and agalsidase  $\beta$  (Fabrazyme®)

("Fabrazyme," 2020; "Replagal," 2018). ERT is applied intravenously every other week and is generally suitable for all patients tolerating this therapy. Many studies have shown that ERT effectively reduces substrate accumulation, improves symptoms and reduces complication rates in patients (Germain et al., 2015; Pastores et al., 2001; Schaefer et al., 2009; Schiffmann et al., 2003; Schiffmann et al., 2001). However, it is often associated with severe side effects such as headache, fever, and shivers that sometimes even lead to therapy stop, and is inconvenient due to its i.v. application (Wilcox et al., 2004).

In 2016, a new drug with a different approach was approved for treatment of FD: the oral chaperone migalastat (Galafold®) ("Galafold," 2019). The functional mechanism is based on the fact that some mutant forms of  $\alpha$ -GalA still possess residual activity, but are degraded prematurely due to misfolding. Migalastat intervenes in the degradation process of misfolded  $\alpha$ -GalA by stabilizing the mutant  $\alpha$ -GalA and restoring its activity (Markham, 2016; McCafferty et al., 2019). While its oral application, the few side effects, and the promising first clinical results are great achievements in FD therapy, this type of treatment is amenable for merely 35-50% of all mutations (Hughes et al., 2017), leaving the remaining patients with the only option ERT.

A new promising therapeutic approach that is currently investigated in a phase 3 clinical trial, is substrate reduction therapy (SRT) with lucerastat. SRT aims at reducing substrate amount to such a level that remaining residual activity of mutant enzymes is sufficient to prevent pathological substrate accumulation. (Lachmann et al., 2001). Studies showed that lucerastat reduces Gb3 levels in in-vitro models of human skin fibroblasts (Welford et al., 2018) and Gb3 concentration in plasma and urine in-vivo of all FD subjects, independent of their mutation (Guérard et al., 2018). However, further studies need to confirm the beneficial effects on clinical outcome in patients. In the future, lucerastat might be a therapeutic option for all patients, entailing its advantages of oral application and good tolerance (Guerard et al., 2017; Guérard et al., 2018).

A totally different approach that is currently investigated in phase 1/2 trials is a personalized lentiviral gene therapy called AVR-RD-01®. In this therapeutic approach, patients donate blood samples to collect stem cells via apheresis.

Subsequently, a therapeutic  $\alpha$ -GalA gene is introduced into the patients' stem cells before returning them to the patient as one-time infusion with a potentially life-long effect. Though first results in a very small cohort sound promising, more and larger studies are required to determine whether this therapeutic approach can be implemented into clinical practice (Khan et al., 2021). Depending on symptoms and organ manifestations, complementary symptom-oriented therapy can be offered, including medication such as anticonvulsants or antidepressants for FD-associated pain (Politei et al., 2016) or angiotensin converting enzyme inhibitors for nephropathy (Waldek and Feriozzi, 2014), and interventional therapy such as implantation of an implantable cardiac device or organ transplant (Akhtar et al., 2018).

### **2.1.7 Challenges in FD**

Despite great advances in FD management over the past years, there are still many issues that clinicians have to meet, such as:

- Identifying each patient

This remains difficult due to several reasons: First, FD is insufficiently well-known, even to medical professionals and hence, probably a high number of patients remains undiagnosed and untreated (Cimaz et al., 2011). Second, FD is a many-faced illness with wide symptom variety hampering simple diagnosis. Third, an unknown number of  $\alpha$ -GalA mutation carriers do not develop clinical signs and remain undiagnosed, but can inherit the mutation to the next generation (Desnick et al., 2003). Fourth, it is most likely that not all  $\alpha$ -GalA mutations are known so far, thus pathogenicity assessment of new  $\alpha$ -GalA variants is challenging (Cairns et al., 2018). All these aspects taken together often lead to missed or delayed diagnosis and hence start of therapy.

- Monitoring disease progression and therapy

Even though it was shown that ERT provides benefit for patients on a long-term basis, it is challenging for clinicians to assess therapy success and need for therapy adaptation in the short-term. Proving reduction of substrate accumulation via repeated biopsies is not practicable due to its invasiveness

(Cairns et al., 2018). In this respect, biomarkers play a crucial role. An important subject of current research is investigation of such FD-specific biomarkers to reflect disease burden and therapy response. Plasma lyso-Gb3 has been described as a reliable biomarker (Auray-Blais et al., 2010; Niemann et al., 2014; Sakuraba et al., 2018), but also in urine and other tissue, lyso-Gb3 deposits have been described (Auray-Blais et al., 2010; Togawa et al., 2010). Also, Gb3 itself has been detected in blood cells and urinary sediment (Rozenfeld et al., 2009; Üçeyler et al., 2018) and could be used as a biomarker, although further studies need to assess its reliability.

- Finding the most suitable therapy for each patient

Not all patients receive FD-specific therapy immediately after the diagnosis is made. If a patient is asymptomatic, watchful waiting with regular follow-up investigations can be an option. However, choosing the right moment to start and the type of therapy can be challenging. As mentioned above, not all patients carry migalastat-amenable mutations, while others develop severe side effects during ERT or antibodies against its compounds, which substantially limits treatment options (Cairns et al., 2018; McCafferty and Scott, 2019; Wilcox et al., 2004).

These are merely some of many challenging aspects, but they already show that FD is and will remain an ongoing challenge. Continuously extending the existing knowledge by basic and clinical research is therefore crucial.

## **2.2 Theoretical background for Study I**

### **2.2.1 Involvement of the peripheral nervous system**

#### **2.2.1.1 Clinical presentation**

Regarding the peripheral nervous system (PNS), FD-associated pain and small fiber neuropathy (SFN) dominate the clinical picture.

SFN emerges from an affection of mostly the thinly myelinated A $\delta$ - and unmyelinated C-fibers of the PNS and is associated with a reduction or loss of intraepidermal innervation (Møller et al., 2007; Üçeyler et al., 2013a). Clinically, this is reflected by impaired thermal perception with a predilection for cold sensation, and elevated heat-pain detection thresholds (Dütsch et al., 2002; Low et al., 2007).

FD-associated pain is not only one of the first, but also one of the most disabling symptoms in FD. In a study investigating 352 pediatric patients, it was shown that 59% boys and 41% girls reported FD-associated pain, present as episodic pain crises or chronic pain on a moderate to severe level (Hopkin et al., 2008). In many patients, FD-associated pain persists during adulthood, as a prevalence of 71-81% among men and 40-65% among females demonstrates (Hoffmann et al., 2007; Üçeyler et al., 2014). Patients describe different types of pain:

- evoked pain: triggered by e.g. pressure or hot/cold objects
- pain attacks: episodic pain that occurs spontaneously
- pain crisis: severe pain on the whole body that can last up to several days
- permanent pain: pain that lasts > 24 hours or most time of the day.

Reported by 66% and 47% patients respectively, evoked pain and pain attacks are most often mentioned as pain types. However, pain quality and location are equal among all types of pain; FD patients mainly characterize pain as burning,

less common as electrifying, squeezing or pressing and typically located in feet and hands (Hoffmann et al., 2007; Üçeyler et al., 2014). In most cases, FD-associated pain is triggerable, usually by physical activity, thermal stimuli, and fever, and may relieve during FD-specific treatment, although permanent analgesic medication or medication on-demand remain an important complement (Politei et al., 2016). The relation between SFN and FD-associated pain has only scarcely been investigated and is still unclear. Progress of SFN and FD-associated pain differ over time, as severity of SFN is likely to increase over time while FD-associated pain often abates with age (Biegstraaten et al., 2012).

#### **2.2.1.2 Pathophysiology of FD-associated pain**

While the exact pathomechanism of FD-associated pain is not fully understood, there is evidence that its primary pathophysiology is, as in other FD symptoms, associated with accumulation of substrates such as Gb3 or lyso-Gb3 (Rozenfeld et al., 2017; Schiffmann, 2006). Gb3 deposits have been found in a range of different neural tissues, including dorsal root ganglia (DRG) and axons of peripheral neurons (Schiffmann et al., 2002). However, there is growing evidence that FD-associated pain may also have a more peripheral origin. Gb3 deposits that have been shown in skin and small vessels could also contribute to FD-associated pain (John MacDermot et al., 2001).

Surely, the sole accumulation of Gb3 is not sufficient to explain the pathophysiology of FD symptoms such as FD-associated pain. The exact impact of Gb3 on cell function is currently investigated and studies have shown that Gb3 and its derivatives can

- induce inflammation and oxidative stress (Biancini et al., 2012), leading to deoxyribonucleic acid (DNA) damage and thus, apoptosis (Chimenti et al., 2015; Shen et al., 2008);
- activate signal cascades such as the Notch1 signaling cascade (Sanchez-Niño et al., 2015)

- and thus, lead to secretion of pro-inflammatory cytokines like tumor necrosis factor- $\alpha$  (TNF) and interferon- $\gamma$  (IFN- $\gamma$ ) (De Francesco et al., 2013), which in turn increases Gb3 accumulation (Üçeyler et al., 2019);
- disturb signal transduction pathways like nociception (Schiffmann, 2009);
- impede proteins such as ion channels, in their cellular function (Hofmann et al., 2018; Park et al., 2011).

## **2.2.2 Cutaneous nociception**

### **2.2.2.1 Relevant structures and processes**

Nociception is the way the somatosensory nervous system processes noxious stimuli. Nociceptors are the nerve endings of the primary afferent A $\delta$ - and C-fibers in various tissues, including inner organs, viscera, and the skin. Those stimuli are then transmitted along the A $\delta$ - and C-fibers to the spinal cord and the cerebral cortex, where the painful sensation is perceived (Vaskar, 2015). In the skin, nerve endings of A $\delta$ - and C-fibers form the majority of all primary afferent fibers and are specialized concerning their activation: chemospecific nociceptors, thermoreceptors, and mechanoreceptors were found, but also polymodal nociceptors, responsive to different stimuli, were described (Millan, 1999). However, not only A $\delta$ - and C-fibers are important in nociception, but also the surrounding cells since interaction between neural and non-neural cells via cytokines can modify nociception. For cutaneous nociceptors, dermal fibroblasts and epidermal keratinocytes play a role in that respect. Recent studies increasingly put the role of non-neuronal skin cells in cutaneous nociception into focus. Together they build a complex, interdependent network communicating in reciprocal ways via pronociceptive neurotransmitters such as substance P, calcitonin-gene related peptide, glutamate, acetylcholine, or neurokinin A; and their receptors. (Scholzen et al., 1998; Ständer et al., 2009; Talagas et al., 2019). These mediators are released by both neuronal and non-neuronal skin cells and can induce release of pro-inflammatory cytokines such as IL6, IL-1 $\beta$ ,

and TNF that contribute to nociceptor sensitization. However, these cytokines can also induce release of pronociceptive mediators. Via membrane receptors, nociceptors detect this stimuli and convert them into an action potential that is then transmitted to the central nervous system (CNS) (Julius et al., 2001; Koltzenburg, 2000; Vaskar, 2015).

#### **2.2.2.2 Role of dermal fibroblasts**

Fibroblasts can be found in connective tissue all over the body. Skin fibroblasts form the majority of cells in the dermal layer of the human skin and are embedded among extracellular matrix and other cell types such as sweat glands, blood vessels and also nociceptors (Vig et al., 2017). Dermal fibroblasts communicate with their environment in reciprocal way and respond to changes therein with adaptation of cellular processes (Kessler-Becker et al., 2004) and hence, play an important role in inflammation by expression of cytokines and chemokines (Saalbach et al., 2007). Human and animal models have shown that fibroblasts express a variety of cytokines and chemokines such as interleukin-6 (IL-6), IL-8, and IL-10, transforming growth factor- $\beta$ 1 (TGF- $\beta$ 1), TNF and chemokine (C-C motif) ligands 2 (CCL2), 5 (CCL5) and 7 (CCL7), and also leukotrienes such as leukotriene B<sub>4</sub>, which are all involved in inflammatory processes (Grimbacher et al., 1998; Jain et al., 2011; Mahmoudi et al., 2019). In various tissues, fibroblasts are considered sentinel cells since they are sensible to inflammatory triggers in their environment and can regulate responses (Díaz-Araya et al., 2015; Fukuda et al., 2017; Smith et al., 1997). Nevertheless, fibroblasts are not only involved in acute inflammatory processes, but also in the transition from acute to chronic inflammation as they consistently express cytokines like IFN- $\beta$  as well as chemokines, retaining immune cells in the inflamed area (Buckley, 2011; Buckley et al., 2001). Since inflammatory processes in the surrounding tissue contribute to activation and sensitization of nociceptors (Moalem et al., 2006), dermal fibroblasts can play a part in pain sensation due to their close contact with cutaneous nociceptors.



### 2.2.2.3 Ion channels in dermal fibroblasts

By establishing the patch-clamp technique, developed in the 1970ies and decorated with the Nobel Prize, Erwin Neher and Bert Sakmann signaled the start of an era of ion channel research (Dale et al., 2007; "The Nobel Prize in Physiology or Medicine 1991," n.d.; Sakmann et al., 1984). However, while excitatory cells were analyzed extensively, non- excitatory cells such as dermal fibroblasts have only scarcely been investigated with this technique. Hence, a large number of ion channels has been described in excitatory cells such as DRG neurons, of whom many were revealed as potential "pain targets", e.g. several voltage-gated  $\text{Na}^+$ -,  $\text{K}^+$  -, and  $\text{Ca}^{2+}$ - channels (Vaskar, 2015). In contrast, only a small number of ion channels was described in the membrane of dermal fibroblasts:

- Volume-regulated anion channels (VRACs) (Lakomá et al., 2016)
- Voltage-regulated  $\text{Cl}^-$  channels (CIC2) (Lakomá et al., 2016)
- Stretch-activated cation channels (Stockbridge et al., 1988)
- Voltage-dependent  $\text{Ca}^{2+}$  channels (Chen et al., 1988)
- Voltage-gated  $\text{Na}^+$  channels (Estacion, 1991)
- Different types of  $\text{K}^+$  channels:
  - o voltage-gated  $\text{K}^+$  channels
  - o inward rectifier  $\text{K}^+$  channels
  - o small-conductance  $\text{Ca}^{2+}$ -activated  $\text{K}^+$  channels ( $\text{K}_{\text{Ca}}$  3.1) and
  - o large-conductance  $\text{Ca}^{2+}$ -activated  $\text{K}^+$  channels ( $\text{K}_{\text{Ca}}$  1.1).(Estacion, 1991; Oliván-Viguera et al., 2017)

While little is known about ion channels that are expressed in the membrane of dermal fibroblasts, even less is known about their function therein, such as their potential role in activation or sensitization of nociceptors by fibroblasts. There is evidence that ion channels in fibroblasts are involved in detection of mechanical stress, changes in cell volume and coordination of signaling cascades by receptor interaction (Stockbridge and French, 1988; Tian et al., 2014). Also, functional alterations in these ion channels as parts of diseases are mostly

unknown. In dermal fibroblasts of FD patients, for example, two types of Cl<sup>-</sup> channel are altered: VRACs are more effectively blocked by their selective inhibitor when compared to dermal fibroblasts of healthy controls, and CIC2 channels synthesized in both FD and control cells, but can only be found in the membrane of control cells (Lakomá et al., 2016). However, the pathophysiological basis of these observations as well as their impact on cell function or connection to FD-associated pain remain unclear.

### **2.2.3 Aims of Study I**

There is growing evidence that Gb3 accumulation is the primary underlying pathology in FD. The concept of cutaneous nociception increasingly unveils the crucial role of non-neuronal skin cells in pain. We hypothesized that Gb3 accumulation in dermal fibroblasts may disturb cellular function, including ion channel function. The aim of this study was to investigate the potential role of dermal fibroblasts in cutaneous nociception and their contribution to FD-associated pain. Therefore, the following questions were addressed:

- Is the Gb3 load in dermal fibroblasts of FD patients higher than in those of healthy controls?
- Which ion channels are present in the membrane of dermal fibroblasts?
- Are there differences in ion channel function between dermal fibroblasts of FD patients and healthy controls?
- If so, how could these be linked to FD-associated pain?
- Which other functional alterations in dermal fibroblasts of FD patients could contribute to FD-associated pain?

## **2.3 Theoretical background of Study II**

### **2.3.1 3D-structure defects in enzymes**

#### **2.3.1.1 3D-structure of enzymes**

Most enzymes are proteins, i.e. they are long, unbranched amino acid chains whose order is determined by the base sequence of the DNA in the corresponding gene. Each amino acid of the protein is encoded by a codon, a base triplet in the gene. The sole amino acid sequence forms the primary structure of the protein and contains all information that is necessary for the correct folding of the protein into its 3D-structure. This spatial structure of the complete amino acid chain including all residues is referred to as the tertiary structure of the protein. If several amino acid chains aggregate to a protein complex, the single amino acid chains are referred to as its subunits (Rassow, 2012). The resulting native 3D-structure of a protein or a protein complex - which most enzymes are - arises from bonding forces between the residues of the amino acids in different segments and is crucial for the function of the protein (Netzker, 2012). Hence, proteins like enzymes are vulnerable towards mutations in the corresponding gene segment since these can induce alterations in their primary structure and consequently in their 3D-structure, resulting in altered protein function.

#### **2.3.1.2 Impact of 3D-structure defects of enzymes in hereditary Diseases**

Determining the 3D-structure of protein complexes such as enzymes is an elaborate process that can be performed using X-ray crystallography (Rassow, 2012). Despite its complexity, the 3D-structures of several enzymes that are involved in hereditary diseases have been determined and published, especially for LSDs (Clark et al., 2009; Gorelik et al., 2016; Lieberman et al., 2007; Mark et

al., 2003). For example, in Niemann-Pick disease types A and B, sphingomyelin accumulates in lysosomes because the enzyme acid sphingomyelinase (ASMase) is deficient due to mutations in the corresponding gene segment. Similar to FD, several types of mutations have been described, including missense and nonsense mutations or deletions (Schuchman, 2007). After determining the 3D-structure of ASMase, amino acid exchanges due to Niemann-Pick disease A and B missense mutations were mapped. Exchanges were found in different segments of the enzyme – some were located in the active site, some in saposin domains (activator domains for hydrolysis (Kishimoto et al., 1992)) and others on the protein surface, each with different impact on ASMase's function and hence clinical manifestation in patients (Gorelik et al., 2016). Similar discoveries have been made for the enzyme  $\beta$ -glucosidase in Gaucher disease (Lieberman et al., 2007). These observations emphasize that investigation of alterations in the 3D-structure of enzymes can play an important role in understanding the pathophysiology of diseases.

#### **2.3.1.3 3D-structure of $\alpha$ -GalA and its defects in FD**

While the base sequence of the  $\alpha$ -GalA gene and hence the primary structure of  $\alpha$ -GalA enzyme were revealed in 1989 (Kornreich et al., 1989), it took almost 15 further years until its 3D-structure was described. When X-ray crystallography was used to determine the spatial structure of  $\alpha$ -GalA, it was discovered that  $\alpha$ -GalA is a homodimeric protein, i.e. consists of two identical subunits, and is formed by 398 amino acids. The active site, where the catalytic reaction takes place, is formed by 15 amino acids and the side-chains of their residues, respectively. Although distant in the primary structure, these amino acid residues interact via hydrogen bonds, van der Waals forces, and polar interactions in the 3D-structure (Garman and Garboczi, 2004a). Fig. 3 depicts the 3D-structure of  $\alpha$ -GalA.

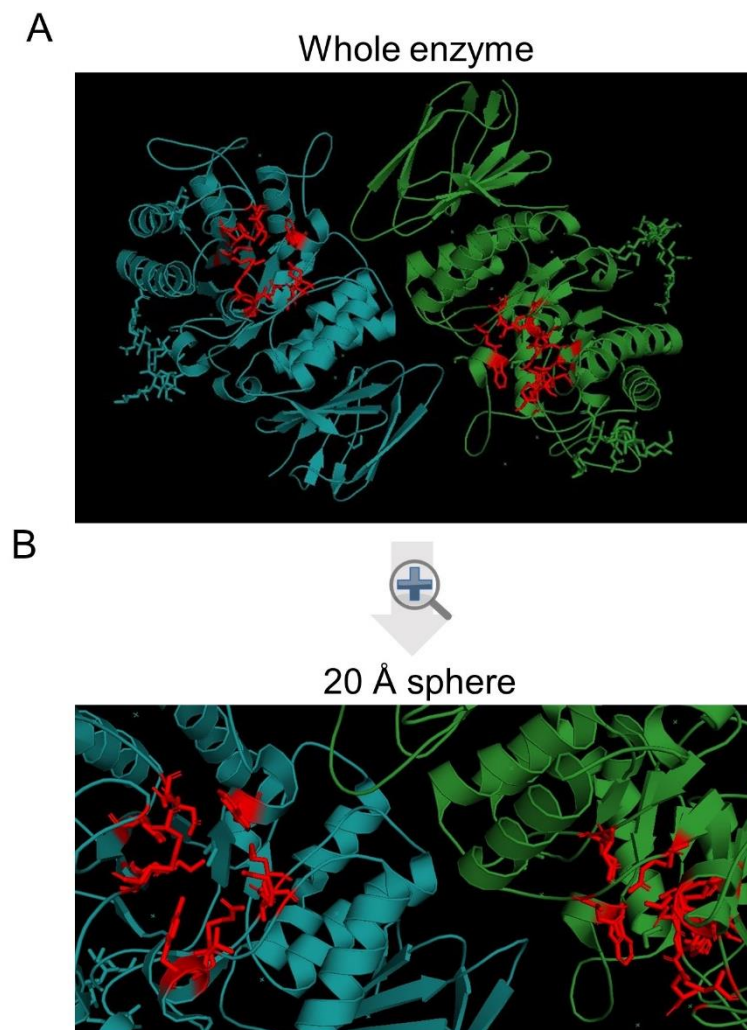


**Figure 3. 3D-structure of  $\alpha$ -GalA**

3D-structure of  $\alpha$ -GalA was downloaded from the PDB Europe into Pymol Graphics System. A) Overview of the 3D-structure of the whole enzyme. The two subunits are colored in blue and green, the amino acids forming the active site are marked in red and their residues are shown to demonstrate their spatial proximity despite their distance in the primary structure. B) Zoom into the active site, reaching 20Å sphere, in the same color mode as A. Abbreviations:  $\alpha$ -GalA= $\alpha$ -Galactosidase A; PDB=Protein databank.

Following determination of  $\alpha$ -GalA 3D-structure, amino acid exchanges due to FD missense mutations in the  $\alpha$ -GalA gene were mapped. It turned out that plenty of the 398 amino acids, spread in different segments of the enzyme, were affected. The amino acid exchanges were grouped based on their location:

- Exchanges of an amino acid forming part of the active site
- Exchange of an amino acid in  $\alpha$ -GalA core
- Exchange of an amino acid that at another location, mostly on the protein surface.

Although it was clear already that the 3D-structure of  $\alpha$ -GalA might help clinicians to assess the impact of novel FD mutations (Garman and Garboczi, 2004a), clinical data of FD patients with known or new mutations has not yet been analyzed in that respect.

### **2.3.2 Aims of Study II**

Symptom variety is large among FD patients due to many different individual mutations found in the  $\alpha$ -GalA gene. Previous findings have shown that amino acid exchanges due to missense mutations are located in various parts of 3D-structure of  $\alpha$ -GalA, but can be grouped into three different location types. Based upon this, the hypothesis was that the amino acid exchange (AAE) location type in the 3D-structure of  $\alpha$ -GalA has impact on symptom onset and disease severity. The aim of this study was to map amino acid exchanges in the 3D-structure of  $\alpha$ -GalA, assign them to a location type and investigate the differences in clinical symptoms between the different location types. Hence, the following questions were addressed:

- Which AAE location types can be found in FD patients?
- How frequent are the different AAE location types?
- Are there differences in laboratory and clinical findings of FD patients when they are grouped according to their individual AAE location type?

### **3 Materials and Methods**

#### **3.1 Study I**

##### **3.1.1 Study cohort**

###### **3.1.1.1 FD patient cohort**

40 adult patients with genetically confirmed FD, who were seen at the Fabry Center for Interdisciplinary Therapy at the University Hospital of Würzburg, Germany were included between August 2015 and December 2018. All patients consented to study participation after oral and written information. The study was approved by the Würzburg Medical Faculty Ethics Committee (#135/15).

###### **3.1.1.2 Control cohort**

Ten adult healthy control subjects were recruited from among friends and acquaintances of the patients and provided skin samples for cell culture experiments. Subjects were only included if no case or suspicion of FD had occurred within their families and after they had consented to study participation after oral and written information.

###### **3.1.1.3 Subgroups in the study cohort**

As shown in Fig. 4, the FD patient cohort was divided into subgroups for parts of the experiments. For other experiments, a selection of several FD patients was made.

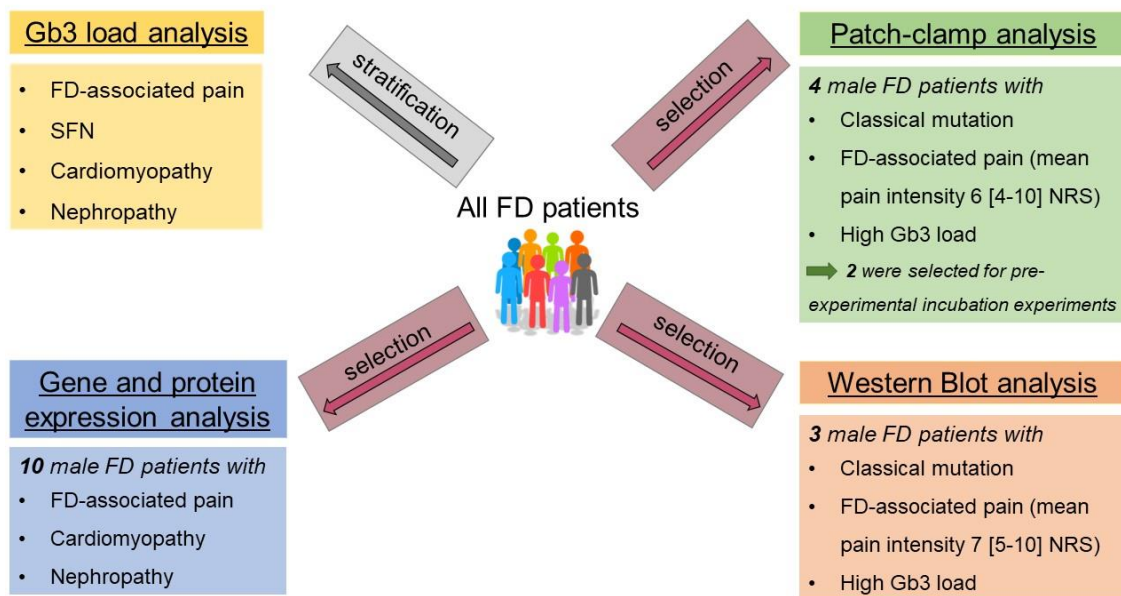


**Figure 4. FD patient subgroups and selections**

The Figure shows how the FD patient cohort was divided and how patients were selected, respectively, for various analyses. Abbreviations: FD=Fabry disease; Gb3=Globotriaosylceramide; NRS=Numeric rating scale; SFN=Small fiber neuropathy.

Methods of collection of all mentioned parameters for stratification within the FD patient cohort as well as the referring experiments will be explained in the following (sections 3.1.2 - 3.1.6).

Also among the healthy control group, individuals were chosen for gene and protein expression analysis (five males), patch-clamp analysis (four males) and Western Blot analysis (three males).

### **3.1.2 FD mutation analysis: classical and non-classical mutations**

All FD mutations were entered into the International Fabry Disease Genotype-Phenotype Database (Chen, 2016) and the corresponding phenotype was extracted.



### **3.1.3 Clinical phenotyping**

#### **3.1.3.1 Neurological assessment**

##### *3.1.3.1.1 Medical history and neurological examination*

All FD patients reported their medical history and underwent complete neurological examination. In particular, patients were asked for anhidrosis or hypohidrosis, dysesthesia, presence and quality of pain, and their medication. Also, signs of past cerebral stroke were assessed by interview and clinically.

##### *3.1.3.1.2 Würzburg Fabry Pain Questionnaire*

To further assess FD-associated pain, all patients filled in the German version of the Würzburg Fabry Pain Questionnaire (Magg et al., 2015). The questionnaire consists of 15 questions and addresses:

- presence of permanent and/or pain crisis and/or pain attacks and/or evoked pain (Üçeyler et al., 2014)
- maximum and average pain intensity on a numeric rating scale (NRS) from 0 (no pain) to 10 (maximum pain imaginable)
- pain quality (e.g. burning or stabbing)
- pain triggers (e.g. heat or infection)
- pain location.

##### *3.1.3.1.3 Quantitative sensory testing (QST)*

To test skin sensitivity, QST was performed according to a standardized protocol of the German Research Network for the Study of Neuropathic Pain (Deutscher Forschungsverbund Neuropathischer Schmerz e.V.) (Rolke et al., 2006). QST was performed at the feet (test area), and cheek (control area) examining thermal, tactile, mechanical, vibration, and pressure perception and pain thresholds. Data were compared with published reference data (Magerl et al., 2010).

#### *3.1.3.1.4 Nerve conduction studies*

To exclude polyneuropathy, all FD patients received electroneurography of a sensory nerve (sural nerve) and a motor nerve (tibial nerve) according to a standardized protocol (Kimura, 2013). Data were compared with the normative values of our laboratory.

#### *3.1.3.1.5 Diagnosis of small fiber neuropathy (SFN)*

After exclusion of polyneuropathy, SFN was diagnosed according to published criteria. SFN was assumed when patients reported pain or dysesthesia and met two of the following three criteria (Devigili et al., 2008): pathological findings in QST and/or in neurological examination and/or reduced intraepidermal nerve fiber density in skin punch biopsies (IENFD, s. below).

### **3.1.3.2 Assessment of cardiomyopathy**

All FD patients received echocardiography and, if no contraindications were present, cardiac magnetic resonance imaging (MRI) scans, to check for presence of left ventricular hypertrophy and late gadolinium enhancement (LGE) as indicators of cardiomyopathy (Putko et al., 2015; Serra et al., 2019). The diagnosis of cardiomyopathy was made when at least one of the two characteristics was found.

### **3.1.3.3 Assessment of nephropathy**

Every FD patient provided a urine sample to measure glomerular filtration rate (GFR; reference:  $>60 \text{ ml/min/1.73m}^2$ ), a parameter that indicates nephropathy (Schiffmann et al., 2010; Waldek and Feriozzi, 2014). The diagnosis of nephropathy was made when the GFR fell  $<60 \text{ ml/min/1.73m}^2$ .

### **3.1.4 Skin sample acquisition**

#### **3.1.4.1 Skin biopsy**

40 FD patients (21 men, 19 women) and all healthy controls received a 6-mm skin punch biopsy (punch: Kai Europe GmbH, Solingen, Germany) of the lateral calf, approx. 10 cm about the ankle, under sterile conditions and in local anesthesia (1-2 ml scandicain 1%) according to an established protocol (Üçeyler et al., 2010). After withdrawal, samples were divided in halves. One half was fixed in 4% buffered paraformaldehyde for determination of IENFD, the other half was placed in fibroblast growth medium for cell culture experiments.

#### **3.1.4.2 Determination of IENFD**

After 30 minutes of fixation, skin samples were repeatedly washed with phosphate buffer and subsequently stored in 10% sucrose/0.1M phosphate buffer at 4°C over night. The next day, samples were transferred into Tissue Tek® embedding compound (Sakura Finetek Europe B.V., Alphen aan den Rijn, Netherlands) and frozen in liquid nitrogen-cooled 2-methylbutane for storage at -80°C. 40-µm cryosections were created for nerve fiber staining with antibodies against the pan-axonal marker protein-gene product 9.5 (Ultraclone, UK, 1:800 or Zytomed, Berlin, Germany, 1:200)/ goat anti-rabbit IgG labeled with fluorescent cyanine 3.18. Nerve fiber counting was performed at a Zeiss Axiophot 2 microscope (Zeiss, Oberkochen, Germany) with a CCD camera (Visitron Systems, Tuchheim, Germany) and SPOT advanced software (Windows version 4.5, Diagnostic Instruments, Inc., Sterling Heights, MI, USA). For each study participant, three sections were analyzed by a blinded investigator, following published guidelines (Lauria et al., 2010).

### **3.1.4.3 Primary fibroblast culture**

Under sterile conditions, skin samples were cut into twelve equal pieces and placed in culture flasks in groups of three. To enable attachment to the flask ground, only ten µl of fibroblast growth medium, containing DMEM (+) l-glutamine, 10% FCS and 1% PenStrep (all Thermo Fischer Scientific, Darmstadt, Germany), were added initially. Each after an hour-long incubation at 37°C and on the next day, 2.5 ml of fibroblast growth medium were added to the flask. During the primary culture period, medium was changed every three days and fibroblasts were transferred to a higher passage at about 80% confluence via trypsinization (TrypLE Express, Thermo Fischer Scientific, Darmstadt, Germany).

### **3.1.5. Cell culture experiments**

#### **3.1.5.1 Analysis of Gb3 deposits in fibroblasts**

##### *3.1.5.1.1 Immunocytochemistry for Gb3*

Two days in advance to the staining, fibroblasts were transferred onto coverslips and further incubated in medium until they were safely attached to the ground, but still solitary. On the first day of staining, fibroblasts were incubated with 4% buffered paraformaldehyde fixing solution for 10 minutes, triple-washed with phosphate buffered saline (PBS) and before being incubated with 0.3% triton/PBS for permeabilization and subsequently with 10% bovine serum albumin/PBS for blocking, for 5 minutes and 1 hour, respectively. Following blocking process, fibroblasts were incubated with monoclonal antibodies against Gb3 (TCI Deutschland GmbH, Eschborn, Germany; 1:250) or else, as a negative control (one for each subject), kept in blocking solution at +4 °C overnight. On the second day, fibroblasts were repeatedly washed with PBS before an hour-long incubation with donkey-anti-mouse IgG labeled with

alexa flour 488 fluorescent probe (Jackson ImmunoResearch, Ely, UK). Afterwards, fibroblasts were newly washed with PBS, then incubated with 4',6-diamidin-2-phenylindol (DAPI; Sigma Aldrich Chemie GmbH, Schnelldorf, Germany) and finally covered with aqua-poly/mount (PolySciences, Warrington, FL, USA).

#### 3.1.5.1.2 Determination of Gb3 load

Using a fluorescent microscope (Ax10, Zeiss, Oberkochen, Germany) with a CARV2-system and Visiview software (Visitron GmbH, Puchheim, Germany), a blinded investigator performed a semi-quantitative determination of Gb3 load. Therefore, each coverslip was comparted into five equal regions. In each region, 10 fibroblasts were regarded concerning presence of Gb3 deposits and morphology. The Gb3 load was then calculated using the formula

$$\text{Gb3 load} = \frac{\frac{\alpha}{10} + \frac{\beta}{10} + \frac{\gamma}{10} + \frac{\delta}{10} + \frac{\varepsilon}{10}}{5}$$

$\alpha / \beta / \gamma / \delta / \varepsilon = \text{fibroblasts with Gb3 deposits in region 1 / 2 / 3 / 4 / 5}$

The number of swollen fibroblasts was calculated in the same manner, but included only those fibroblasts that had Gb3 deposits *and* a swollen morphology.

#### 3.1.5.2 Incubation experiments

Fibroblasts of ten male, severely affected FD patients (all with FD-associated pain, cardiomyopathy and nephropathy) and five male healthy controls were selected for incubation experiments for quantitative real-time-PCR (qRT-PCR) experiments, enzyme-linked immunosorbent assays (ELISA) and Western Blot analysis (please see below and Fig.4). Fibroblasts were transferred into 6-well plates and T-25 flasks, respectively, and initially incubated with medium until they reached approx. 80% confluence. To model inflammation, fibroblasts were

incubated with 500 U TNF and 500 U IFN $\gamma$  (both Thermo Fisher scientific, Darmstadt, Germany). As negative controls (one for each subject), fibroblasts were kept in regular medium. After 24h, fibroblasts and supernatant were harvested and stored at -20°C.

To analyze the effect of Gb3 clearance on ions channels, half of the male FD patients selected for patch-clamp analysis, were likewise selected for preceeding incubation experiments (please refer to Fig. 4). Fibroblasts were transferred onto coated coverslips and initially incubated with medium, followed by a 24h-long incubation with 1.32  $\mu$ g/ml agalsidase- $\alpha$  (Replagal®, Shire, Lexington, KY, USA) to clear Gb3. Afterwards, they were analyzed electrophysiologically. As negative controls (one for each subject), fibroblasts were kept in regular medium.

### **3.1.5.3 Patch-clamp analysis**

Fibroblasts of four male FD patients suffering from FD-associated pain and with high Gb3 load (s. above and Fig. 4) and four male healthy controls were investigated using patch-clamp analysis. Two of the FD patients were selected for pre-experimental incubation with 1.32  $\mu$ g/ml agalsidase- $\alpha$  (s. above and Fig.4). Two days before patch-clamp analysis, fibroblasts were transferred onto coated coverslips, enabling stable attachment, but hindering conflation. Prior to experiment, bath and pipette solution were prepared, containing 135 mM NaCl, 5.4 mM KCl, 1.8 mM CaCl<sub>2</sub>, 1 mM MgCl<sub>2</sub>, 10 mM glucose, and 5 mM HEPES (bath solution) and 140 mM KCL, 1 mM MgCl<sub>2</sub>, 2 mM EGTA, 5 mM HEPES, and 2 mM CaCl<sub>2</sub>, pH 7.4 (pipette recording solution). Patch pipettes were produced by use of borosilicate glass capillaries (Kimble Chase Life Science and Research Products, Meiningen, Germany), and heat-polished, reaching an input resistance of 2 to 3 M $\Omega$ . On solitary fibroblasts, whole-cell recordings were performed at room temperature. Current recordance was conducted at -40mV, using an EPC9 patch-clamp amplifier (HEKA, Ludwigshafen, Germany) with a sampling rate of 20 kHz. A PULSE/PULSEFIT software package (HEKA, Lambrecht, Germany) on a Macintosh computer-controlled stimulation and data

acquisition, while data analysis was executed with IGOR software (WaveMetrics, Lake Oswego, OR, USA). Division of current amplitude (in pA) by cell size (in pF) yielded current density (pA/pF).

With a perfusion system (Solution Exchange System ALAVC3–8, ALA Scientific Instruments, Farmingdale, NY, USA), recorded currents were characterized via application of various channel blockers (all from Merck, Darmstadt, Germany), listed in Table 4.

**Table 4. List of ion channel blockers applied for patch-clamp analysis**

| <b>Name</b>      | <b>Effect</b>  | <b>Concentration</b> |
|------------------|--|----------------------|
| 9-AC             | blocks $\text{Cl}^-$ channels                              | 100 $\mu\text{M}$    |
| CsCl             | blocks HCN channels  | 100 mM               |
| ChTX             | blocks $\text{K}_{\text{Ca}1.1}$ channel                   | 100 nM               |
| Cholin chloride* | replaces $\text{Na}^+$ und $\text{K}^+$ in their atomicity | 140 mM               |
| DCPIB            | blocks VRAC channel  | 10 $\mu\text{M}$     |
| DIDS             | blocks $\text{Cl}^-$ channels                              | 100 $\mu\text{M}$    |
| Diltiazem        | blocks $\text{Ca}^{2+}$ channels                           | 20 $\mu\text{M}$     |
| $\text{GdCl}_3$  | blocks $\text{Ca}^{2+}$ channels                           | 50 $\mu\text{M}$     |
| NS 6180          | blocks $\text{K}_{\text{Ca}3.1}$ channel                   | 5 $\mu\text{M}$      |
| TEA              | blocks $\text{K}^+$ channels                               | 5 mM                 |
| TRAM 34          | blocks $\text{K}_{\text{Ca}3.1}$ channel                   | 100 $\mu\text{M}$    |
| TTX              | blocks voltage dependent $\text{Na}^+$ channels            | 100 nM               |

\*cholin chloride is not an actual channel blocker, but an organic compound replacing  $\text{Na}^+$  und  $\text{K}^+$  in their atomicity, with thus similar effect

Abbreviations: 9-AC=9-anthracenecarboxylic acid; ChTX=charybdotoxin; CsCl= caesium chloride; DCPIB=4-(2-butyl-6,7-dichloro-2-cyclopentylindan-1-on-5-yl)oxybutyric acid; DIDS=4,4'-diisothiocyano-2,2'-stilbenedisulfonic acid; HCN= hyperpolarization-activated cyclic nucleotide-gated channel; NS 6180=4-[[3-(trifluoromethyl)phenyl]methyl]-2H-1,4-benzothiazin-3(4H)-one; TEA=tetraethylammonium; TRAM 34=1-[(2-chlorophenyl)diphenylmethyl]-1H-pyrazole; TTX= tetrodotoxin; VRAC=volume-regulated anion channel.

### **3.1.5.4 Gene expression analysis**

#### *3.1.5.4.1 mRNA extraction*

After harvesting fibroblasts (using QIAzol Lysis Reagent®; Qiagen, Hilden, Germany) following incubation experiments (s. above), mRNA extraction was performed with reagents and instruction of a miRNeasy Mini Kit (Qiagen, Hilden, Germany) and a Polytron 1600E® centrifuge (Luzern, Switzerland). mRNA samples were placed in a -80°C freezer for storage.

#### *3.1.5.4.2 Reverse transcription PCR*

Next, mRNA was transcribed to cDNA using TaqMan Reverse Transcription® reagents and cyclers by Thermo Fischer scientific (Darmstadt, Germany). 5 µl random hexamer, 10 µl 10x buffer, 22 µl MgCl<sub>2</sub>, 20 µl dNTP, 2 µl RNase Inhibitor, 6.2 µl multiscribe RT and 2 µl Oligo-D and distilled water were added to mRNA and all samples were centrifuged before transcription to cDNA in a Peqlab Advanced Primus 96® cycler, incubating samples at 25 °C for ten minutes, at 48 °C for 60 minutes and finally at 95 °C for five minutes. cDNA samples were stored at -20°C.

#### *3.1.5.4.3 qRT-PCR*

Gene expression by qRT-PCR was performed with reagents, cyclers and software by Thermo Fischer scientific (Darmstadt, Germany) for the following targets:

- potassium calcium-activated channel subfamily-M- $\alpha$ -1 (Hs01119904\_m1), encoding K<sub>Ca</sub>1.1 channel
- transmembrane receptors notch homolog 1 (Notch1; Hs01062014\_m1)
- TNF (Hs00174128\_m1)
- IFN $\gamma$  (Hs00989291\_m1)
- chemokine C-C motif ligand 2 (CCL-2; Hs00234140\_m1)
- transforming growth factor- $\beta$ 1 (TGF- $\beta$ 1; Hs00998133\_m1).



As samples to be investigated, 5 µl cDNA were mixed with 0.25 µl of the corresponding primer, 2 µl TaqMan® Universal PCR Master Mix and 1.75 µl nuclease-free water. As an endogenous control of each sample, 2.5 µl cDNA were mixed with 0.25 µl 18s rRNA primer, 4.25 µl nuclease-free water, 2µl TaqMan® Universal PCR Master Mix. Additionally, negative control and a calibrator sample (the sample of that control person whose threshold cycle (Ct) values came closest to the calculated mean of all control Ct values for the corresponding primer) were added to each plate. Each sample to be investigated was pipetted on the plate in triplicates, each 18s rRNA control in duplicates. Measurement was performed using a StepOnePlus cycler, incubating probes 50°C for two minutes, then at 95 °C for ten minutes, running 40 cycles at 95°C in 15 s and finally at 60°C for one minute. Data was analyzed with the corresponding StepOne Software Version 2.1 and evaluated according to the  $\Delta\Delta C_t$  method (Winer et al., 1999).

### **3.1.5.5 Protein expression analysis**

#### **3.1.5.5.1 ELISA**

After incubation experiments (s. above), supernatant of unstimulated fibroblasts was analyzed via ELISA (MyBioSource, sensitivity 0.1 ng/ml, San Diego, CA, USA) to measure protein level of the K<sub>Ca</sub>1.1 channel in fibroblasts. As a first step, cell debris was removed by centrifuging the samples at 1000g for 15 minutes. Subsequently, samples were handled according to the instructions in the ELISA kit and finally, the optical density of all samples was determined at 450 nm with a Multiskan™ FC Microplate Photometer (Thermo Fisher scientific, Darmstadt, Germany) as correlate for the level of K<sub>Ca</sub>1.1 channel in the fibroblasts.

#### 3.1.5.5.2 Western Blot analysis

Out of the incubation samples of the ten male FD patients and the five male healthy controls (s. above), we selected each three patient and control samples for Western Blot analysis. At the end of the incubation, medium was removed and fibroblasts were washed with PBS before detachment from the T-25 flask and homogenization with lysis buffer for storage at -20°C.

For Western Blot experiment, 20 µg total protein of each sample were transferred into 12.5% sodium dodecyl sulfate polyacrylamide electrophoresis gel for electrical separation by protein size. Then, samples were transferred onto polyvinylidene difluoride membrane (Hartenstein GmbH, Würzburg, Germany), that was blocked 5% milk buffer and incubated with antibodies against

- nuclear factor kappa-light-chain-enhancer of activated B-cells p65 (NF-κB p65; Santa Cruz Biotechnology, Inc., Dallas, TX, USA) and
- phosphorylated NF-κB p65 (p-NF-κB p65; Santa Cruz Biotechnology, Inc., Dallas, TX, USA)
- α-actin (Merck KGaA, Darmstadt, Germany), as loading control

at +4°C over night. The next day, the membrane was washed with 0.05% tween/PBS buffer for 30 minutes before one-hour-long incubation with donkey-anti-mouse horseradish peroxidase antibody (DIANOVA GmbH, Hamburg, Germany) at room temperature. Following the immunoreaction, the membrane was washed a second time with 0.05% tween/PBS buffer before visualization of immunoreactive bands with chemiluminescent reagent (GE Healthcare, Diegem, Belgium) and quantification with ChemiDoc™ Touch Imaging System (Bio-Rad Laboratories GmbH, München, Germany). Density of signal saturation was analyzed with the image processing tool of ImageJ software (Abràmoff et al., 2004) in raw data format with a light background of 50. Finally, division of the signal saturation density p-NF-κB p65 by that of NF-κB p65 yielded the p-NF-κB p65/NF-κB p65 ratio which was used for inter-sample comparisons. A-actin signal was evaluated in each probe to assure comparability of protein amount and hence, signal saturation density.

### **3.1.6 Statistical analysis and figure preparation**

Statistical analysis and graph preparation was performed using SPSS Statistics for Windows, Version 25.0. (IBM Corp, Armonk, NY, USA) and GraphPad Prism version 8.0.0 (for Windows, GraphPad Software, San Diego, CA, USA). Prior to comparative analysis, data distribution was determined with a Kolmogorov-Smirnov test. For inter-group comparison of metric variables, a *t*-test (for normally distributed data) or a Mann-Whitney-*U*-test (for non-normally distributed data) was used. Dichotomous variables were analyzed with a  $\chi^2$  test. Significance level was set to  $p < 0.05$ .

## **3.2 Study II**

### **3.2.1 Study cohort**

80 adult patients with genetically confirmed FD, who were seen at the Fabry Center for Interdisciplinary Therapy at the University Hospital of Würzburg, Germany were included between August 2015 and October 2019. All patients consented to study participation after oral and written information. The study was approved by the Würzburg Medical Faculty Ethics Committee (#135/15).

### **3.2.2 Subgroups in the study cohort**

Fig. 5 demonstrates how the study cohort was divided by sex, AAE location type and age (the latter for clinical parameters only). Since the clinical phenotype of patients carrying active site and buried mutations resembled each other, they were combined for analysis and compared with patients carrying other mutations.

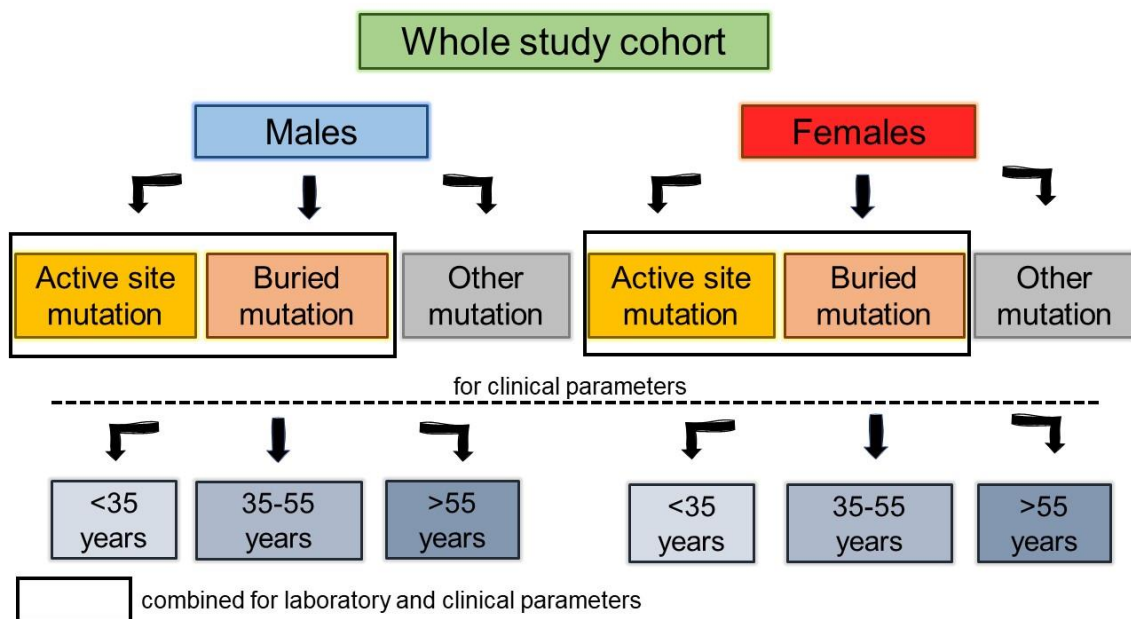


**Figure 5. Subgroups in the study cohort**

First, the study cohort was divided by sex. Each group was then subdivided by AAE location type and, for clinical parameters, further by age. Patients with active site and buried mutation were combined for analysis of clinical and laboratory parameters. Abbreviation: AAE=amino acid exchange.

Method of collection of the different AAE location types will be explained in section 3.2.2.2.

## 3.2.2 FD mutation analysis

### 3.2.2.1 Distinction between classical and non-classical mutations

The analysis was performed in the same manner as in Study I. For details, please refer to section 3.2.1.

### **3.2.2.2 Distinction by AAE location in the $\alpha$ -GalA 3D-structure**

3D-structure of  $\alpha$ -GalA, available at free disposal at the Protein Databank Europe (Garman et al., 2004b) was illustrated in Pymol 1.8 Graphics System (Schrodinger, 2015). Both the amino acid code and the 3D-structure of  $\alpha$ -GalA were depicted. Each amino acid exchange due to a single FD missense mutation was entered into the amino acid code and marked in the 3D-structure of  $\alpha$ -GalA. Based on the location of the consecutive amino acid exchange, FD missense mutations were subdivided into three groups, following the description by Garman and Garboczi (Garman and Garboczi, 2004a):

- Mutations inducing an exchange of an amino acid building part of the active site (= active site mutation)
- Mutations inducing an exchange of an amino acid in  $\alpha$ -GalA core with consecutive enzyme misfolding (= buried mutation)
- Mutations inducing an exchange of an amino acid on the protein surface (= other mutation)

### **3.2.3 Clinical phenotyping**

#### **3.2.3.1 Neurological assessment**

Neurological assessment was performed in the same manner as in Study I. For details, kindly refer to section 3.1.3.1.

#### **3.2.3.2 Assessment for cardiomyopathy**

As in Study I, every FD patient received echocardiography and, if no contraindications were present, cardiac MRI scans, to check for presence of left ventricular hypertrophy and LGE as indicators of cardiomyopathy (Putko et al., 2015; Serra and Marziliano, 2019).

Additionally, as summarized in Table 5, severity of cardiomyopathy was assessed by calculating a score based on the degree of left ventricular hypertrophy and LGE (i.e. 0-3 points for each category); carrying a cardiac device such as a pacemaker or an implantable cardioverter-defibrillator, hindering MRI scans, was scored 3 points.

**Table 5. Cardiomyopathy score**

| Points  | 0                                    | 1  | 3                                     |
|---|--------------------------------------|--|---------------------------------------|
| <b>Left ventricular hypertrophy</b>   |                                      |  |                                       |
| Septal wall thickness [mm]<br>and/or<br>Left ventricular mass index [g/m <sup>2</sup> ] | <12<br><br><95 (women)<br><115 (men) | 12-14<br><br>95-120 (women)<br>115-135 (men) | >14<br><br>>120 (women)<br>>135 (men) |
| <b>LGE</b>  | None                                 | Any intramural                               | Transmural or<br>>2 segments          |
| <b>Cardiac device</b>   | No                                   |  | Yes                                   |

Abbreviation: LGE=late gadolinium enhancement.

The calculated sum score differentiated between mild and severe cardiomyopathy. A sum score  $\leq 3$  was classified as mild cardiomyopathy, a sum score  $\geq 4$  points as severe cardiomyopathy.

### **3.2.3.3 Assessment for nephropathy**

Every FD patient provided a urine sample to measure the GFR (reference:  $>60$  ml/min/1.73m<sup>2</sup>), urine albumin, and creatinine as parameters indicating nephropathy (Schiffmann et al., 2010; Waldek and Feriozzi, 2014). Urine albumin/creatinine ratio (reference:  $<30$  mg/g) was calculated to categorize albuminuria according to Kidney Disease: Improving Global Outcomes. Category A2 ( $<30$  mg/g) was declared incipient nephropathy, category A3 ( $<300$  mg/g) overt nephropathy (Work, 2018).

### **3.2.4 FD-related laboratory tests**

All FD patients underwent blood withdrawal to measure  $\alpha$ -GalA activity in leukocytes (reference: 0.4 - 1.0 nmol/minute/mg protein; Podskarbi Laboratory, Munich, Germany) and lyso-Gb3 levels in plasma (reference: <0.9 ng/ml; Centogene, Rostock, Germany) by liquid chromatography and mass spectrometry.

### **3.2.5 Statistical analysis and figure preparation**

Statistical analysis and graph preparation was performed using SPSS Statistics for Windows, Version 25.0. (IBM Corp, Armonk, NY, USA) and GraphPad Prism version 8.0.0 (for Windows, GraphPad Software, San Diego, CA, USA). Data distribution was determined with a Kolmogorov-Smirnov test. Since data was non-normally distributed, a Mann-Whitney-*U*-test was used for comparison.

Significance level was set to  $p < 0.05$ .

Vectors for illustration purposes were obtained for free from Public Domain Vectors (<https://publicdomainvectors.org/>).

## **4 Results**

### **4.1 Study I**

#### **4.1.1 Epidemiology**

40 FD patients and ten healthy controls took part in Study I. The FD patient cohort consisted of 21 men and 19 women, and their median age was 47 [17-75] years (46 [17-64] years among men; 47 [25-75] years among women). The healthy control cohort consisted of seven men and three women, and their median age was 42 [21-65] years (38 [24-57] years among men; 46 [21-65] years among women).

#### **4.1.2 Characterization of the FD patient cohort**

##### **4.1.2.1 Genetic findings**

Table 6 gives an overview of the individual genotypes and phenotypes of the FD study cohort. The majority of FD patients carried a missense mutation, while nonsense or intron mutations were found less often. Regarding the resulting phenotype, classical and non-classical mutation were present in comparable numbers of patients.



**Table 6. Genetic findings in the FD cohort**

| Mutation               | N of patients |    |
|------------------------|---------------|----|
|                        | M             | F  |
| <b>Mutation type</b>   |               |    |
| Missense mutation      | 17            | 14 |
| Nonsense mutation      | 4             | 4  |
| Intron mutation        | 0             | 1  |
| <b>Phenotype</b>       |               |    |
| Classical mutation     | 12            | 10 |
| Non-classical mutation | 9             | 9  |

Abbreviations: M=male; N=number; F=female

#### **4.1.2.2 Clinical findings**

##### *4.1.2.2.1 All main organ manifestations in FD*

Table 7 summarizes the most important clinical findings among the FD study cohort in Study I. Regarding the nervous system, FD-associated pain was the most often reported symptom, while cerebral stroke was generally rare. Among the inner organs, the heart was most often affected.

**Table 7. Clinical findings and specific therapy in the FD study cohort**

| Disease manifestation      | N of patients |             |
|----------------------------|---------------|-------------|
|                            | M             | F           |
| <b>Nervous System</b>      |               |             |
| Cerebral stroke            | 2/21 (10%)    | 1/19 (5%)   |
| FD-associated pain         | 17/21 (81%)   | 14/19 (73%) |
| SFN                        | 9/21 (43%)    | 5/19 (26%)  |
| <b>Inner organs</b>        |               |             |
| Cardiomyopathy             | 15/21 (72%)   | 9/19 (47%)  |
| Nephropathy                | 9/21 (43%)    | 4/19 (19%)  |
| <b>FD-specific therapy</b> |               |             |
| ERT                        | 9/21 (43%)    | 5/19 (26%)  |
| Migalastat                 | 9/21 (43%)    | 6/19 (31%)  |
| None                       | 3/21 (14%)    | 8/19 (43%)  |

Abbreviations: ERT=Enzyme Replacement Therapy; FD=Fabry disease; SFN=Small fiber neuropathy.

#### 4.1.2.2.2 FD-associated pain

Regarding only FD-associated pain, analysis revealed that both average and maximum pain intensities were comparable between men and women (Fig. 6).

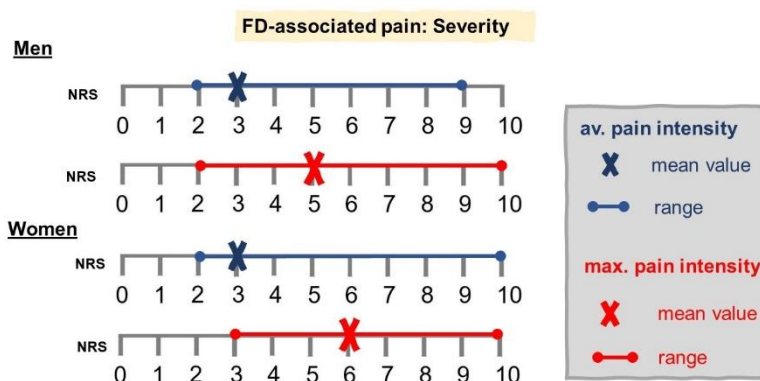


**Figure 6. Average and maximum pain intensity among FD patients**

All patients filled in the FPQ including questions on average and maximum pain intensity on a NRS from 0-10. Both average and maximum pain intensity were comparable between FD men and women. Abbreviations: av=average; FD=Fabry disease; max=maximum; NRS=Numeric rating scale.

As shown in Fig. 7, most patients reported several pain triggers, most often heat and fever (Fig. 7a-c). 'Other' pain triggers were stress and pressure. The majority of patients described pain of one two different qualities, most often burning pain, followed by stabbing pain (Fig. 6d-f). The 'other' pain quality was tingling.

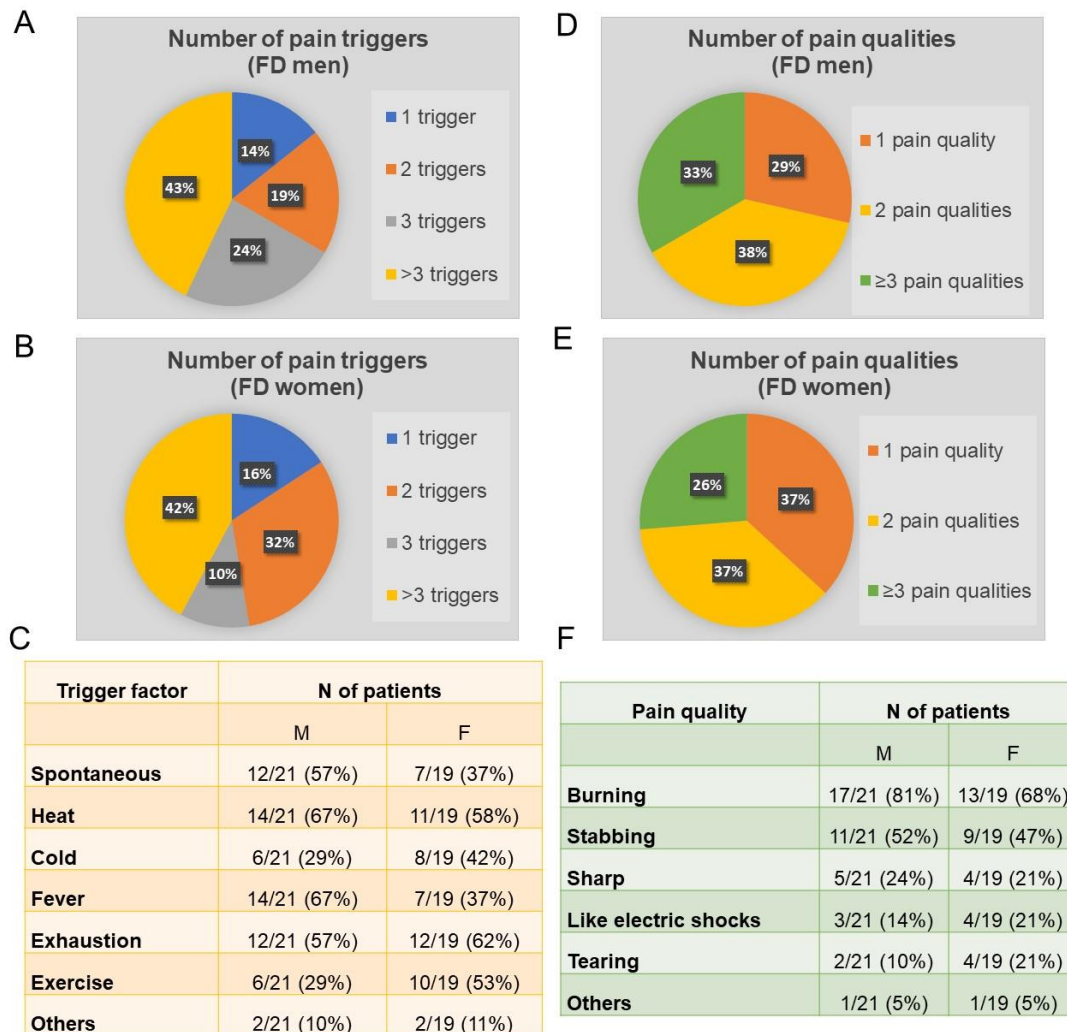


**Figure 7. Pain triggers and pain qualities among FD patients**

All patients filled in FPQ, including questions concerning pain triggers and pain quality. A) Number of pain triggers among FD men. B) Number of pain triggers among FD women. C) Frequency of pain triggers in exact numbers. D) Number of pain qualities among FD men. E) Number of pain qualities among FD women. F) Frequency of pain qualities in exact numbers. Abbreviations: F=Female; FD=Fabry disease; FPQ=Fabry Pain Questionnaire M=Male; N=Number.

### 4.1.3 Gb3 load analysis

#### 4.1.3.1 Median Gb3 load and median number of swollen cells in fibroblasts of FD patients and healthy controls

Fig. 8 shows Gb3 load in fibroblasts of FD patients and healthy controls. While Gb3 deposits (see arrows) were found in many cells and in large amounts in fibroblasts of the FD patient (Fig. 8a), Gb3 deposits were scarce in fibroblasts of the healthy control (Fig. 8b). This optical difference was confirmed by the analysis of fibroblasts of all FD patients and healthy controls: the median Gb3 load and the number of swollen cells were higher in fibroblasts of FD patients than in healthy controls (Fig. 8c-d;  $p < 0.01$ ).

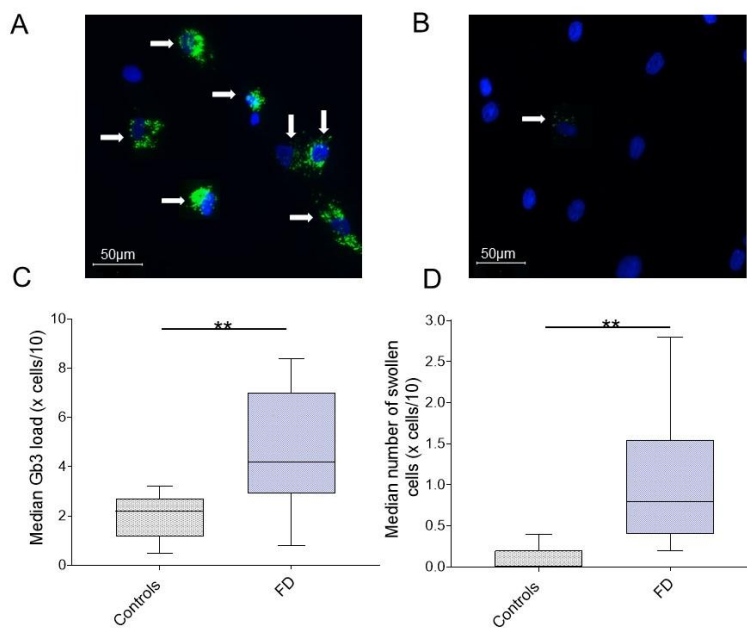


**Figure 8. Gb3 deposition in dermal fibroblasts**

Gb3 deposition in fibroblasts was shown with monoclonal antibodies against Gb3, cell nuclei were visualized with DAPI. A) Large Gb3 deposition in FD fibroblasts. B) Scarce Gb3 deposition in control fibroblasts. C) Median Gb3 load is higher in FD fibroblasts when compared to control fibroblasts. D) Median number of swollen cells is also higher in FD fibroblasts when compared to control fibroblasts. Abbreviations: DAPI= 4',6-diamidin-2-phenylindol; FD=Fabry disease; Gb3=Globotriaosylceramide; n=number of patients. \*\* $p < 0.01$ . Scale bar = 50 µm.

#### 4.1.3.2 Median Gb3 load and median amount of swollen cells in fibroblasts of different FD subgroups

As shown in Fig. 9, stratification of the FD cohort neither for disease manifestation in the PNS (FD-associated pain and SFN; Fig.9-b) nor for disease manifestation in the inner organs (cardiomyopathy and nephropathy; Fig. 9c-d) revealed a difference in median Gb3 load or number of swollen cells between the subgroups.

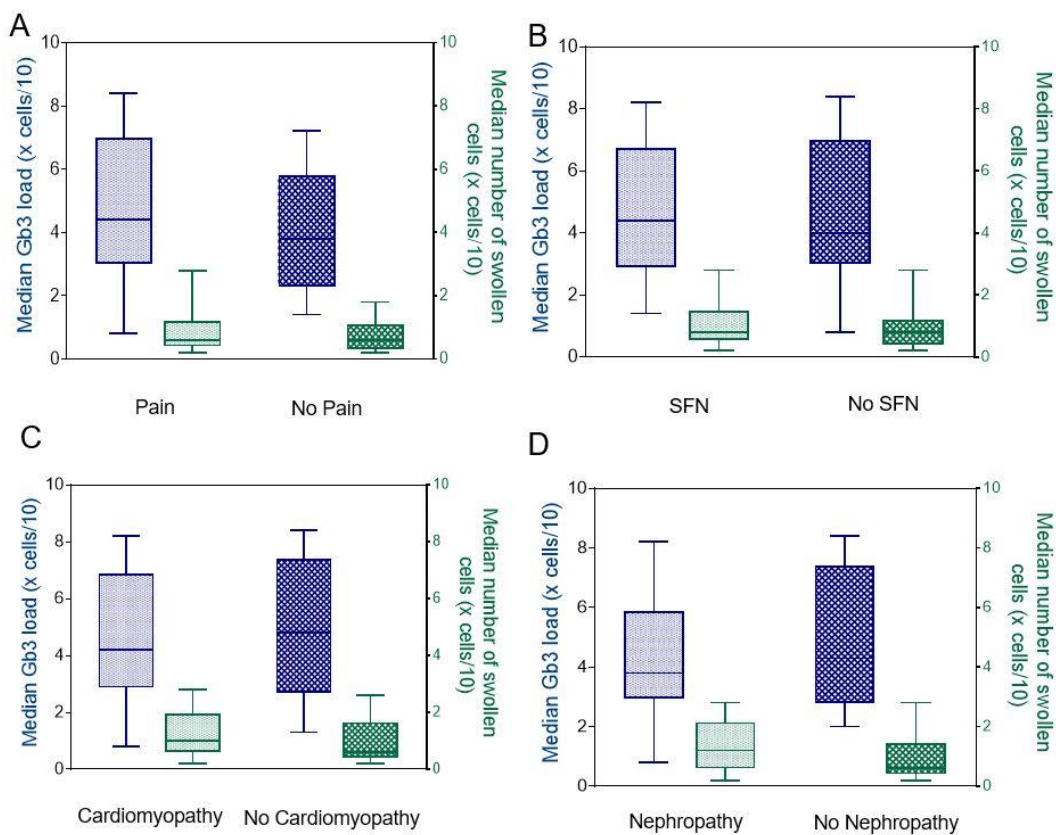


**Figure 9. Median Gb3 load and median number of swollen cells in fibroblasts of different FD subgroups**

Gb3 deposition in FD fibroblasts was shown with monoclonal antibodies against Gb3, and additionally, cell nuclei were visualized with DAPI. The Figure shows that no difference in median Gb3 load (blue box plots) or median number of swollen cells (green box plots) was found when stratifying for different clinical parameters. Abbreviations: DAPI= 4'0.6-diamidin-2-phenylindol; FD=Fabry disease; Gb3=Globotriaosylceramide.

#### 4.1.3.3 Median Gb3 load at different ERT-biopsy intervals

For those patients who received ERT, the time interval between ERT infusion and biopsy was noted to check the impact of Gb3 degradation by ERT. As seen in Fig. 10, this revealed a decrease and re-increase of median Gb3 load in FD fibroblasts over time, depending on the ERT-biopsy interval. If this interval was only one day, the median Gb3 load in the FD fibroblasts was still high. With a four days interval between ERT and biopsy, median Gb3 load was at a very low level, comparable with those of controls (compare with Fig. 8c, right box plot). However, when the interval grew again, median Gb3 load re-increased over time, and reached similar amounts as with a one day interval at a 12-13 days interval. At an 18-days interval, median Gb3 load had grown even higher.

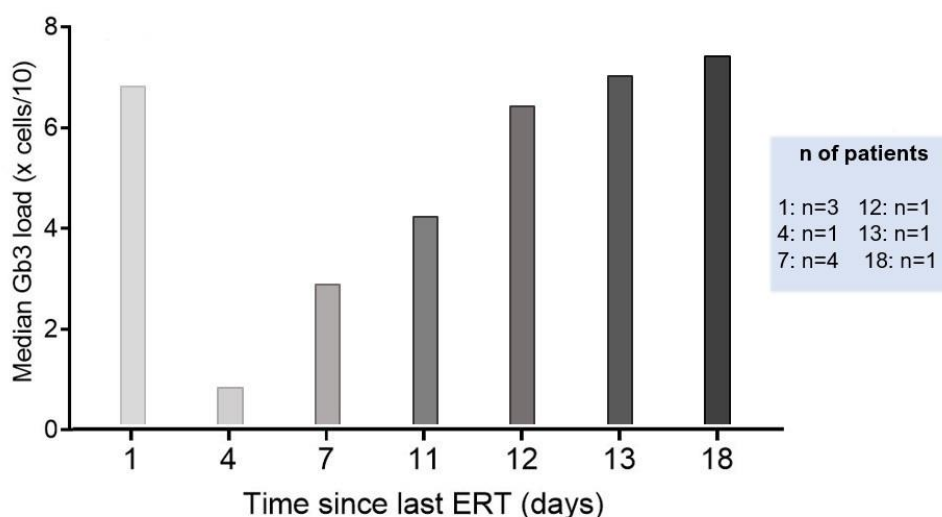


**Figure 10. Median Gb3 load at different ERT-biopsy intervals**

Gb3 deposition in FD fibroblasts was shown with monoclonal antibodies against Gb3, and additionally, cell nuclei were visualized with DAPI. Median Gb3 load was analyzed semi-quantitatively by a blinded investigator calculating the Gb3 deposits in ten cells in five equal regions of the coverslip. The Figure illustrates that median Gb3 load varies with different ERT-biopsy intervals. When this interval was short, median Gb3 load was still high. As the interval grew, median Gb3 load decreased initially and then slowly re-increased with greater intervals, reaching levels similar as with a one day interval at a 12-13 days interval and exceeding this level at an 18-days interval. Abbreviations: DAPI = 4',6-diamidin-2-phenylindol; ERT=Enzyme replacement therapy; FD=Fabry disease; Gb3=Globotriaosylceramide; n=number of patients.

#### 4.1.3.4 Median Gb3 load in two consecutive biopsies of two male FD patients

To confirm the observations of section 4.1.3.3, two FD patients received consecutive biopsies at two different ERT-biopsy intervals. Fig. 11 shows that both in the first patient (Fig. 11a) and in the second patient (Fig. 11b), median Gb3 load was higher in fibroblasts of second biopsy, taken after a greater ERT-biopsy interval.

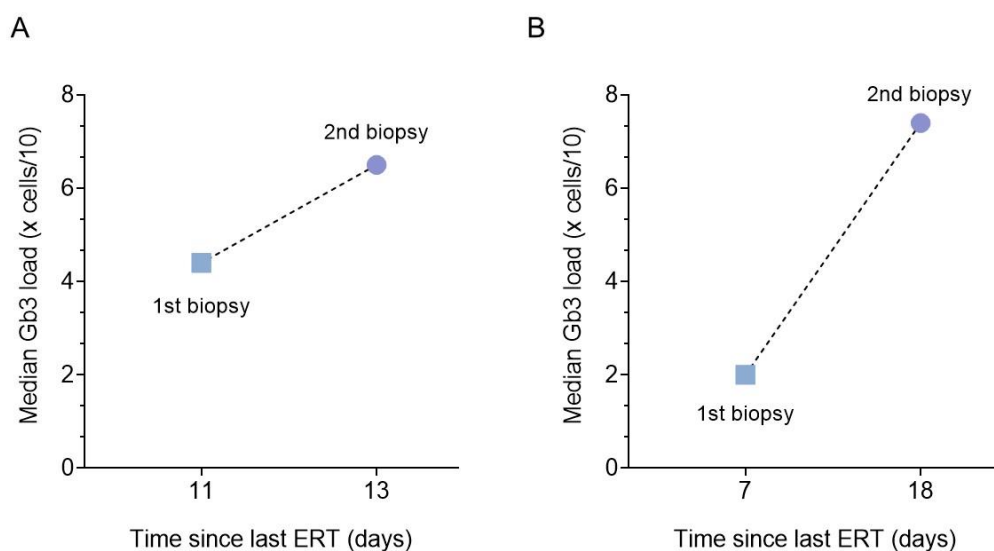


**Figure 11. Median Gb3 load in two consecutive biopsies**

Gb3 deposition in FD fibroblasts was shown with monoclonal antibodies against Gb3, and additionally, cell nuclei were visualized with DAPI. Median Gb3 load was analyzed semi-quantitatively by a blinded investigator calculating the Gb3 deposits in ten cells in five equal regions of the coverslip. A) In the fibroblasts of first patient, median Gb3 load was higher in second biopsy with a greater ERT-biopsy interval. B) Also in the fibroblasts of the second patient, median Gb3 load was higher in second biopsy with a greater ERT-biopsy interval. Abbreviations: DAPI = 4'-6-diamidin-2-phenylindol; ERT=Enzyme replacement therapy; FD=Fabry disease; Gb3=Globotriaosylceramide.

#### **4.1.4 Patch-clamp analysis**

##### **4.1.4.1 Description of the measured current**

To investigate electrical characteristics of dermal fibroblasts, patch-clamp technique was applied using whole-cell recordings. Fig. 12 shows that at baseline conditions, only unspecific electrical activity was measured (Fig. 12a) which did not change substantially upon application of a variety of channel blockers (for list please refer to Table 4). However, after increasing the intracellular  $\text{Ca}^{2+}$  concentration, a current was observed that was only active over +20 mV (Fig. 12b-c). Application of tetraethylammonium (TEA) induced a reduction of current density, indicating that the channel in question was a  $\text{Ca}^{2+}$  activated  $\text{K}^{+}$ -Channel. To further specify the channel, blockers of  $\text{Ca}^{2+}$  activated  $\text{K}^{+}$ -Channels were applied. While 4-[[3-(trifluoromethyl)phenyl]methyl]-2H-1,4-benzothiazin-3(4H)-one (NS6180) and 1-[(2-chlorophenyl)diphenylmethyl]-1H-pyrazole (TRAM 34) had no effect (Fig. 12d-e), application of charybdotoxin (ChTX) lead to reduction of current amplitude (Fig. 12f). These observations taken together lead to the conclusion that the channel in question was a  $\text{Ca}^{2+}$  activated  $\text{K}^{+}$ -Channel 1.1 ( $\text{K}_{\text{Ca}1.1}$ ).



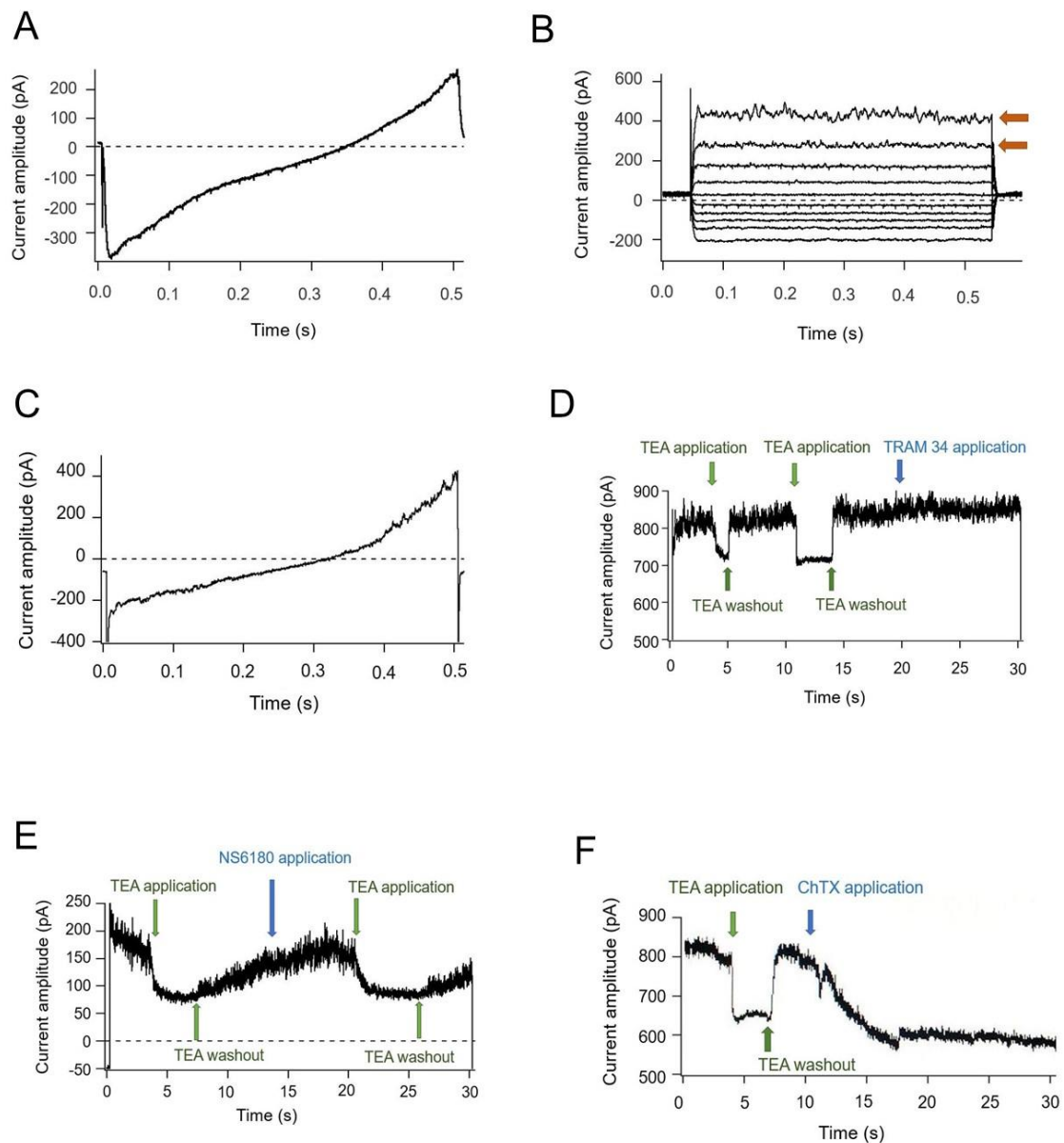


**Figure 12. Characterization of  $K_{Ca1.1}$  channel in dermal fibroblasts**

To investigate electrical characteristics of dermal fibroblasts, patch-clamp technique was applied using whole-cell recordings. A) Unspecific electric activity at baseline condition. B) Currents measured at different holding potentials and under increased intracellular  $Ca^{2+}$  conditions. In the depolarizing range, electric activity was elevated (arrows). C) Current under increased intracellular  $Ca^{2+}$  conditions. D-F) Continuous recording during application of 5mM TEA, 100  $\mu$ M TRAM 34, 5  $\mu$ M NS6180, and 100 nM ChTX, showing decrease of current amplitude upon TEA and ChTX application, but no effect of TRAM 34. Abbreviations: ChTX=Charybodotoxin; NS6180=4-[[3-(trifluoromethyl)phenyl]methyl]-2H-1,4-benzothiazin-3(4H)-one; TEA=tetraethylammonium; TRAM34=1-[(2-chlorophenyl)diphenylmethyl]-1H-pyrazole.

#### 4.1.4.2 Functional difference of K<sub>Ca</sub>1.1 between FD and healthy control fibroblasts

Following the characterization of K<sub>Ca</sub>1.1 in dermal fibroblasts, the channel's function was analyzed in both FD and healthy control fibroblasts. Fig.13 shows current densities under different experimental conditions: in untreated fibroblasts, current density of K<sub>Ca</sub>1.1 was lower in FD fibroblasts compared to healthy controls ( $p<0.01$ ). However, after incubation with agalsidase- $\alpha$ , current density increased dramatically, reaching a level that was 7-fold higher than those of control fibroblasts ( $p<0.01$ ).

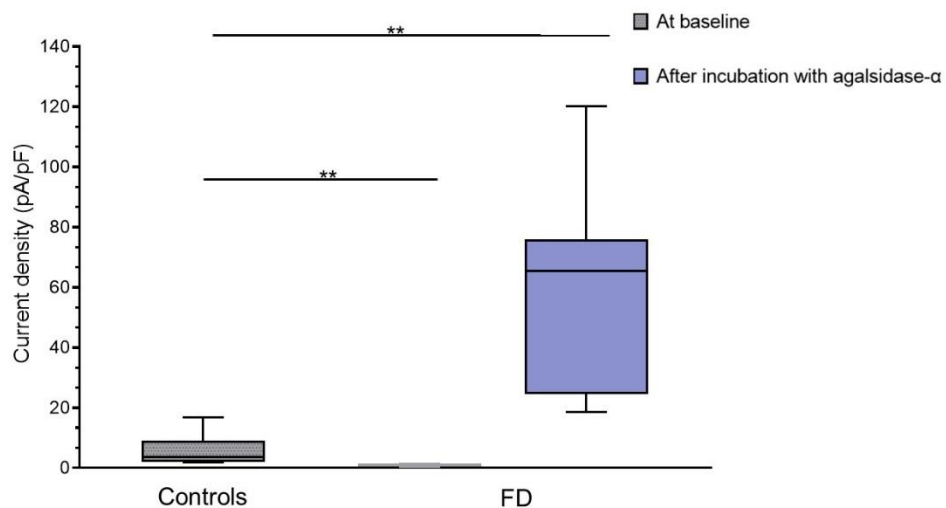


**Figure 13. K<sub>Ca</sub>1.1 function in FD and control fibroblasts**

Patch-clamp technique was applied on dermal fibroblasts of FD and control fibroblasts. FD fibroblasts were incubated with 1.32  $\mu\text{g/ml}$  agalsidase- $\alpha$  for 24h. The Figure demonstrates that K<sub>Ca</sub>1.1 current density was lower in FD fibroblasts than in controls at baseline, but increased over-proportionally upon incubation with agalsidase- $\alpha$ , reaching 7-fold the level of control current density. Abbreviations: FD=Fabry disease; K<sub>Ca</sub>1.1= Ca<sup>2+</sup>-activated K<sup>+</sup>-channel 1.1. \*\* $p<0.01$ .

#### 4.1.5 Gene and protein expression of K<sub>Ca</sub>1.1 in fibroblasts of FD patients and healthy controls

To investigate the mechanisms underlying the observations described in section 4.1.4.2, the gene expression of K<sub>Ca</sub>1.1 channel (encoded by the potassium calcium-activated channel subfamily-M- $\alpha$ -1-gene) and its protein concentration were analyzed. Fig. 14 shows that both gene expression (Fig. 14a) and protein concentration (Fig. 14b) of the K<sub>Ca</sub>1.1 channel were higher in FD fibroblasts than in healthy controls ( $p < 0.05$  for both).

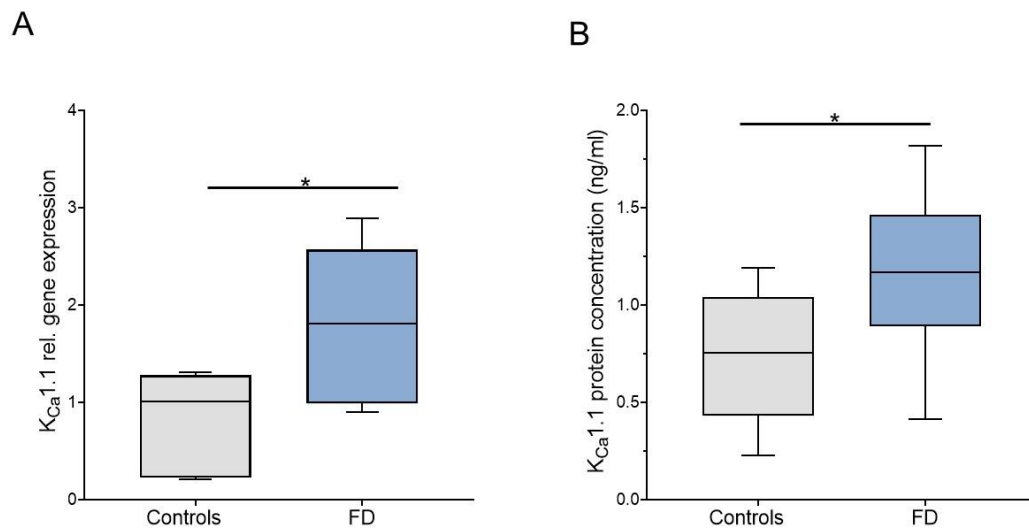


**Figure 14. K<sub>Ca</sub>1.1 gene and protein expression in FD and control dermal fibroblasts**

K<sub>Ca</sub>1.1 gene expression analysis was performed on dermal fibroblasts using qRT-PCR, K<sub>Ca</sub>1.1 protein concentration was measured with an ELISA. A) K<sub>Ca</sub>1.1 gene expression was higher in FD fibroblasts than in control fibroblasts. B) K<sub>Ca</sub>1.1 protein concentration was also higher in FD fibroblasts when compared to those of controls. Abbreviations: ELISA = enzyme-linked immunosorbent assay; FD = Fabry disease; K<sub>Ca</sub>1.1 = Ca<sup>2+</sup>-activated K<sup>+</sup>-channel 1.1; qRT-PCR = quantitative real-time PCR. \* $p < 0.05$ .

#### **4.1.6 Gene expression of various cytokines and chemokines in fibroblasts of FD patients and healthy controls**

To further investigate the role of fibroblasts in FD-associated pain, the gene expression of several cytokines and chemokines was analyzed in fibroblasts of FD patients and healthy controls (kindly refer to Fig. 4 for case selection) before and after stimulation with TNF and IFN $\gamma$ , respectively (Fig. 15).

##### Notch 1:

Notch1 gene expression was higher in FD patients than in healthy controls prior to and after stimulation with TNF (Fig. 15a;  $p < 0.05$  each).

##### CCL2:

CCL2 gene expression was higher in FD patients when compared to healthy controls before and after stimulation with TNF (Fig. 15b;  $p < 0.05$  each).

##### TGF- $\beta$ 1:

Unlike Notch 1 and CCL2, gene expression of TGF- $\beta$ 1 did not differ between FD patients and healthy controls at baseline. However, after stimulation with TNF, gene expression of TGF- $\beta$ 1 was higher in FD patients than in healthy controls (Fig. 15c;  $p < 0.05$ ).

##### IFN $\gamma$ :

Fig. 15d demonstrates the amount of samples with detectable IFN $\gamma$  gene expression. No IFN $\gamma$  gene expression could be measured in any sample of healthy controls, neither before nor after stimulation with TNF. Among the samples of FD patients, IFN $\gamma$  gene expression was detected in 40% of samples before and in 70% of samples after stimulation with TNF. Since IFN $\gamma$  gene expression could not be measured in any healthy control, no calibrator could be determined, hindering the usual data analysis with the  $\Delta\Delta C_t$  method. However, data allowed a  $\chi^2$  test that showed that IFN $\gamma$  gene expression differed between FD patients and healthy controls before and after stimulation with TNF ( $p < 0.05$  each).

## TNF:

No difference in TNF gene expression was detected when comparing FD patients and healthy controls, neither before nor after stimulation with IFN $\gamma$  (Fig. 15e).

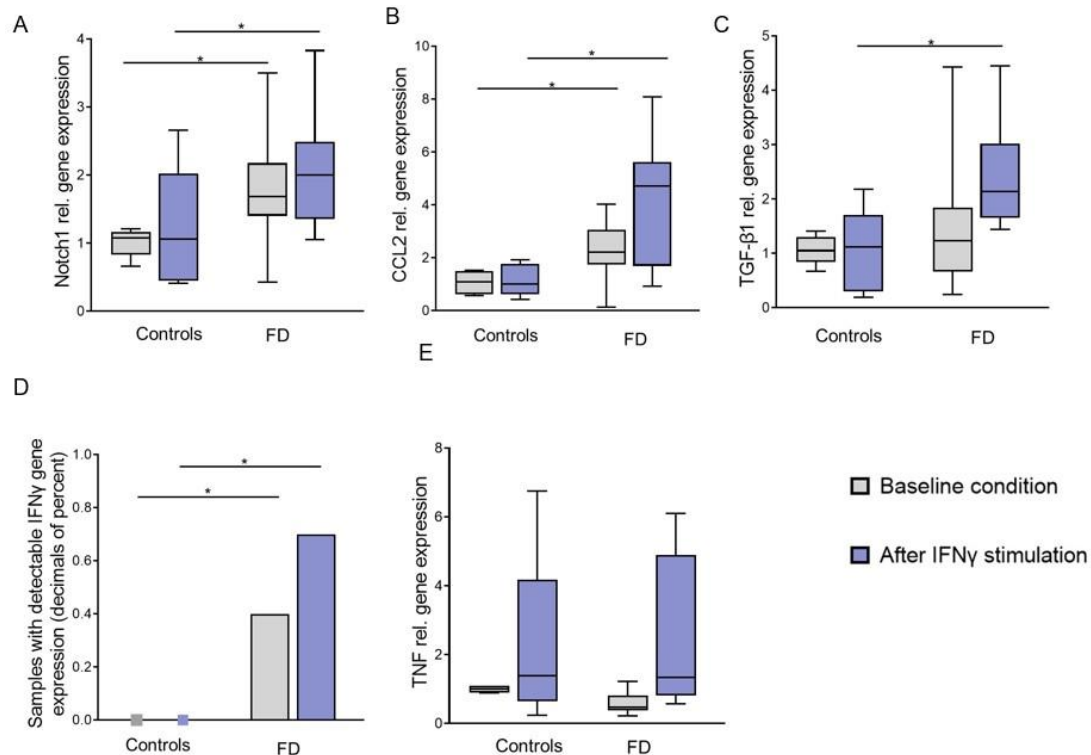


**Figure 15. Gene expression of various cytokines and chemokines in FD and control fibroblasts**

Gene expression analysis was performed on dermal fibroblasts using qRT-PCR. For stimulation experiments, fibroblasts were incubated with 500U TNF or IFN $\gamma$  (the latter only for measurement of TNF gene expression) for 24h. A-B) Notch 1 and CCL2 gene expression were higher in FD fibroblasts when compared to control fibroblasts, both before and after stimulation with TNF. C) TGF- $\beta$ 1 gene expression was only higher in FD fibroblasts than in control fibroblasts after TNF stimulation. D) IFN $\gamma$  was expressed in more samples of FD patients compared to healthy controls, both before and after TNF stimulation. E) TNF gene expression did not differ between FD and control fibroblasts, neither before nor after stimulation with IFN $\gamma$ . Abbreviations: CCL2= chemokine C-C motif ligand 2; FD = Fabry disease; IFN $\gamma$ =Interferon- $\gamma$ ; qRT-PCR = quantitative real-time PCR; Notch1= transmembrane receptors notch homolog 1; TNF= Tumor necrosis factor  $\alpha$ . TGF- $\beta$ =transforming growth factor- $\beta$ 1. \*p<0.05.

#### 4.1.7 Analysis of pNF- $\kappa$ B p65 in fibroblasts of FD patients and healthy controls pre- and post-TNF stimulation

To further comprehend the cytokine expression pathways in dermal fibroblasts, activation of NF- $\kappa$ B to pNF- $\kappa$ B p65 was analyzed using Western Blot before and after stimulation with TNF. Fig.16 depicts Western Blot bands and shows that NF- $\kappa$ B (Fig. 16a) and pNF- $\kappa$ B p65 (Fig. 16b) were detectable, but varying in intensity in all samples, while loading control  $\alpha$ -actin was detectable in comparable amounts in all samples.

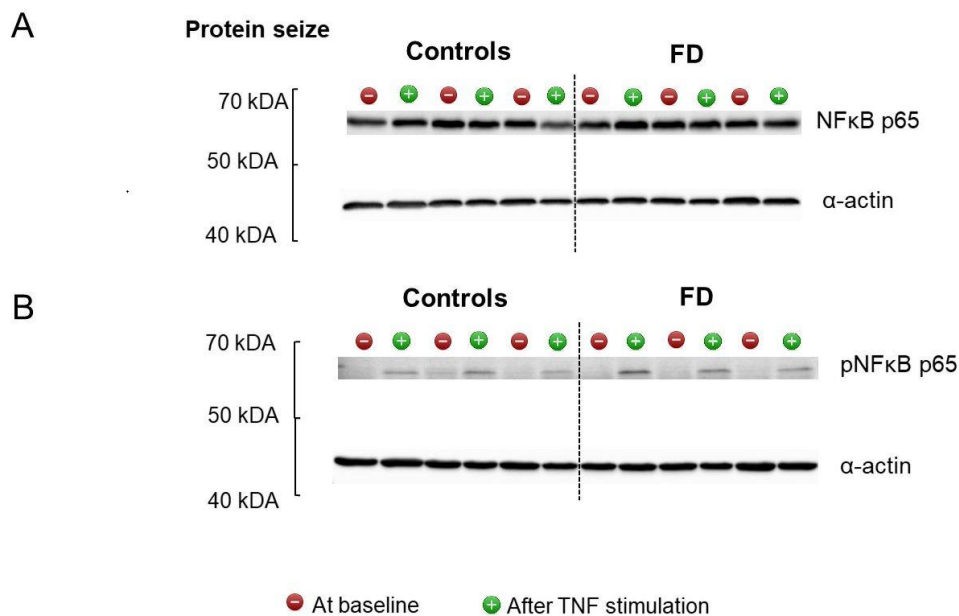


**Figure 16. Western Blot analysis for NF- $\kappa$ B p65 in dermal fibroblasts**

Western Blot analysis was performed with dermal fibroblasts of FD patients and healthy controls before and after stimulation with TNF using antibodies against NF- $\kappa$ B, pNF- $\kappa$ B p65 and  $\alpha$ -actin. A) Western Blot bands of NF- $\kappa$ B and loading control  $\alpha$ -actin. B) Western Blot bands of pNF- $\kappa$ B and loading control  $\alpha$ -actin. Abbreviations: FD = Fabry disease; NF $\kappa$ B p65 = nuclear factor kappa-light-chain-enhancer of activated B-cells p65; pNF $\kappa$ B p65= phosphorylated NF $\kappa$ B p65; TNF= tumor necrosis factor- $\alpha$ .

As seen in Fig. 17, the analysis showed that the median pNF- $\kappa$ B/NF- $\kappa$ B p65 ratio was low at baseline conditions in FD and control fibroblasts (0.018 in FD fibroblasts vs 0.030 in control fibroblasts). After TNF stimulation, median pNF- $\kappa$ B/ NF- $\kappa$ B p65 ratio rose by factor 24 in FD fibroblast (to 0.441) and factor 13 in control fibroblasts (to 0.380). Hence, increase in pNF- $\kappa$ B/ NF- $\kappa$ B p65 ratio in FD fibroblasts was almost twice as much as in control fibroblasts. Due to the low number of samples (n=3 in each subgroup), this observation failed to reach statistical significance.

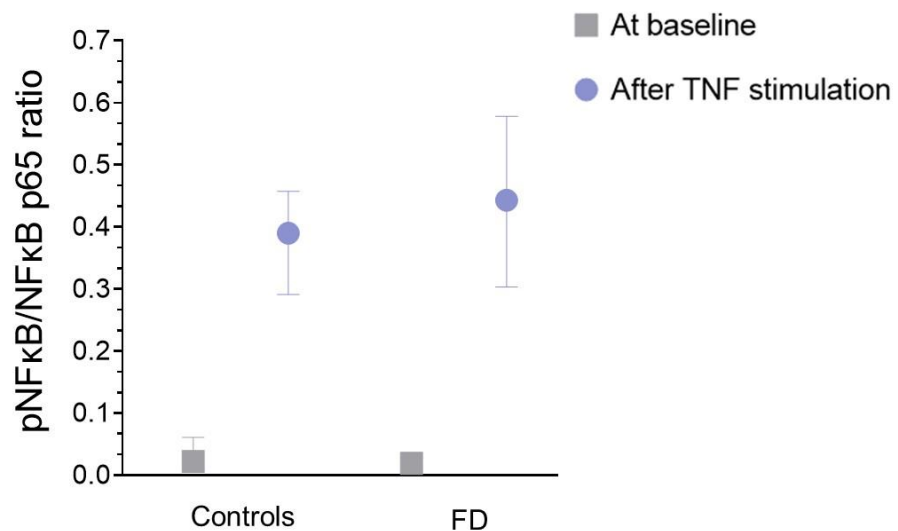


**Figure 17. Analysis of median pNF- $\kappa$ B/NF- $\kappa$ B p65 in Western Blot**

Western Blot analysis was performed with dermal fibroblasts of FD patients and healthy controls before and after stimulation with TNF using antibodies against NF- $\kappa$ B, pNF- $\kappa$ B p65 and  $\alpha$ -actin (loading control). The Figure shows the median pNF- $\kappa$ B/ NF- $\kappa$ B p65 ratio which was low in both groups at baseline conditions, but rose after TNF stimulation. In FD fibroblast, increase in median pNF- $\kappa$ B/ NF- $\kappa$ B p65 ratio was almost twice as much in control fibroblasts. Abbreviations: FD = Fabry disease; NF $\kappa$ B p65 = nuclear factor kappa-light-chain-enhancer of activated B-cells p65; pNF $\kappa$ B p65= phosphorylated NF $\kappa$ B p65; TNF = tumor necrosis factor- $\alpha$ .

## 4.2 Study II

### 4.2.1 Epidemiology

80 FD patients took part in Study II of whom 32 were men and 48 were women. The median age was 52 [20-77] years (47 [21-68] years among men; 53 [20-77] years among women).

### 4.2.2 Genetic characterization of the study cohort

#### 4.2.2.1 Frequency of classical and non-classical mutations in the study cohort - separated by sex

For both FD men and women, the slender majority the patients carried a mutation predictably leading to a classical phenotype, as seen in Table 8.

**Table 8. Percent distribution of classical and non-classical FD mutations in the study cohort, separated by sex**

| Mutation               | N of patients carrying the mutation |             |
|------------------------|-------------------------------------|-------------|
|                        | M                                   | F           |
| Classical mutation     | 17/32 (53%)                         | 27/48 (56%) |
| Non-classical mutation | 15/32 (47%)                         | 21/48 (44%) |

Abbreviation: n=number.

#### 4.2.2.2 AAE location types in $\alpha$ -GalA 3D-structure

##### 4.2.2.2.1 *Frequency of AAE location types as wells as the frequency of each individual mutation*

Among both FD men (1/32, 3%) and women (3/48, 6%), active site mutations occurred by far to the rarest (overall 4/80, 5%). Buried and other mutations were found in comparable numbers (buried mutations: 35/80, 41% overall; 12/32,



41% men; 22/48, 46% women vs other mutations: 41/80, 51% overall; 18/32, 56% men; 23/48, 48% women). Table 9 summarizes the frequency of the location types as well as that of each individual mutation. Overall, 25 different mutations were found and distributed as follows:

- one active site mutation
- 16 different buried mutations
- eight different other mutations.

**Table 9. AAE location type of the individual mutations and their frequency**

| Mutation             |                             | N of patients |             |
|----------------------|-----------------------------|---------------|-------------|
| Nucleotid exchange   | Amino acid exchange (abbr.) | M             | F           |
| Active site mutation |                             | 1/32 (3%)     | 3/48 (6%)   |
| c.515G>A             | p.Cys172Tyr (C172Y)         | 1 (3%)        | 3 (6%)      |
| Buried mutations     |                             | 13/32 (41%)   | 22/48 (46%) |
| c.202C>T             | p.Leu68Phe (L68F)           | 1 (3%)        |             |
| c.334C>T             | p.Arg112Cys (R112C)         |               | 1 (2%)      |
| c.386T>C             | p.Leu129Pro (L129P)         | 2 (6%)        | 2 (4%)      |
| c.404C>T             | p.Ala135Val (A135V)         | 2 (6%)        | 5 (10%)     |
| c.408T>A             | p.Asp136Glu (D136E)         | 1 (3%)        | 2 (4%)      |
| c.471T>G             | p.Gln157His (Q157H)         |               | 1 (2%)      |
| c.484T>G             | p.Trp162Gly (W162G)         | 1 (3%)        | 1 (2%)      |
| c.486G>T             | p.Trp162Cys (W162C)         | 1 (3%)        |             |
| c.559A>G             | p.Met187Val (M187V)         |               | 1 (2%)      |
| c.708G>C             | p.Trp236Cys (W236C)         | 1 (3%)        | 2 (4%)      |
| c.784T>C             | p.Trp262Arg (W262R)         | 1 (3%)        |             |
| c.806T>G             | p.Val269Gly (V269G)         |               | 1 (2%)      |
| c.860G>C             | p.Trp287Ser (W287S)         |               | 1 (2%)      |
| c.1021G>A            | p.Glu341Lys (E341K)         | 1 (3%)        |             |
| c.1025G>T            | p.Arg342Leu (R342L)         | 2 (6%)        | 3 (6%)      |
| c.1250T>G            | p.Leu471Arg (L417P)         |               | 2 (6%)      |
| Other mutations      |                             | 18/32 (56%)   | 23/48 (48%) |
| c.155G>C             | p.Cys52Ser (C52S)           |               | 1 (2%)      |
| c.188G>A             | p.Cys63Tyr (C63Y)           | 1 (3%)        | 1 (2%)      |
| c.416A>G             | p.Asn139Ser (N139S)         | 3 (9%)        | 2 (4%)      |
| c.427G>A             | p.Ala143Thr (A143T)         |               | 4 (8%)      |
| c.644A>G             | p.Asn215Ser (N215S)         | 13 (39%)      | 10 (20%)    |
| c.902G>A             | p.Arg301Gln (R301Q)         |               | 3 (6%)      |
| c.963G>C             | p.Gln321His (Q321H)         | 1 (3%)        | 1 (2%)      |
| c.973G>A             | p.Gly325Ser (G325S)         |               | 1 (2%)      |

Abbreviation: abbr.=abbreviation; n=number.

#### 4.2.2.2.2 Illustration of AAEs in the $\alpha$ -GalA 3D-structure

Each individual mutation was mapped in the  $\alpha$ -GalA 3D-structure and depicted along with the fellow mutations of the same AAE location type. Fig. 18 presents all occurring mutations in the study cohort, grouped by AAE location type.

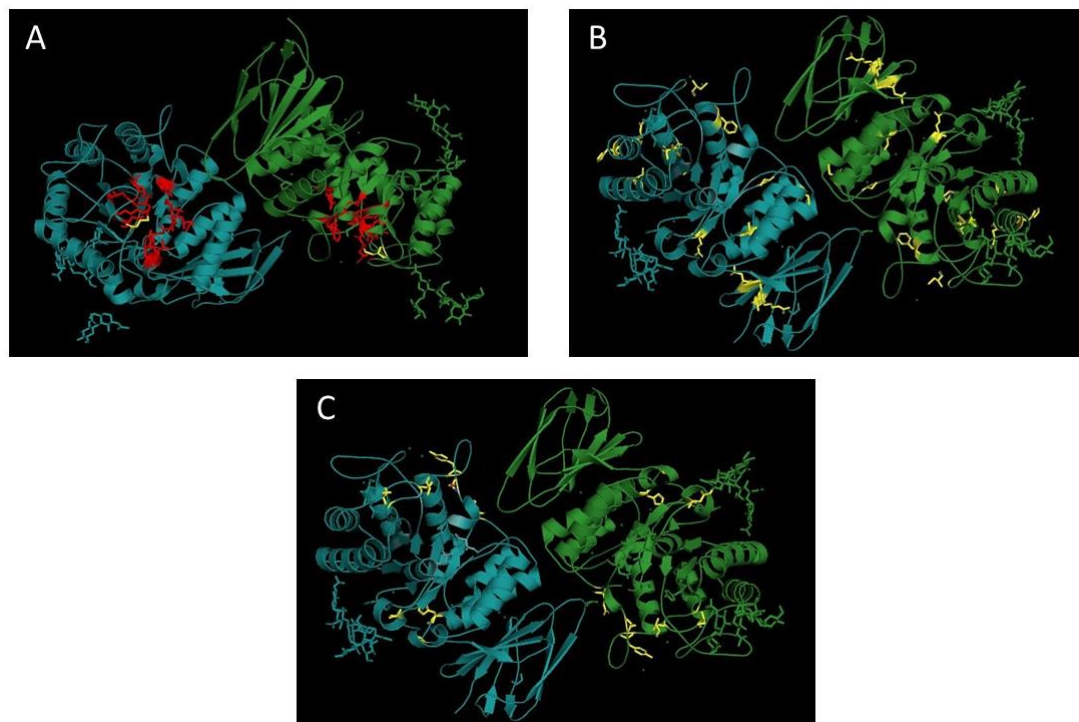


**Figure 18. AAE location types in the  $\alpha$ -GalA 3D-structure**

3D-structure of  $\alpha$ -GalA was downloaded from the PDB Europe into Pymol Graphics System.

A) Active site mutation. The wildtype amino acid residues are marked in red, while the mutated amino acid residue is marked in yellow. B) Buried mutations. The mutated amino acid residues (marked in yellow) can be found in the core of  $\alpha$ -GalA. C) Other mutations. The mutated amino acid residues (marked in yellow) can be found solely on the protein surface, not in the core of  $\alpha$ -GalA. Abbreviation:  $\alpha$ -GalA=  $\alpha$ -Galactosidase A; PDB=Protein databank.

#### 4.2.2.2.3 *Frequency of classical and non-classical mutations in the study cohort separated by AAE location type*

While the frequency of classical and non-classical mutations was comparable when only dividing the study cohort by sex, a different observation was made when dividing the cohort by AAE location type. As demonstrated in Table 10, the active site mutation and the vast majority of buried mutations lead to a classical phenotype, while the majority of other mutations lead to a non-classical phenotype.

**Table 10. Percent distribution of classical and non-classical mutations in the study cohort, separated by AAE location type**

| Mutation                      | AAE location type |             |           |
|-------------------------------|-------------------|-------------|-----------|
|                               | Active site       | Buried      | Other     |
| <b>Classical mutation</b>     | 1/1 (100%)        | 15/16 (94%) | 3/8 (37%) |
| <b>Non-classical mutation</b> | 0/1 (0%)          | 1/16 (6%)   | 5/8 (63%) |

Abbreviation: AAE=amino acid exchange

### **4.2.3 Clinical characterization of patient subgroups**

#### **4.2.3.1 Clinical characterization of male FD patients**

##### *4.2.3.1.1 Clinical characterization of male patients younger than 35 years ('<35y-group')*

Fig. 19 gives an overview of the symptoms and FD-specific treatment in the male <35y-group.

- Nervous system

While cerebral stroke was rarely seen in patients carrying active site/buried mutations and not at all in those with other mutations, symptoms related to an affection of the PNS such as SFN or anhidrosis/hypohidrosis were found more often, especially among patients with active site/buried mutations. FD-associated pain was only reported by a patient with active site/buried mutations.







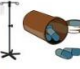
- Inner organs

Cardiomyopathy was more frequent in patients with active site/buried mutations than in those with other mutations, and severe cardiomyopathy was found merely in patients with active site/buried mutations. Nephropathy was less common in this age group, however, both patient groups suffered from overt nephropathy.

- FD-specific therapy

Most patients in this age group were already being treated. All patients with active site/buried mutations were on ERT, while the vast majority of those patients with other mutations was treated with migalastat.

**A**

| Active site/Buried  | ♂ <35y-group   | Other   |
|---|--|---|
| <b>NERVOUS SYSTEM</b>   |  |   |
| <b>Cerebral stroke</b><br>1/3 (33%)   |   | <b>Cerebral stroke</b><br>0/5 (0%)  |
| <b>FD-associated pain</b><br>1/3 (33%)  |   | <b>FD-associated pain</b><br>0/5 (0%)   |
| <b>SFN</b><br>2/3 (67%)   |   | <b>SFN</b><br>1/5 (20%)   |
| <b>Anhidrosis/hypohidrosis</b><br>2/3 (67%)   |   | <b>Anhidrosis/hypohidrosis</b><br>3/5 (60%)   |
| <b>INNER ORGANS</b>   |  |   |
| <b>Cardiomyopathy</b><br>In total: 2/3 (67%)<br>Mild: 1/2 (50%) Severe: 1/2 (50%)         |   | <b>Cardiomyopathy</b><br>In total: 1/5 (20%)<br>Mild: 1/1 (100%) Severe: 0/1 (0%)         |
| <b>Nephropathy</b><br>In total: 1/3 (33%)<br>Incipient: 0/1 (0%) Overt: 1/1 (100%)        |   | <b>Nephropathy</b><br>In total: 1/5 (20%)<br>Incipient: 0/1 (0%) Overt: 1/1 (100%)        |
| <b>FD-SPECIFIC THERAPY</b>  |  |   |
| <b>FD-specific therapy</b><br>In total: 2/3 (67%)<br>ERT: 2/2 (100%) Migalastat: 0/2 (0%) |  | <b>FD-specific therapy</b><br>In total: 4/5 (80%)<br>ERT: 1/4 (25%) Migalastat: 3/4 (75%) |

**B**

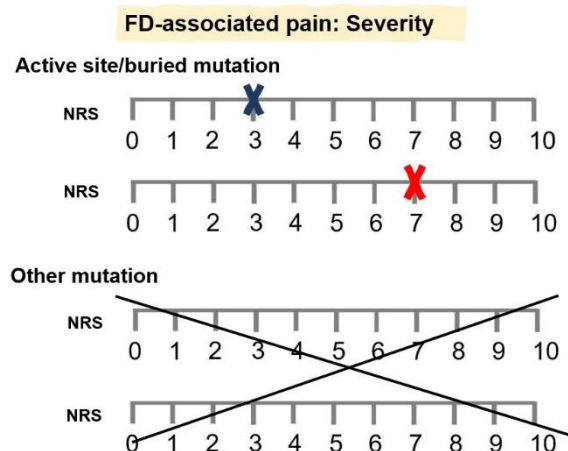


**Figure 19. Clinical characterization of male patients younger than 35 years**

The Figure gives a synopsis of the main symptoms and disease-specific therapy options in FD, comparing patients with active site/buried mutation and other mutation. A) Clinical symptoms. B) Severity of FD-associated pain. Abbreviations: av=average; ERT=Enzyme replacement therapy; FD=Fabry disease; max=maximum; NRS=Numeric rating scale; SFN=Small fiber neuropathy.

#### 4.2.3.1.2 *Clinical characterization of male patients between 35 and 55 years ('35-55y-group')*

Fig. 20 gives an overview of the symptoms and FD-specific treatment in the male 35-55y-group.

- Nervous system

While cerebral stroke was rarely seen also in this age group, affection of the PNS was detectable in many cases. Among patients with active site/buried mutations, SFN and anhidrosis/hypohidrosis were very common, and FD-associated pain was in fact reported by all patients with this AAE location type. These symptoms were found less often in patients with other mutations; moreover, FD-associated pain was less severe.

- Inner organs

Cardiomyopathy was found in all patients with active site/buried mutations and most patients with other mutations. It was severe in all cases of active site/buried mutations, and most of those with other mutations. Once more, nephropathy was less common, but all cases suffered from overt nephropathy.

- FD-specific therapy

Most patients of this age group received FD-specific therapy. All patients with active site/buried mutations were on ERT, while the vast majority of those with other mutations was treated with migalastat.

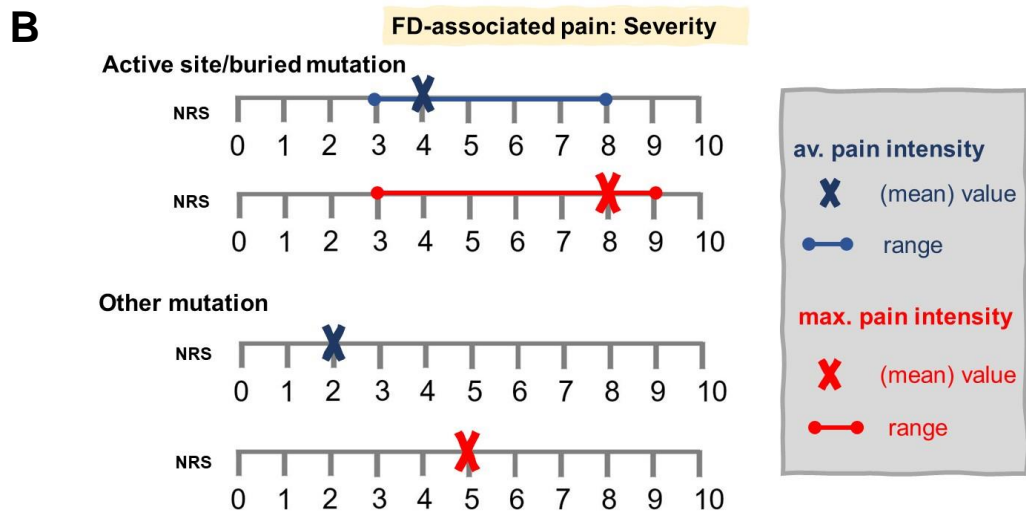
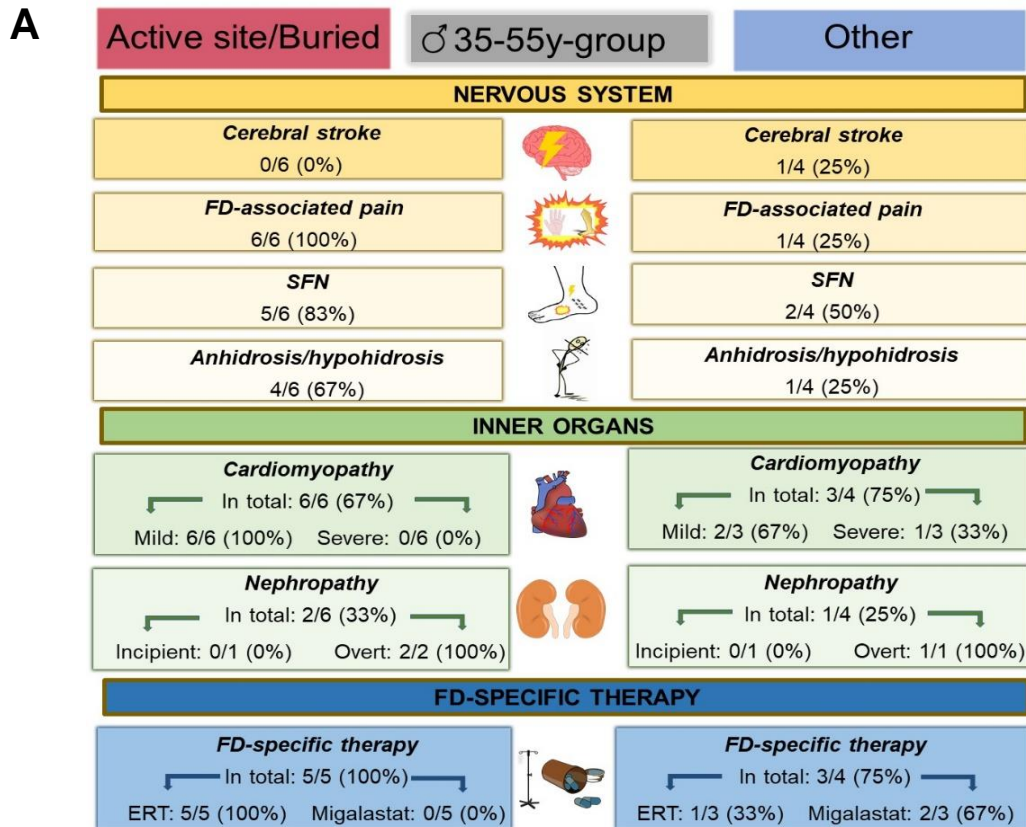


**Figure 20. Clinical characterization of male patients between 35 and 55 years**

The Figure gives a synopsis of the main symptoms and disease-specific therapy options in FD, comparing patients with active site/buried mutation and other mutation. A) Clinical symptoms. B) Severity of FD-associated pain. Abbreviations: av=average; ERT=Enzyme replacement therapy; FD=Fabry disease; max=maximum; NRS=Numeric rating scale; SFN=Small fiber neuropathy.



#### 4.2.3.1.3 *Clinical characterization of male patients older than 55 years ('>55y-group')*

Fig. 21 gives an overview of the symptoms and FD-specific treatment in the male >55y-group.

- Nervous system

While cerebral stroke was rarely seen in patients with active site/buried mutations, affection of the PNS was very common among these patients, concerning all investigated symptoms. Among patients with other mutations, CNS and PNS were affected less often; moreover, FD-associated pain was less severe.

- Inner organs

Cardiomyopathy was found in all patients of this age group, of whom the majority suffered from the severe form. Nephropathy was also common in this age group. Among patients with active site/buried mutations, nephropathy was overt in most cases, while patients with other mutations mainly had an incipient nephropathy.

- FD-specific therapy

All patients with active site/buried mutations and most patients with other mutation received FD-specific therapy. While patients with active site/buried mutations were all on ERT, the vast majority of patients with other mutations was treated with migalastat.

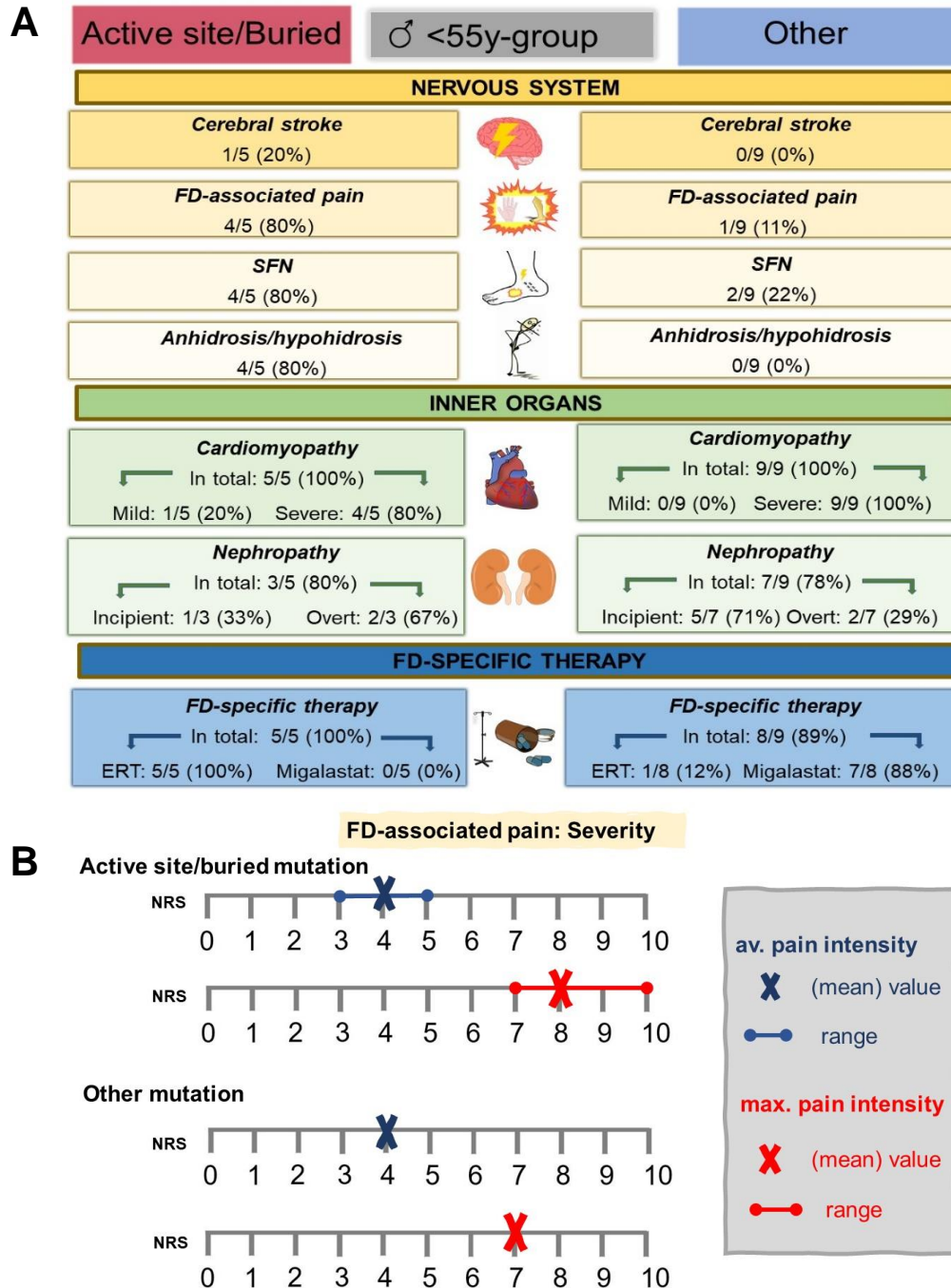


**Figure 21. Clinical characterization of male patients older than 55 years**

The Figure gives a synopsis of the main symptoms and disease-specific therapy options in FD, comparing patients with active site/buried mutation and other mutation. A) Clinical symptoms. B) Severity of FD-associated pain. Abbreviations: av=average; ERT=Enzyme replacement therapy; FD=Fabry disease; max=maximum; NRS=Numerics rating scale; SFN=Small fiber neuropathy.

#### 4.2.3.1.4 *Clinical characterization of all male patients*

Fig. 22 gives an overview of the symptoms and FD-specific treatment of all male FD patients.

- Nervous system

While the CNS was generally rarely affected, an affection of the PNS, manifested as FD-associated pain, SFN, and anhidrosis/hypohidrosis was more frequent in patients with active site/buried mutations. Moreover, FD-associated pain was more severe among these patients.

- Inner organs

Cardiomyopathy was common among men, and in many cases severe. Nephropathy was found in about half of all male patients, with more cases of overt nephropathy among those with active site/buried mutations.

- FD-specific therapy

Most patients received FD-specific therapy; all patients with active site/buried mutations were on ERT, while the majority of those with other mutations received migalstat.

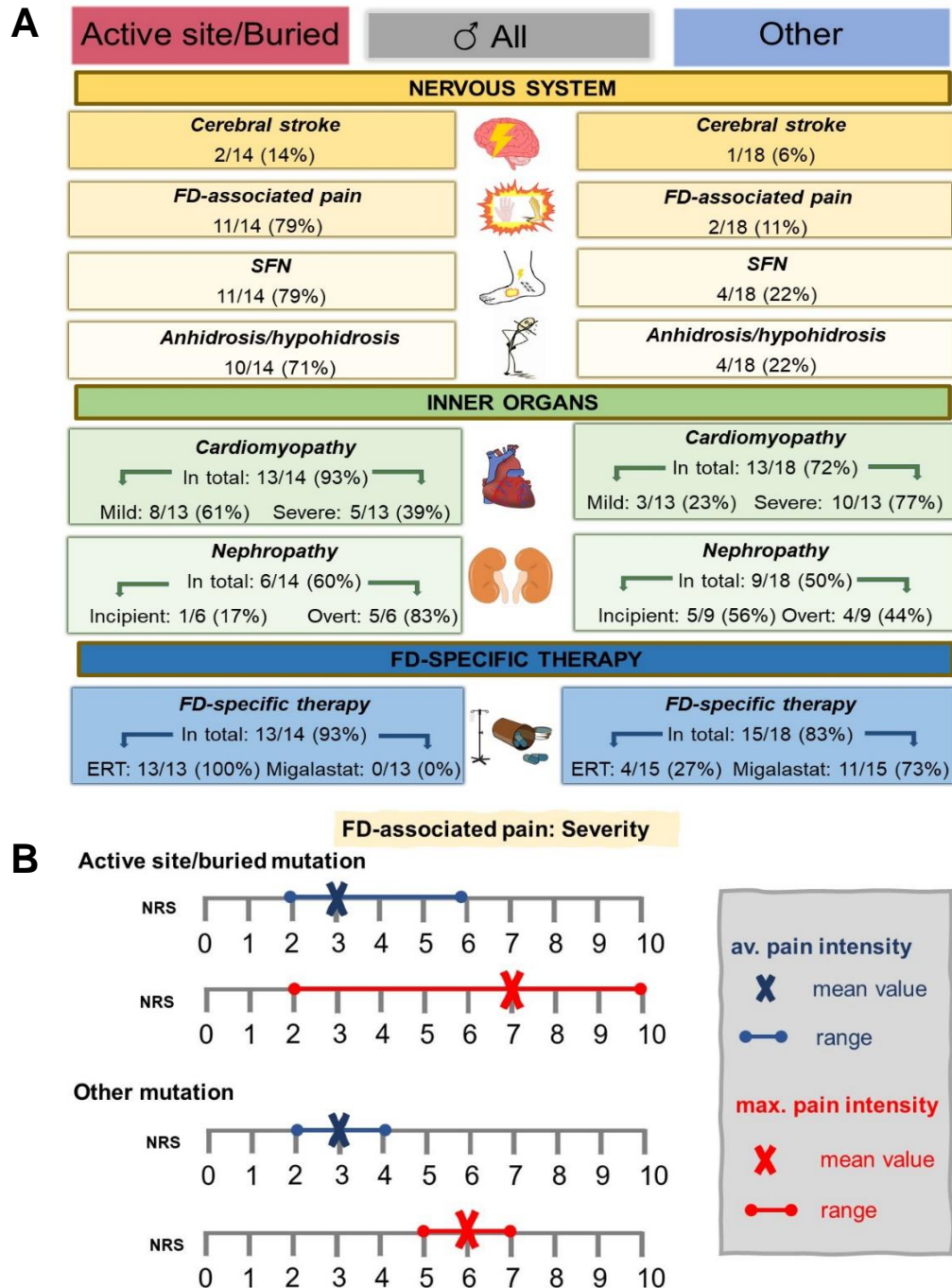


**Figure 22. Clinical characterization of all male patients**

The Figure gives a synopsis of the main symptoms and disease-specific therapy options in FD, comparing patients with active site/buried mutation and other mutation. A) Clinical symptoms. B) Severity of FD-associated pain. Abbreviations: av=average; ERT=Enzyme replacement therapy; FD=Fabry disease; max=maximum; NRS=Numeric rating scale; SFN=Small fiber neuropathy.

#### **4.2.3.2 Clinical characterization of female FD patients**

##### *4.2.3.2.1 Clinical characterization of female patients younger than 35 years (<35y-group)*

Fig. 23 gives an overview of the symptoms and FD-specific treatment in the female <35y-group.

- Nervous system

An affection of the nervous system was not detected among patients with other mutations, and only presented as FD-associated pain in patients with active site/buried mutations. No other symptoms related to an affection of the nervous system were found.

- Inner organs

While cardiomyopathy was not present in any patient of this age group, nephropathy was detected in some cases. In the group with active site/buried mutations, nephropathy was overt, while nephropathy was incipient in the group with other mutations.

- FD-specific therapy

Only one patient with an active/site buried mutation, and no patient with an other mutation received FD-specific therapy; the treated patient was on migalastat.

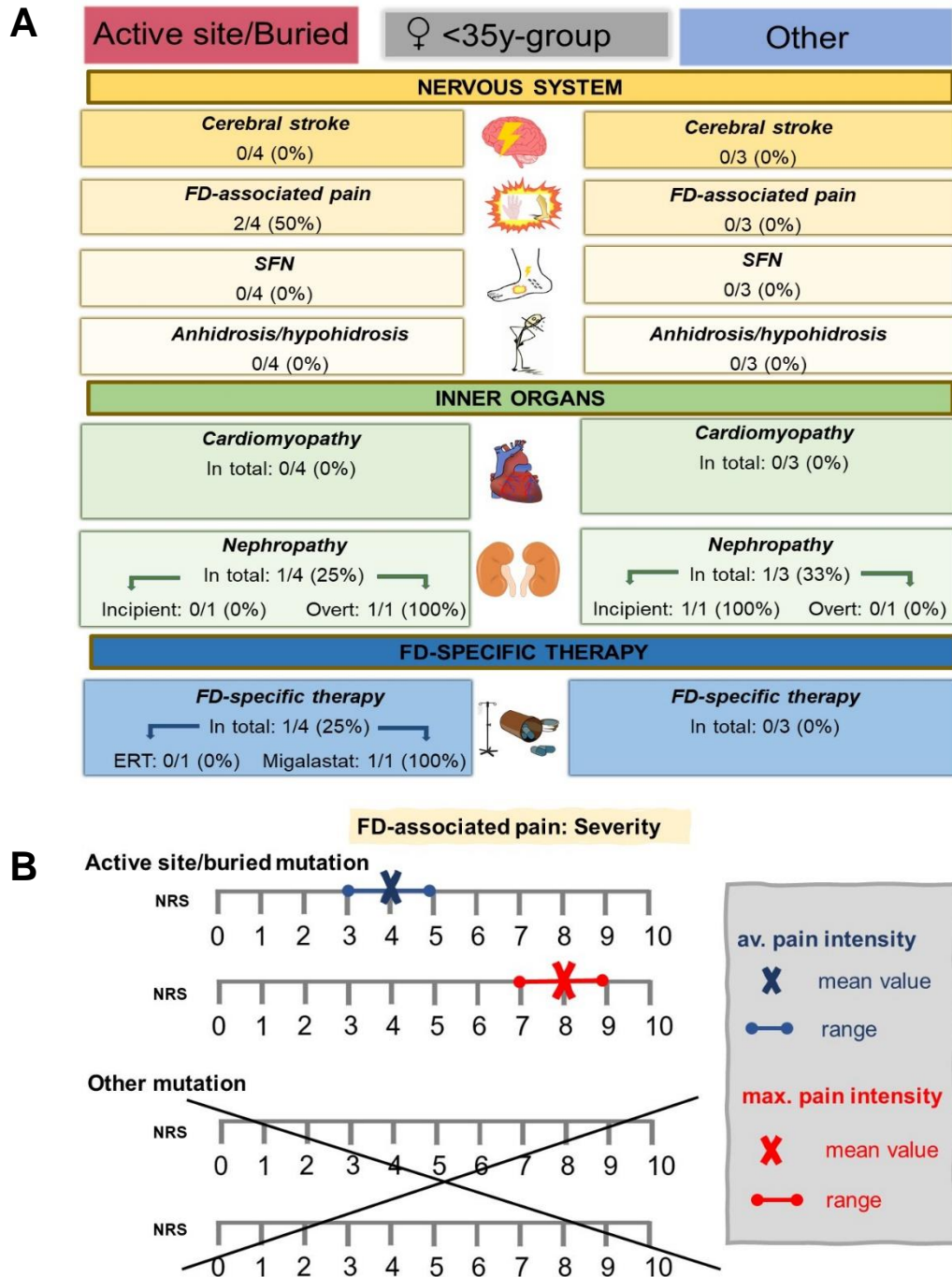


**Figure 23. Clinical characterization of female patients younger than 35 years**

The Figure gives a synopsis of the main symptoms and disease-specific therapy options in FD comparing patients with active site/buried mutations and other mutations. A) Clinical symptoms. B) Severity of FD-associated pain. Abbreviations: av=average; ERT=Enzyme replacement therapy; FD=Fabry disease; max=maximum; NRS=Numeric rating scale; SFN=Small fiber neuropathy.

#### 4.2.3.2.2 *Clinical characterization of female patients between 35 and 55 years ('35-55y-group')*

Fig. 24 gives an overview of the symptoms and FD-specific treatment in the female 35-55y-group.

- Nervous system

Both the CNS and the PNS were affected in less than half of female patients in this age group. However, the PNS was affected in more women with active site/buried mutations than in those with other mutations. FD-associated pain was also more severe in patients with active site/buried mutations.

- Inner organs

Cardiomyopathy was detected in more patients with active site/buried mutations than in those with other mutations. Most patients suffered from severe cardiomyopathy. Over half of the women with active site/buried mutations suffered from nephropathy (in most cases incipient), while none of those patients with other mutations had nephropathy.

- FD-specific therapy

Many patients received FD-specific therapy. More women with active site/buried mutation were treated with ERT than with migalastat, while this was evenly distributed among those patients carrying other mutations.

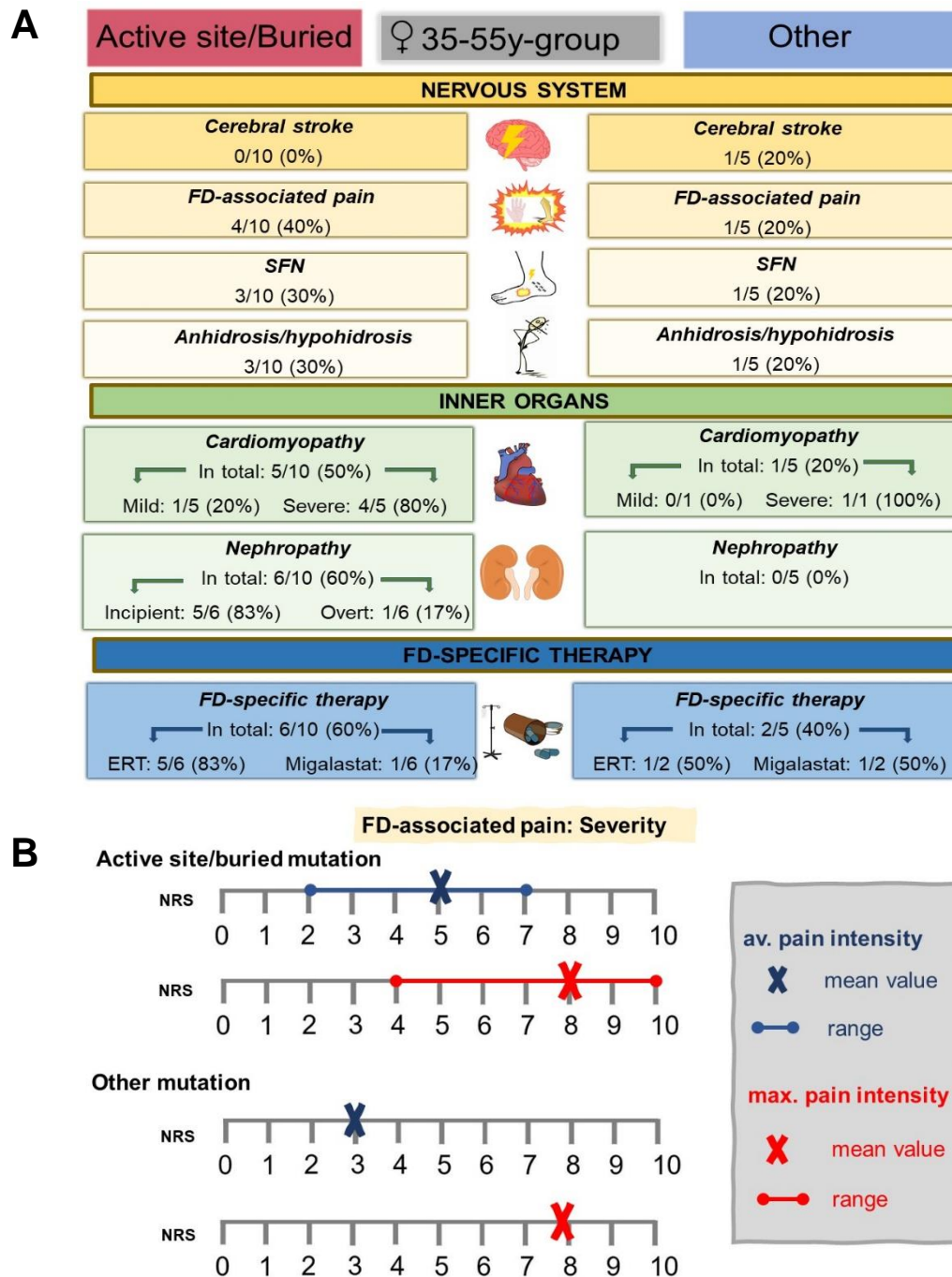


**Figure 24. Clinical characterization of female patients between 35 and 55 years**

The Figure gives a synopsis of the main symptoms and disease-specific therapy options in FD, comparing patients with active site/buried mutations and other mutations. A) Clinical symptoms. B) Severity of FD-associated pain. Abbreviations: av=average; ERT=Enzyme replacement therapy; FD=Fabry disease; max=maximum; NRS=Numeric rating scale; SFN=Small fiber neuropathy.



#### 4.2.3.2.3 *Clinical characterization of female patients older than 55 years ('>55y-group')*

Fig. 25 gives an overview of the symptoms and FD-specific treatment in the female >55y-group.

- Nervous system

While cerebral stroke was rare in among all patients in this subgroup, an affection of the PNS, especially presenting as FD-associated pain and SFN, was more frequent in patients with active site/buried mutations. Also, FD-associated pain was more severe in these patients.

- Inner organs

Cardiomyopathy was detected in almost all patients with active site/buried mutations, and about half of those with other mutations; in most cases, cardiomyopathy was mild. Nephropathy was almost twice as frequent in patients with active site/buried mutations than in those with other mutations, and was incipient in most cases.

- FD-specific therapy

The vast majority of women in this age group received FD-specific therapy. Most women with active site/buried mutations were on ERT, while about each a half of patients with other mutations received ERT and migalastat, respectively.

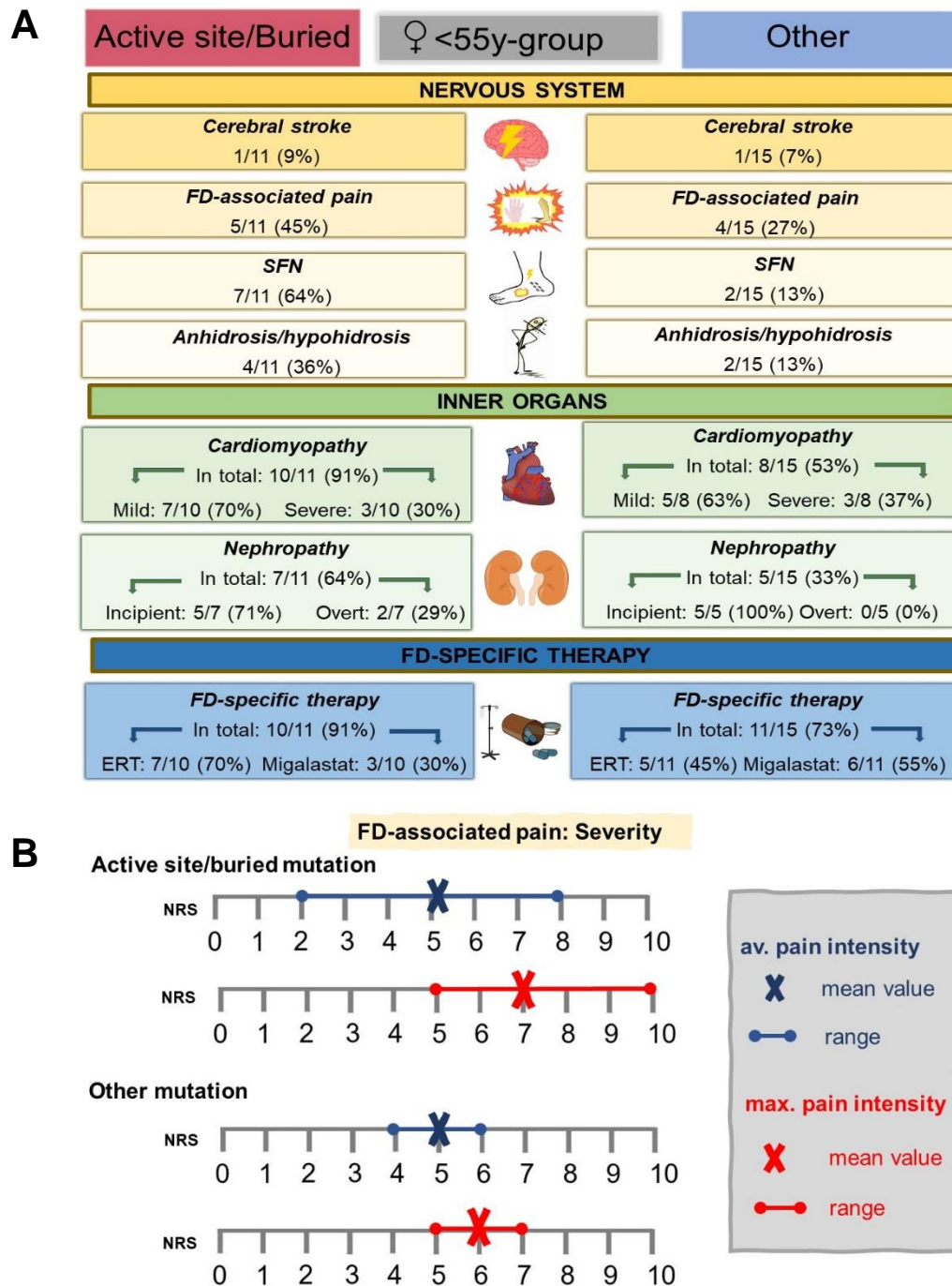


**Figure 25. Clinical characterization of female patients older than 55 years**

The Figure gives a synopsis of the main symptoms and disease-specific therapy options in FD, comparing patients with active site/buried mutation and other mutations. A) Clinical symptoms. B) Severity of FD-associated pain. Abbreviations: av=average; ERT=Enzyme replacement therapy; FD=Fabry disease; max=maximum; NRS=Numeric rating scale; SFN=Small fiber neuropathy.

#### 4.2.3.2.4 Clinical characterization of all female patients

Fig. 26 gives an overview of the symptoms and FD-specific treatment of all female patients.

- Nervous system

While cerebral stroke was generally rare among women, the PNS was affected in more women with active site/buried mutations than in those with other mutations. FD-associated pain was more severe in patients with active site/buried mutations.

- Inner organs

Cardiomyopathy was more common in women with active site/burieds mutation than in those with other mutations. Mild and severe form were evenly distributed. Nephropathy was also found in more patient with active site/burieds mutation. While some women with active site/buried mutations suffered from overt nephropathy, all patients with other mutations had incipient nephropathy.

- FD-specific therapy

The majority of women received FD-specific therapy. While most patients with active site/buried mutations were on ERT, more than half of the women with other mutations received migalastat.

Additionally, when comparing FD men and women, it was apparent that disease onset was later in women than in men (compare Figs. 24 and 28).

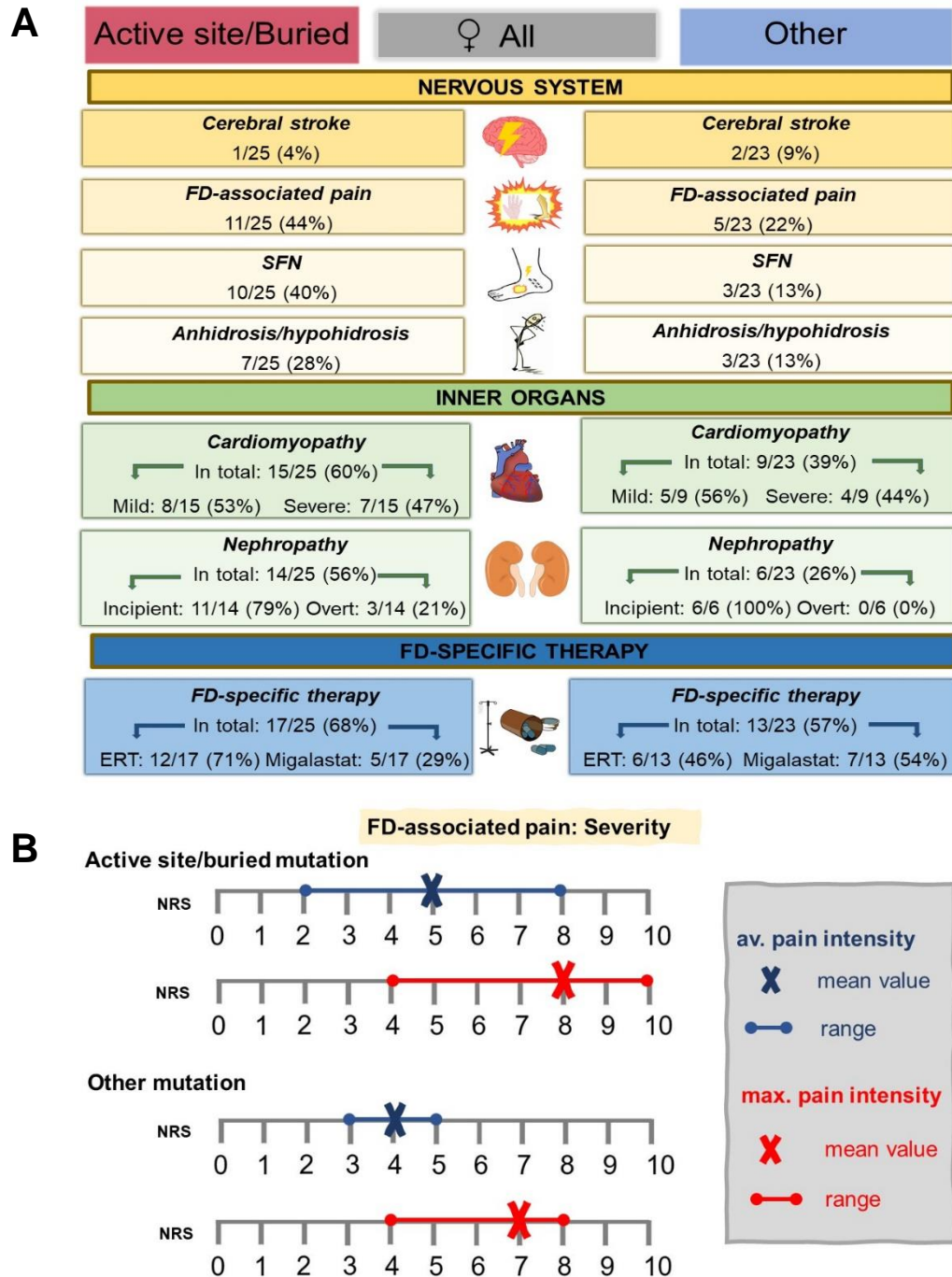


**Figure 26. Clinical characterization of all female patients**

The Figure gives a synopsis of the main symptoms and disease-specific therapy options in FD, comparing patients with active site/buried mutation and other mutations. A) Clinical symptoms. B) Severity of FD-associated pain. Abbreviations: av=average; ERT=Enzyme replacement therapy; FD=Fabry disease; max=maximum; NRS=Numeric rating scale; SFN=Small fiber neuropathy.

#### 4.2.4 $\alpha$ -GalA activity and plasma lyso-Gb3 levels

As seen in Fig. 27, median  $\alpha$ -GalA activity was lower in both male and female patients with active site/buried mutations when compared to those with other mutations (Fig. 27a;  $p<0.01$  for men;  $p<0.05$  for women). In line with these results, plasma lyso-Gb3 levels were higher in both male and female patients with active site/buried mutation than in those with buried mutation (Fig 27b;  $p<0.01$  for men;  $p<0.05$  for women).

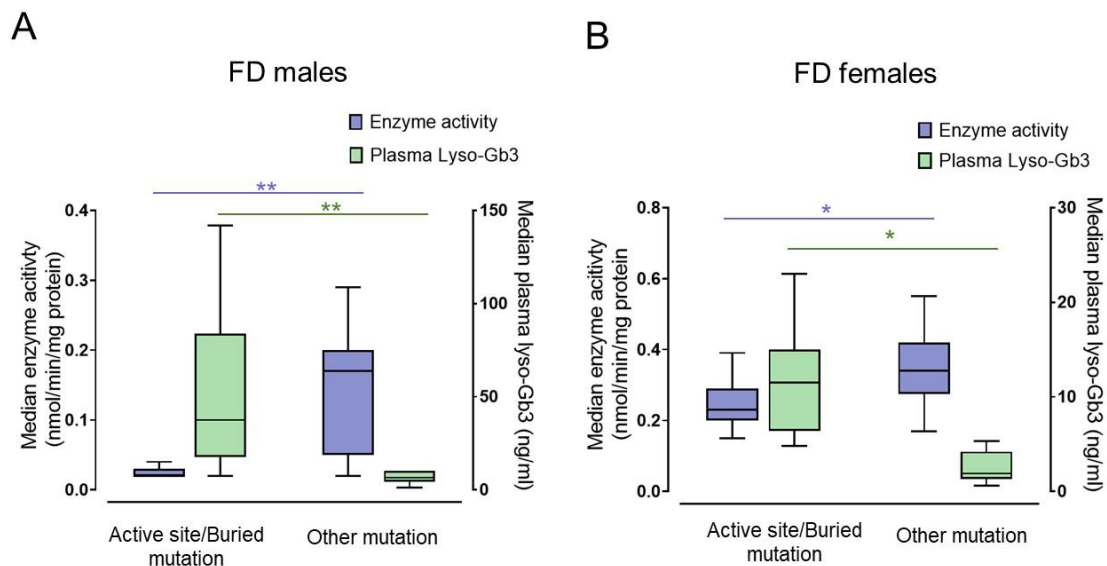


**Figure 27.  $\alpha$ -GalA activity and lyso-Gb3 levels**

Enzyme activity was measured in leukocytes (norm: 0.4-1.0 nmol/min/mg protein) and lyso-Gb3 level was determined in plasma (norm:  $<0.9$  ng/ml). A) FD males: while enzyme activity was lower in patients with active site/buried mutation, plasma lyso-Gb3 level was higher. B) FD females: while enzyme activity was lower in patients with active site/buried mutation, plasma lyso-Gb3 level was higher. Abbreviations: FD=Fabry disease; Gb3=Globotriaosylceramide. \* $p<0.05$ ; \*\* $p<0.01$ .

## 5 Discussion

### 5.1 Study I

Study I investigated electrical characteristics and cytokine expression patterns of human dermal fibroblasts, comparing cells of FD patients with those of healthy controls. Our investigations revealed that Gb3 load in dermal fibroblasts of FD patients was higher than in those of healthy controls. In those patients who received ERT, Gb3 load varied with the time interval between previous ERT and biopsy day. Further, dermal fibroblasts express  $K_{Ca}1.1$  channels, whose function was reduced in FD fibroblasts under baseline conditions, i.e. when cellular Gb3 load was high. However, upon Gb3 cleavage by ERT, a sudden over-proportionate increase of  $K_{Ca}1.1$  activity in FD fibroblasts was observed. Investigations of cytokine expression patterns showed an activation of the Notch1 signaling pathway in FD fibroblasts already at baseline, but even more evidently under pro-inflammatory conditions. Hints towards elevated pNF- $\kappa$ B p65 levels in FD fibroblasts in a pro-inflammatory environment further supported this finding. Hence, Study I confirms the hypothesis that functional alterations in  $K_{Ca}1.1$  activity due to Gb3 accumulation and elevated cytokine expression may be a link between FD fibroblasts and cutaneous nociceptors that may contribute to FD-associated pain.

When regarding genetic and clinical findings in different FD cohorts, varying i.e. in ethnicity and sample size, patient characteristics of Study I are well in line with those of previous studies: concerning genetic findings, a variety of many different mutations can be found, even in smaller cohorts. However, the majority of FD patients carries a missense mutation (Schaefer et al., 2005). Among clinical aspects, PNS and cardiac involvement are generally frequent, while renal and even more so CNS involvement are less common (KD MacDermot et al., 2001; Üçeyler et al., 2014; Vedder et al., 2007). FD-associated pain is typically located in hands and feet, often triggerable by external stimuli such as heat or cold, and internal stimuli such as fever or infections (Hoffmann et al.,

2007; MacDermot and MacDermot, 2001; Üçeyler et al., 2014). Hence, Study I largely confirms previous studies in terms of patient characteristics, organ involvement and pain parameters (Arends et al., 2018; Gibas et al., 2006; Maag et al., 2008; Mehta et al., 2004).

In FD, pathological accumulation of Gb3 and its derivatives due to dysfunctional  $\alpha$ -GalA is regarded as the 'root of all evil' by many experts (Aerts et al., 2008; Namdar et al., 2012). Gb3 deposits have been detected in many human tissues and cells, such as in glomerular podocytes or cardiomyocytes (Alroy et al., 2002; Chien et al., 2016; Germain et al., 2007), in endothelial cells (Shen et al., 2008), in neuronal cells (Kaneski et al., 2016), and also in fibroblasts of different organs (Lakomá et al., 2016; Song et al., 2016). Results of Study I are in line with these findings, showing high Gb3 load in human dermal fibroblasts.

While methods for Gb3 visualization are well established, the pathophysiological mechanisms underlying cellular dysfunction based on Gb3 accumulation are incompletely understood.

One hypothesis, how cellular Gb3 deposits may disturb cellular function is interference with proteins such as ion channels. Previous studies have shown that accumulation of Gb3 can interfere with various ion channels in different tissues:  $\alpha$ -GAL deficient mice, one of the currently investigated mouse models of FD, showed reduced activity of pain-related Nav1.7 channels in DRG sensory neurons which was reversed by Gb3 cleavage via incubation with ERT or SRT (Hofmann et al., 2018). Although the exact mechanism of Gb3 interference with Nav1.7 channels remained unclear, the authors concluded that Nav1.7 dysfunction may disrupt cell membrane homeostasis and hence, could play an important role in PNS symptoms in FD. Further, Gb3 induced dysfunction of the intermediate-conductance  $\text{Ca}^{2+}$ -activated  $\text{K}^+$  ( $\text{K}_{\text{Ca}3.1}$ ) channel in endothelial cells of  $\alpha$ -GAL deficient mice by down-regulating gene and protein expression and by interfering with the activation process (Park et al., 2011). In human cells, its derivative lyso-Gb3 reduced  $\text{K}_{\text{Ca}3.1}$  function in aortic fibroblasts by downregulating its gene and protein expression via hindering phosphorylation processes (Choi et al., 2016; Choi et al., 2015). As a consequence, collagen synthesis and differentiation into myofibroblasts was impaired and hence,

weakened the vessel wall, which potentially elevates the risk for cardiovascular events.

Although describing different ways of interaction, these studies exemplify, how Gb3 can interfere with ion channels and hence, induce critical cellular impairment.

The link between Gb3 accumulation and ion channel dysfunction was also drawn in Study I, investigating not only Gb3 load in human dermal fibroblasts, but also  $K_{Ca1.1}$  activity in the cell membrane. This activity was reduced in FD fibroblasts under baseline conditions (i.e. during high Gb3 load), but increased over-proportionally upon Gb3 cleavage. Elevated gene and protein expression of  $K_{Ca1.1}$  in FD fibroblasts supported these findings. Fig. 28 gives a synopsis of the potential relations between Gb3 deposits and  $K_{Ca1.1}$  function:

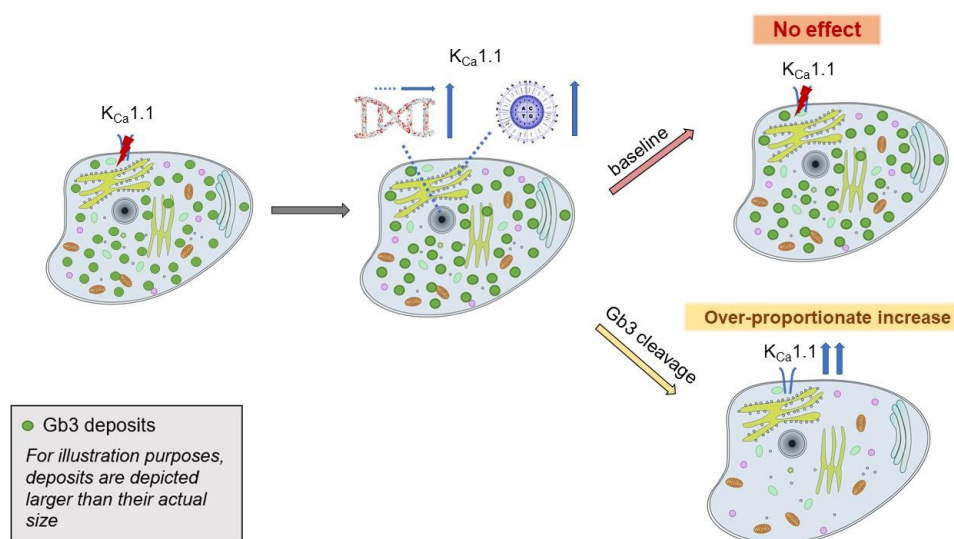


**Figure 28. Potential relations between  $K_{Ca1.1}$  gene and protein expression and activity in FD dermal fibroblasts**

The Figure shows how  $K_{Ca1.1}$  activity and its gene and protein expression in FD fibroblasts could be related: at baseline,  $K_{Ca1.1}$  activity is reduced due to Gb3 accumulation, inducing compensatory increase in its gene and protein. While this escape mechanism remains inefficient in natural condition (i.e. when Gb3 load remains high), its activity increases over-proportionately after Gb3 cleavage, based on the elevated gene and protein expression. Abbreviations: FD=Fabry disease; Gb3=Globotriaosylceramide;  $K_{Ca1.1}$ =  $Ca^{2+}$ -activated  $K^{+}$ -channel 1.1.



However, it remains unclear whether the negative consequences of K<sub>Ca</sub>1.1 dysfunction also recover upon Gb3 cleavage, since K<sub>Ca</sub>1.1 is integrated in cellular function in complex ways:

Human Ca<sup>2+</sup>-activated K<sup>+</sup> channels form a family of eight different ion channels that are all activated by intracellular Ca<sup>2+</sup>. As a member of K<sub>Ca</sub>1 channels, K<sub>Ca</sub>1.1 is both Ca<sup>2+</sup>- and voltage-gated. Although K<sub>Ca</sub>1.1 can *per se* be activated by Ca<sup>2+</sup> and voltage independently, sole increase of intracellular Ca<sup>2+</sup> or depolarization do not suffice to raise the probability of open K<sub>Ca</sub>1.1 channels to a measurable level. Hence, high intracellular Ca<sup>2+</sup> and depolarization are both required for enough K<sub>Ca</sub>1.1 channels to open, such that K<sub>Ca</sub>1.1 activity can be measured. Since K<sub>Ca</sub>1.1 has a large single channel conductance of about 100-300 pS, it is also referred to as BK channel (abbreviating Big K<sup>+</sup> conductance) or MaxiK channel (Garneau et al., 2010; B Wang et al., 2009). While Study I did not include investigations on the implications of K<sub>Ca</sub>1.1 dysfunction, it is known from previous studies that the K<sub>Ca</sub>1.1 channel is distributed among both excitable and non-excitable cells and plays a role in various cellular functions: it is functionally connected to receptors such as β-adrenergic- or angiotensin II-receptors and enzymes like proteinkinase B, regulating metabolism, cell signaling, and also apoptosis (Tian et al., 2014; Toro et al., 2014). Further, it modulates secretion of e.g. luteinizing hormone that is stimulated by gonadotropin-releasing hormone, fine tunes neurotransmitter release and regulates pathways that are triggered by changes of intracellular Ca<sup>2+</sup> concentration (Gribkoff et al., 2001; Lu et al., 2006; Waring et al., 2009). It can also play a role in inflammatory processes as its dysfunction induces activation of NF-κB p65 and expression of CCL2 (Park et al., 2006; Tajhya et al., 2016). While Study I showed that Gb3 accumulation induces dysfunction of K<sub>Ca</sub>1.1 activity in FD dermal fibroblasts, it failed to detect further ion channels in their membrane, despite application of various ion channel blockers (kindly refer to Table 4 for the list) and thorough analysis. However, it is likely that Gb3 does indeed interfere with more ion channels, also in dermal fibroblasts, where other ion channels have already been described (Estacion, 1991; Lakomá et al., 2016). The underlying cause for the diversity of these findings could be variation

in the origin of material (*Study I* and *Lakomá et al.*: lateral calf of adults; *Estación*: foreskin of newborns) and cell age (*Study I*: passages 3-5; *Estación*: passages 4-16 (mainly 8-12); *Lakomá*: passages 5-10).

In addition to that, it is important to mention that not only exactly how and with what Gb3 can interfere, also how long it can disturb cellular dysfunction has been described differently:

On the one hand, Hofmann and colleagues and *Study I* consistently report on an immediate, short-term effect of Gb3 on ion channel function, which is reversible by Gb3 cleavage. On the other hand, a previous study – in fact not investigating ion channel function, but autophagy processes – showed that Gb3 cleavage did not recover cellular function (Braun et al., 2019), hinting towards potential long-term effects of Gb3 accumulation.

When summarizing these observations, Gb3 may interfere

- with different ion channels: Na<sup>+</sup> and K<sup>+</sup> channels
- in various tissues: mouse DRG neurons, human aortic fibroblasts and human dermal fibroblasts
- in diverse ways: down-regulation of gene and protein expression and hindering activation processes
- with various times of effect: short-term consequences and long-term impact.

Despite this *prima facie* divergence, the unanimous gist of all studies is that Gb3 accumulation can induce ion channel dysfunction, which can lead to cellular impairment and hence, be directly linked to FD-associated symptoms and disease manifestation in various organ systems.

In addition to ion channel investigations, *Study I* included experiments on cytokine expression patterns and the Notch1 signaling pathway in dermal fibroblasts.

Notch1 is a transmembrane receptor whose signaling cascade is crucial for many cellular processes, including cell proliferation and differentiation, making it of great interest in cancer and leukemia research (Borggreve et al., 2009).

However, as Notch1 can also activate the NF- $\kappa$ B pathway, inducing higher expression of cytokines and chemokines such as IFN $\gamma$ , TGF- $\beta$ 1, and CCL2 (Monsalve et al., 2009; Rozenfeld and Feriozzi, 2017; Shin et al., 2006; Shin et al., 2014), Notch1 is also involved in inflammatory processes, and induction of fibrosis and sclerosis (Sanz et al., 2010). Elevated levels of Notch1 have been found in neurons of adult rats after nerve injury (Sun et al., 2012) and in models of diabetic neuropathy (both in vivo and in vitro) (Chen et al., 2017), emphasizing its role in the PNS, nerve fiber dysfunction and pain development. Also, Notch1 plays a role in pathological processes in FD. For example, in FD glomerular podocytes, the Notch1 pathway may be triggered by Gb3 and lyso-Gb3, contributing to inflammation, fibrosis and eventually, organ impairment (Rozenfeld and Feriozzi, 2017; Sanchez-Niño et al., 2015). Also, a direct association between Gb3 and elevated cytokine expression has been described before (Sakiri et al., 1998; Zetterström et al., 1998). Study I is in line with those results, as it shows elevated levels of Notch1, cytokines, and chemokines such as TGF- $\beta$ 1, IFN $\gamma$  or CCL2 in FD fibroblasts, which are known to play a role in inflammation and pain (Tsuda et al., 2009; Van Steenwinckel et al., 2011; Xiao-Min Wang et al., 2009). While CCL2 and IFN $\gamma$  were increased in FD fibroblasts at baseline and under inflammatory conditions, TGF- $\beta$ 1 was only elevated upon inflammation. These observations have been made before, in some cases using lipopolysaccharide instead of TNF to mimic inflammation (Ho et al., 2008; Lieberman et al., 1989; Sheng et al., 1995; Üçeyler et al., 2019), and match the clinical findings that FD patients report pain mainly during fever and infections. Although not proven in Study I, fibroblasts may then release cytokines into their surroundings, where cutaneous nociceptors are located, and thus contribute to FD-associated pain. Summarizing the major points outlined above, Fig. 29 illustrates their potential relations as well as their combined impact on the behaviour of cutaneous nociceptors in FD:

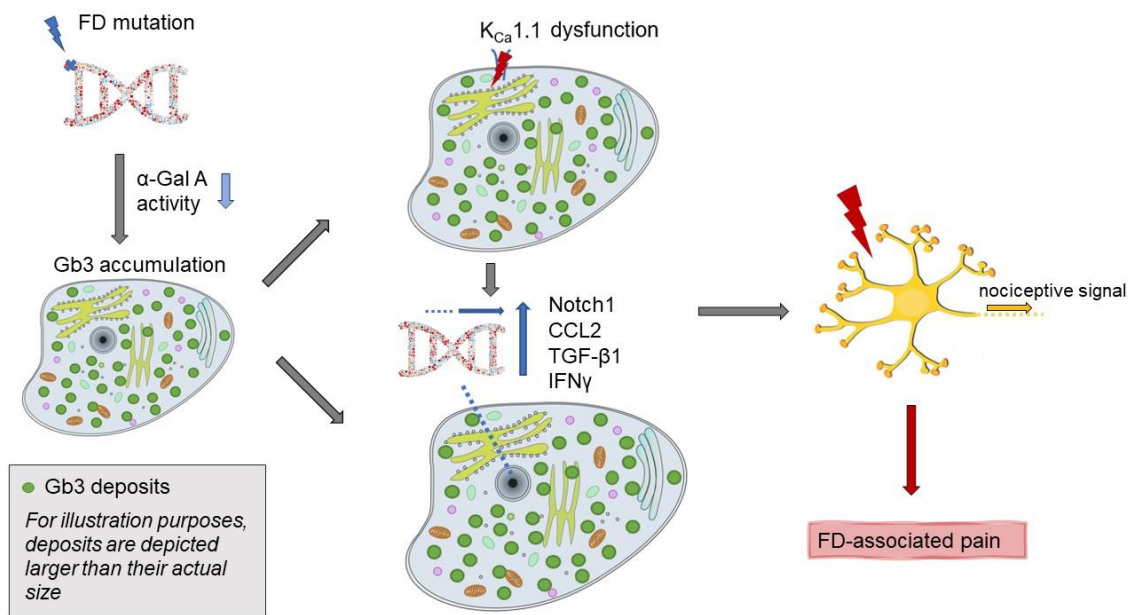


**Figure 29. Potential relations between FD mutation, dysfunction in FD dermal fibroblasts and FD-associated pain**

The Figure shows how a FD mutation may eventually be related to FD-associated pain: due to the FD mutation  $\alpha$ -GalA activity is reduced, and hence, Gb3 accumulates in FD fibroblasts. This can lead to K<sub>Ca</sub>1.1 dysfunction, as well as higher gene expression of various cytokines and chemokines, enhanced by K<sub>Ca</sub>1.1 dysfunction. These mechanism may sensitize cutaneous nociceptors and thus, contribute to FD-associated pain. Abbreviations: FD=Fabry disease; Gb3=Globotriaosylceramide; K<sub>Ca</sub>1.1= Ca<sup>2+</sup>-activated K<sup>+</sup>-channel 1.1.

## 5.2 Study II

Study II investigated the clinical phenotype of 80 adult FD patients carrying missense mutations and determined the corresponding locations of the amino acid exchanges in the 3D-structure of  $\alpha$ -GalA.

The investigations revealed that the AAE can either be found in the active site, buried in the core of  $\alpha$ -GalA, or at an other location, mostly on the protein surface.

While active site mutations were rare, buried mutations and other mutations were found more often. Further, the active site and the vast majority of buried mutations were associated with a classical FD phenotype, while most of the other mutations lead to a non-classical FD phenotype.

Also, when regarding the clinical symptoms, a correlation between AAE location and disease burden was found. Active site and buried mutations lead to a severe clinical phenotype, presenting with early disease onset, multi-organ manifestation and severe FD-associated pain. In contrast, patients with other mutations generally reported FD symptoms that occurred later in life and were limited to few inner organs; in most cases the nervous system was spared and patients described less severe FD-associated pain.

Clinical findings were paralleled by laboratory parameters: patients with active site or buried mutations had lower residual  $\alpha$ -GalA activity and higher plasma lyso-Gb3 levels.

Overall, Study II gives evidence that the location of the AAE in the 3D-structure of  $\alpha$ -GalA due to FD missense mutations has a critical impact on disease burden and demonstrates that stratification of FD missense mutation based hereupon may become a useful additional tool in the management of FD patients.

Although the clinical distinction of classical and non-classical FD has long been established (Clarke et al., 1971; Opitz et al., 1965), it is still difficult to classify new variants in the  $\alpha$ -GalA gene immediately upon detection. This is due to the fact that the classification into the classical and non-classical phenotype requires i.a. the long-term observation of a larger cohort of individuals with the

same mutation. While measurements of  $\alpha$ -GalA activity and plasma lyso-Gb3 levels can give hints towards the potential phenotype, these sole laboratory findings cannot build a solid basis for the management of patients with new variants. As increasingly more variants are being found and more therapy options become available, scientists and clinicians face the problem of how to categorize the individual mutation as well as if and how to treat the patients. Additionally, this classification system is not only stretched to its limits when new variants occur, it can also be conflicting in the assessment of longer known variants as it lacks a clear pathophysiological basis explaining why some variants lead to a classical phenotype, some to a non-classical phenotype and some not at all to FD. Hence, certain variants are regarded as pathogenic and therefore, FD-inducing by some scientists, but as apathogenic and therefore as a mere benign polymorphism by others. These inconsistent and conflicting assessments were e.g. observed for the variants R118C (Ferreira et al., 2015; Talbot et al., 2018), A143T (Hauth et al., 2018; Lenders et al., 2016), and D313Y (du Moulin et al., 2017; Niemann et al., 2012; Oder et al., 2016). For variant N215S, classification varied even within one study: one individual was classified as having the classical phenotype, while the other patients were classified as having the non-classical phenotype (Arends et al., 2017). Due to a growing number of newly discovered variants in the  $\alpha$ -GalA gene, these conflicts are likely to continue in the future.

Seizing the results of previous studies describing the 3D-structure of  $\alpha$ -GalA, Study II considered this problem by taking the AAE location type into consideration for the clinical assessment of FD patients.

The importance of the integrity of the 3D-structure of  $\alpha$ -GalA and impact of AAE due to FD missense mutations has yet only scarcely been investigated, especially towards their correlation with clinical symptoms. However, previous studies on this topic have described that most AAE occur in the core of  $\alpha$ -GalA, while AAE in or around the active site are less frequent (Garman and Garboczi, 2004a). Amino acid exchanges in these two location types either interfere with substrate binding or disrupt the 3D-structure of  $\alpha$ -GalA with consecutive protein misfolding, and hence, have a clear negative effect on enzyme function.

Further, some amino acids that are neither in the active site nor in the core of  $\alpha$ -GalA, but have other functional relevance, e.g. for bonding forces, or are located on the protein surface, can also be affected in FD ('other' mutation). AAE in this location have a less clearer and varying impact on the 3D-structure and are often better tolerated concerning their function (Garman and Garboczi, 2004a; Matsuzawa et al., 2005; Shabbeer et al., 2006). The results of Study II are well in line with these studies, including FD patients carrying different missense mutations with the three different AAE location types, of which active site mutation were by far the rarest, while buried mutations and other mutations occurred more often. The difference in impact of the different AAE types was reflected by the different clinical phenotypes of patients with active site or buried mutations and other mutations. Moreover, results of Study I go beyond those of previous studies, as it investigated individual clinical symptoms and not only the general classical or non-classical phenotype and additionally, divided the study cohort by age:

On the one hand, this detailed analysis revealed that patients with other mutations, regardless of their individual mutation, developed disease manifestations in fewer organs and later in life than those with active site or buried mutation. Especially women with other mutations were less severely affected. In most patients with other mutations, both men and women, the nervous system was not affected. Interestingly, the number of patients carrying active site or buried mutations and suffering from FD-associated pain and/or hypohidrosis in Study II was higher or comparable with those of previous studies that did not subdivide their cohort, while that of patients with other mutations was well lower (Lidove et al., 2006; Mehta et al., 2004; Orteu et al., 2007). While similar observations were made concerning cardiomyopathy and nephropathy in female patients, the number of male patients with cardiomyopathy and/or nephropathy was comparable to previous studies in both patients with active site/buried and other mutations (KD MacDermot et al., 2001; Mehta et al., 2004).

These observations suggest that the stratification by AAE location type could help to better establish patient subgroups within big FD cohorts, especially regarding the PNS and women in general.

On the other hand, Study II emphasized that each mutation still needs to be regarded separately. For example, the mutation c.644A>G (N215S) belongs to the group of other mutations, but is known to induce a severe to lethal cardiac manifestation in FD (Oder et al., 2017). This exemplifies that some mutations of the other AAE location type can induce a severe disease burden of a single organ and can be life-threatening. Thus, the sole assignment of FD missense mutations to one AAE location type is not sufficient to reliably evaluate their pathogenicity and assess the clinical course of the patient. Regarding each mutation individually remains essential in the clinical management.

In addition to clinical symptoms, Study II also investigated relevant laboratory parameters in FD, namely residual  $\alpha$ -GalA activity and plasma lyso-Gb3 levels. Previous studies have shown that low residual  $\alpha$ -GalA activity correlates with early organ manifestation and severe disease burden (Branton et al., 2002; Wu et al., 2010), which was also observed in Study II. Plasma lyso-Gb3 is considered as a biomarker in FD that can help to differentiate FD patients and the healthy population (Dupont et al., 2013; Niemann et al., 2014), and also classic and non-classic FD (Nowak et al., 2018). On cellular level, lyso-Gb3 is involved in the release of pro-inflammatory cytokines and eventually, in disease manifestation, e.g. in heart and kidneys. (Sanchez-Niño et al., 2015). On clinical level, plasma lyso-Gb3 is therefore used to assess disease burden and potential prognosis (Aerts et al., 2008), as well as to monitor disease process (Nowak et al., 2017) and therapy success (Sakuraba et al., 2018).

However, it is important to keep in mind that laboratory findings should not be regarded separately, but always in context with clinical symptoms. In Study II, this combined analysis was performed and showed matching clinical and laboratory results that suggested a severe clinical phenotype with poor prognosis in patients with active site or buried mutations.



## **5.3 Limitations and strengths**

### **5.3.1 Study I**

One limitation of Study I is that patch-clamp analysis, incubation experiments as well as gene and protein expression investigations, were performed with a relatively low number of samples, focusing on male FD patients with pain. This was due to the arduous nature of those experiments which obliged sample selection. Patch-clamp analysis is an elaborate single-cell investigation that requires thoughtful preparation, execution and conclusion of the observations. As this is a time-intensive process, a reasonable selection had to be made. Since the aim was to put the results of patch-clamp analysis in context with cytokine expression patterns, the same sample selection was also made for incubation experiments with following gene and protein expression investigations. As a consequence of the sample selection, results of the experiments concerned might not be applicable to further patient subgroups like FD men without pain or FD women.

Potential alternatives to the patch-clamp technique such as micro-electrode array may allow the analysis of a much bigger sample, e.g. including different patient subgroups.

As a further limitation, only dermal fibroblasts were analyzed, while other skin cells such as keratinocytes or mast cells were not investigated. Therefore, conclusions about their potential role in FD pain cannot be drawn.

A comprehensive analysis of these cell types would require larger skin biopsies and individual cell culture conditions for each cell type so that enough cells could be harvested for the experiments.

The major strength of Study I is the broad analysis of dermal fibroblasts that contextualized gene and protein expression patterns with ion channel function, also considering inflammatory circumstances and the potential confounder Gb3. The investigations were performed with a well-characterized patient cohort

which can help further understand the different clinical phenotypes of FD. The results indicate that Gb3-associated functional disruption of non-neuronal cells may be relevant in FD-associated pain and may provide the basis for future studies on how non-neuronal cells could be involved in FD-associated pain. Following this course of research might open up new treatment options for FD patients.

### **5.3.2 Study II**

As one limitation, the classification system based on AAE location in the 3D-structure of  $\alpha$ -GalA, as it was used in Study II, can only be applied to missense mutations since nonsense mutations or deletions and insertions mostly hamper the formation of the complete enzyme (Maquat, 2004) and thus, render the localization of the impaired residue impossible. Therefore, a comparative analysis between e.g. patients with missense mutations and nonsense mutations could not be performed.

As the impact of e.g. nonsense mutations on gene transcription and protein translation is complex and variable, an investigation similar to that of missense mutations is challenging and would require in depth analysis of each individual mutation, including i.a. investigation on the mRNA level of the mutant allele, how it could escape non-sense mediated RNA decay, and how the potentially arising protein would be formed and function (Dyle et al., 2020; Frischmeyer et al., 1999).

Further, patients with active site mutations were not regarded as a separate group, but together with patients with buried mutations. This joint analysis had to be carried out because of their relatively low number which is likely due to the fact that only 15 of 397 residues form the active site of  $\alpha$ -GalA (Garman and Garboczi, 2004a; Riera et al., 2015), so that patients with active site mutations comprise the smallest subgroup of all FD patients carrying missense mutations. As a consequence, the combined analysis of patients with active site and buried mutations hindered separate conclusions for these two subgroups.

Larger FD patient cohorts would likely contain enough patients with active site mutations, so that this group could then be analyzed separately.

The major strength of Study II is the implementation of a classification system that is based the direct pathofunctional impact of FD missense mutations, linking  $\alpha$ -GalA structure and function with laboratory and clinical parameters. By considering the alterations in the 3D-structure of  $\alpha$ -GalA, objective and subjective FD manifestations were put in context with  $\alpha$ -GalA pathology, bringing basal FD pathofunction into clinical application. Study II may hence lay the ground for future studies on the impact of alterations in the 3D-structure of  $\alpha$ -GalA, such as experimental or further clinical trials with larger cohorts. They could provide further evidence for the benefiting of this classification system that could in the future serve as an additional stratification and evaluation tool in clinical practice, helping to assess disease burden and potential prognosis of FD patients.

#### **5.4. Overall conclusion**

Study I experimentally investigated how dermal fibroblasts can impact pain in FD. Study II clinically described why looking at the 3D-structure of  $\alpha$ -GalA may be worthwhile for the clinical management of FD patients. Despite this difference in research direction, the two studies conjointly describe that  $\alpha$ -GalA pathology induces functional alterations in cells such as dermal fibroblasts and eventually FD manifestations like e.g. FD-associated pain. Their severity depends i.a. on how the mutation in the  $\alpha$ -GalA gene disrupts the integrity of  $\alpha$ -GalA.

## 6 Summary/Zusammenfassung

### 6.1 English Summary

FD is a genetic lysosomal storage disorder based on mutations in the gene encoding  $\alpha$ -GalA. Missense mutations induce an AAE in the  $\alpha$ -GalA. Pain is a predominant symptom in FD and the pathophysiology is unclear. Evidence is increasing for the concept of cutaneous nociception. Study I aimed at investigating the impact of dermal fibroblasts on FD-associated pain. Skin punch biopsies were obtained from 40 adult FD patients and ten healthy controls and dermal fibroblast cultures were generated. Gb3 deposits were visualized immunocytochemically, patch-clamp analysis was conducted to investigate ion channel activity, and gene and protein expression patterns were analyzed via PCR, ELISA, and Western Blot. FD dermal fibroblasts showed high Gb3 load depending on treatment interval and expressed  $K_{Ca}1.1$  channels. Activity was reduced in FD cells at baseline, but increased over-proportionately upon Gb3-cleavage by ERT. Gene and protein expression of  $K_{Ca}1.1$  was increased in FD cells. FD dermal fibroblasts showed higher gene expression of Notch1 and CCL2, TGF- $\beta$ , and IFN $\gamma$ . Western Blot analysis gave hints towards elevated pNF $\kappa$ B levels under inflammatory conditions. These results show that dermal fibroblasts may be involved in FD-associated pain. Study II aimed at investigating the correlation between the AAE location type in the  $\alpha$ -GalA and the clinical FD phenotype. 80 adult FD patients were investigated and characterized clinically and their  $\alpha$ -GalA activity and lyso-Gb3 level was measured in leucocytes and plasma, respectively. The 3D-structure of  $\alpha$ -GalA was downloaded into Pymol Graphics System and the AAE was depicted and located. The study showed that three different AAE location types can be differentiated: mutations in the active site ('active site'), those buried in the core of  $\alpha$ -GalA ('buried') and those at another location, mostly on the protein surface ('other'). FD patients carrying active site or buried mutations showed a severe clinical phenotype with multi-organ manifestation and early disease onset. Patients with other mutations were less severely affected with oligo-organ

manifestation sparing the nervous system and later disease onset. The clinical impression was paralleled by laboratory findings. Patients with active site or buried mutations had lower  $\alpha$ -GalA activity and higher lyso-Gb3 levels than patients with other mutations. These results demonstrate that stratification of FD patients carrying missense mutations by AAE location type may be an advantageous parameter that can help in the management of FD patients.

## 6.2 Deutsche Zusammenfassung

M. Fabry ist eine genetisch bedingte lysosomale Speichererkrankung aufgrund von Mutationen im Gen der  $\alpha$ -GalA. Missense-Mutationen führen zum Austausch einer Aminosäure in der  $\alpha$ -GalA. Schmerz ist ein häufiges Symptom bei Patient\*innen mit M. Fabry, dessen Pathophysiologie bisher unklar ist, wobei Studien die Beteiligung von Hautzellen beschreiben. Studie I untersuchte die Rolle von dermalen Fibroblasten hierbei. Hierfür wurde bei 40 Patient\*innen mit M. Fabry sowie zehn Kontrollprobanden eine 6-mm Hautstanzbiopsie durchgeführt und zur Kultivierung von dermalen Fibroblasten verwendet. In diesen wurden Gb3-Ablagerungen dargestellt, und die Ionenkanalaktivität der dermalen Fibroblasten via Patch-Clamp Verfahren sowie Gen- und Proteinexpression mittels PCR, ELISA und Western Blot betrachtet. Es zeigte sich, dass dermale Fibroblasten erhöhte Gb3-Ablagerungen beinhalten, abhängig von der Zeit zwischen Enzyersatztherapie und Biospieentnahme, sowie  $K_{Ca}1.1$  Kanäle, deren Funktion in Patientenzellen unter Normalbedingungen reduziert war, der jedoch eine überproportionale Aktivitätszunahme nach Gb3-Abbau mittels ERT zeigte. Die Gen- und Proteinexpression des Kanals war in Patient\*innenzellen erhöht. Zudem zeigte sich in Patient\*innenzellen eine erhöhte Genexpression von Notch1 sowie CCL2, TGF- $\beta$ 1 und IFN $\gamma$ . Der Western Blot lieferte Hinweise auf eine erhöhte Expression von pNF $\kappa$ B unter inflammatorischen Bedingungen. Die Ergebnisse zeigen, dass dermale Fibroblasten zu Schmerz bei M. Fabry beitragen können. Studie II untersuchte den Zusammenhang zwischen dem Ort des Aminosäureaustausches (ASA) in der  $\alpha$ -GalA durch Missense Mutationen und dem klinischen Phänotypen. 80 Patient\*innen mit M. Fabry wurden klinisch charakterisiert, ihre  $\alpha$ -GalA-Aktivität in Leukozyten und Lyso-Gb3 Spiegel im Blutplasma wurde gemessen. Die 3D-Struktur der  $\alpha$ -GalA wurde in Pymol Graphics System geladen und der Ort des ASA dargestellt. Es gab drei verschiedene ASA Gruppen: Mutationen im aktiven Zentrum („active site“), in der Tiefe des Enzyms („buried“) und an anderen Orten, meist an der Oberfläche („other“). Patient\*innen mit active site- oder buried-Mutationen zeigten einen

schweren Phänotypen mit Multi-Organbeteiligung und frühem Krankheitsbeginn. Patient\*innen mit other-Mutationen zeigten eine Beteiligung von wenigen Organen ohne Nervensystem und späteren Krankheitsbeginn. Zudem zeigten Patient\*innen mit active site- oder buried-Mutationen geringe  $\alpha$ -GalA-Aktivität und hohe Lyso-Gb3 Spiegel. Die Ergebnisse zeigen, dass die Einteilung von Patient\*innen mit M. Fabry-Missense Mutationen anhand des Ortes des ASA ein gewinnbringender Parameter bei der Betreuung dieser Patient\*innen sein kann.

## 7 Bibliography

- Abràmoff, M. D., Magalhães, P. J., & Ram, S. J. (2004). Image processing with ImageJ. *Biophotonics Int*, 11(7), 36-42.
- Aerts, J. M., Groener, J. E., Kuiper, S., et al. (2008). Elevated globotriaosylsphingosine is a hallmark of Fabry disease. *PNAS*, 105(8), 2812-2817. doi:10.1073/pnas.0712309105
- Akhtar, M., & Elliott, P. (2018). Anderson-Fabry disease in heart failure. *Biophys Rev*, 10(4), 1107-1119. doi:10.1007/s12551-018-0432-5
- Alroy, J., Sabnis, S., & Kopp, J. B. (2002). Renal pathology in Fabry disease. *Clin J Am Soc Nephrol*, 13(suppl 2), S134-S138. doi:10.1097/01.ASN.0000016684.07368.75
- Arends, M., Biegstraaten, M., Wanner, C., et al. (2018). Agalsidase alfa versus agalsidase beta for the treatment of Fabry disease: an international cohort study. *J Med Genet*, 55(5), 351-358. doi:10.1136/jmedgenet-2017-104863
- Arends, M., Hollak, C. E., & Biegstraaten, M. (2015). Quality of life in patients with Fabry disease: a systematic review of the literature. *Orphanet J Rare Dis*, 10(1), 77. doi:10.1186/s13023-015-0296-8
- Arends, M., Wanner, C., Hughes, D., et al. (2017). Characterization of classical and nonclassical Fabry disease: a multicenter study. *Clin J Am Soc Nephrol*, 28(5), 1631-1641. doi:10.1681/ASN.2016090964
- Auray-Blais, C., Ntwari, A., Clarke, J. T., et al. (2010). How well does urinary lyso-Gb3 function as a biomarker in Fabry disease? *Clin Chim Acta*, 411(23-24), 1906-1914. doi:10.1016/j.cca.2010.07.038
- Biancini, G. B., Vanzin, C. S., Rodrigues, D. B., et al. (2012). Globotriaosylceramide is correlated with oxidative stress and inflammation in Fabry patients treated with enzyme replacement therapy. *Biochim Biophys Acta Mol Basis Dis*, 1822(2), 226-232. doi:10.1016/j.bbadis.2011.11.001
- Biegstraaten, M., Hollak, C. E., Bakkers, M., et al. (2012). Small fiber neuropathy in Fabry disease. *Mol Genet Metab*, 106(2), 135-141. doi:10.1016/j.ymgme.2012.03.010
- Bishop, D. F., Kornreich, R., & Desnick, R. J. (1988). Structural organization of the human alpha-galactosidase A gene: further evidence for the absence of a 3'untranslated region. *PNAS*, 85(11), 3903-3907. doi:10.1073/pnas.85.11.3903
- Borggreffe, T., & Oswald, F. (2009). The Notch signaling pathway: transcriptional regulation at Notch target genes. *Cell Mol Life Sci*, 66(10), 1631-1646. doi:10.1007/s00018-009-8668-7
- Boustany, R.-M. N. (2013). Lysosomal storage diseases—the horizon expands. *Nat Rev Neurol*, 9(10), 583. doi:10.1038/nrneurol.2013.163
- Branton, M. H., Schiffmann, R., Sabnis, S. G., et al. (2002). Natural history of Fabry renal disease: influence of  $\alpha$ -galactosidase A activity and genetic mutations on clinical course. *Medicine*, 81(2), 122-138.
- Braun, F., Blomberg, L., Brodesser, S., et al. (2019). Enzyme replacement therapy clears Gb3 deposits from a podocyte cell culture model of Fabry



- disease but fails to restore altered cellular signaling. *Cell Physiol Biochem*, 52(5), 1139-1150. doi:10.33594/0000000077
- Buckley, C. D. (2011). Why does chronic inflammation persist: An unexpected role for fibroblasts. *Immunol Lett*, 138(1), 12-14. doi:doi.org/10.1016/j.imlet.2011.02.010
- Buckley, C. D., Pilling, D., Lord, J. M., et al. (2001). Fibroblasts regulate the switch from acute resolving to chronic persistent inflammation. *Trends Immunol*, 22(4), 199-204. doi:10.1016/S1471-4906(01)01863-4
- Cairns, T., Müntze, J., Gernert, J., et al. (2018). Hot topics in Fabry disease. *Postgrad Med J*, 94(1118), 709-713. doi:10.1136/postgradmedj-2018-136056
- Chen, C., Corbley, M. J., Roberts, T. M., & Hess, P. (1988). Voltage-sensitive calcium channels in normal and transformed 3T3 fibroblasts. *Science*, 239(4843), 1024-1026. doi:10.1126/science.2449730
- Chen, R. (2016). International Fabry Disease Genotype-Phenotype Database (dbFGP). Retrieved from <http://www.dbfgp.org/dbFgp/fabry/index.html>
- Chen, T., Li, H., Yin, Y., et al. (2017). Interactions of Notch1 and TLR4 signaling pathways in DRG neurons of in vivo and in vitro models of diabetic neuropathy. *Sci Rep*, 7(1), 1-12. doi:10.1038/s41598-017-15053-w
- Chien, Y., Chien, C.-S., Chiang, H.-C., et al. (2016). Interleukin-18 deteriorates Fabry cardiomyopathy and contributes to the development of left ventricular hypertrophy in Fabry patients with GLA IVS4+ 919 G> A mutation. *Oncotarget*, 7(52), 87161. doi:10.18632/oncotarget.13552
- Chimenti, C., Scopelliti, F., Vulpis, E., et al. (2015). Increased oxidative stress contributes to cardiomyocyte dysfunction and death in patients with Fabry disease cardiomyopathy. *Hum Pathol*, 46(11), 1760-1768. doi:10.1016/j.humpath.2015.07.017
- Choi, J. Y., & Park, S. (2016). Role of protein kinase A and class II phosphatidylinositol 3-kinase C2 $\beta$  in the downregulation of KCa3. 1 channel synthesis and membrane surface expression by lyso-globotriaosylceramide. *Biochem Biophys Res Commun*, 470(4), 907-912. doi:10.1016/j.bbrc.2016.01.152
- Choi, J. Y., Shin, M.-Y., Suh, S. H., & Park, S. (2015). Lyso-globotriaosylceramide downregulates KCa3. 1 channel expression to inhibit collagen synthesis in fibroblasts. *Biochem Biophys Res Commun*, 468(4), 883-888. doi:10.1016/j.bbrc.2015.11.050
- Cimaz, R., Guillaume, S., Hilz, M. J., et al. (2011). Awareness of Fabry disease among rheumatologists—current status and perspectives. *J Clin Rheumatol*, 30(4), 467-475. doi:10.1007/s10067-010-1445-z
- Clark, N. E., & Garman, S. C. (2009). The 1.9 Å structure of human  $\alpha$ -N-acetylgalactosaminidase: the molecular basis of Schindler and Kanzaki diseases. *J Mol Biol*, 393(2), 435-447. doi:10.1016/j.jmb.2009.08.021
- Clarke, J. T., Knaack, J., Crawhall, J. C., & Wolfe, L. S. (1971). Ceramide trihexosidosis (Fabry's disease) without skin lesions. *N Engl J Med*, 284(5), 233-235. doi:10.1056/NEJM197102042840503
- Cole, A., Lee, P., Hughes, D., et al. (2007). Depression in adults with Fabry disease: A common and under-diagnosed problem. *J Inherit Metab Dis*, 30(6), 943-951. doi:10.1007/s10545-007-0708-6

- Cooper, D. N., & Youssoufian, H. (1988). The CpG dinucleotide and human genetic disease. *Hum Genet*, 78(2), 151-155. doi:doi.org/10.1007/BF00278187
- Dale, T. J., Townsend, C., Hollands, E. C., & Trezise, D. J. (2007). Population patch clamp electrophysiology: a breakthrough technology for ion channel screening. *Mol Biosyst*, 3(10), 714-722. doi:10.1039/B706152H
- De Francesco, P. N., Mucci, J. M., Ceci, R., et al. (2013). Fabry disease peripheral blood immune cells release inflammatory cytokines: role of globotriaosylceramide. *Mol Genet Metab*, 109(1), 93-99. doi:10.1016/j.ymgme.2013.02.003
- Desnick, R. J. (2018). Fabry disease. In *Nephrology Secrets: First South Asia Edition* (1st ed., pp. 289-292): Elsevier.
- Desnick, R. J., Brady, R., Barranger, J., et al. (2003). Fabry disease, an under-recognized multisystemic disorder: expert recommendations for diagnosis, management, and enzyme replacement therapy. *Ann Intern Med*, 138(4), 338-346. doi:10.7326/0003-4819-138-4-200302180-00014
- Devigili, G., Tugnoli, V., Penza, P., et al. (2008). The diagnostic criteria for small fibre neuropathy: from symptoms to neuropathology. *Brain*, 131(7), 1912-1925. doi:10.1093/brain/awn093
- Díaz-Araya, G., Vivar, R., Humeres, C., et al. (2015). Cardiac fibroblasts as sentinel cells in cardiac tissue: Receptors, signaling pathways and cellular functions. *Pharmacol Res*, 101, 30-40. doi:10.1016/j.phrs.2015.07.001
- Dobrovolny, R., Dvorakova, L., Ledvinova, J., et al. (2005). Relationship between X-inactivation and clinical involvement in Fabry heterozygotes. Eleven novel mutations in the  $\alpha$ -galactosidase A gene in the Czech and Slovak population. *J Mol Med*, 83(8), 647-654. doi:10.1007/s00109-005-0656-2
- du Moulin, M., Koehn, A., Golsari, A., et al. (2017). The mutation p. D313Y is associated with organ manifestation in Fabry disease. *Clin Genet*, 92(5), 528-533. doi:10.1111/cge.13007
- Dupont, F., Gagnon, R., Boutin, M., & Auray-Blais, C. (2013). A metabolomic study reveals novel plasma lyso-Gb3 analogs as Fabry disease biomarkers. *Curr Med Chem*, 20(2), 280-288.
- Dütsch, M., Marthol, H., Stemper, B., et al. (2002). Small fiber dysfunction predominates in Fabry neuropathy. *J Clin Neurophysiol*, 19(6), 575-586.
- Dyle, M. C., Kolakada, D., Cortazar, M. A., & Jagannathan, S. (2020). How to get away with nonsense: Mechanisms and consequences of escape from nonsense-mediated RNA decay. *Wiley Interdiscip Rev RNA*, 11(1), e1560. doi:10.1002/wrna.1560
- Ellaway, C. (2016). Paediatric fabry disease. *Transl Pediatr*, 5(1), 37. doi:10.3978/j.issn.2224-4336.2015.12.02
- Elstein, D., Schachamov, E., Beer, R., & Altarescu, G. (2012). X-inactivation in Fabry disease. *Gene*, 505(2), 266-268. doi:10.1016/j.gene.2012.06.013
- Estacion, M. (1991). Characterization of ion channels seen in subconfluent human dermal fibroblasts. *J Physiol*, 436(1), 579-601. doi:10.1113/jphysiol.1991.sp018568

- Fabrazyme. (2020). Retrieved from <https://www.ema.europa.eu/en/medicines/human/EPAR/fabrazyme>
- Ferreira, C. R., & Gahl, W. A. (2017). Lysosomal storage diseases. *Transl Sci Rare Dis*, 2(1-2), 1-71. doi:10.3233/TRD-160005
- Ferreira, S., Ortiz, A., Germain, D. P., et al. (2015). The alpha-galactosidase A p. Arg118Cys variant does not cause a Fabry disease phenotype: data from individual patients and family studies. *Mol Genet Metab*, 114(2), 248-258. doi:10.1016/j.ymgme.2014.11.004
- Frischmeyer, P. A., & Dietz, H. C. (1999). Nonsense-mediated mRNA decay in health and disease. *Hum Mol Genet*, 8(10), 1893-1900. doi:10.1093/hmg/8.10.1893
- Fukuda, K., Ishida, W., Fukushima, A., & Nishida, T. (2017). Corneal fibroblasts as sentinel cells and local immune modulators in infectious keratitis. *Int J Mol Sci*, 18(9), 1831. doi:10.3390/ijms18091831
- Galafold. (2019). Retrieved from <https://www.ema.europa.eu/en/medicines/human/EPAR/galafold>
- Garman, S. C., & Garboczi, D. N. (2004a). The molecular defect leading to Fabry disease: structure of human  $\alpha$ -galactosidase. *J Mol Biol*, 337(2), 319-335. doi:10.1016/j.jmb.2004.01.035
- Garman, S. C., & Garboczi, D. N. (2004b). Structure of human alpha-galactosidase. Retrieved from [https://www.wwpdb.org/pdb?id=pdb\\_00001r46](https://www.wwpdb.org/pdb?id=pdb_00001r46)
- Garneau, L., Klein, H., Parent, L., & Sauvé, R. (2010). Toward the rational design of constitutively active KCa3. 1 mutant channels. In *Methods in Enzymology* (Vol. 485, pp. 437-457): Elsevier.
- Germain, D. P. (2010). Fabry disease. *Orphanet J Rare Dis*, 5(1), 30. doi:10.1186/1750-1172-5-30
- Germain, D. P., Charrow, J., Desnick, R. J., et al. (2015). Ten-year outcome of enzyme replacement therapy with agalsidase beta in patients with Fabry disease. *J Med Genet*, 52(5), 353-358. doi:10.1136/jmedgenet-2014-102797
- Germain, D. P., Waldek, S., Banikazemi, M., et al. (2007). Sustained, long-term renal stabilization after 54 months of agalsidase  $\beta$  therapy in patients with Fabry disease. *Clin J Am Soc Nephrol*, 18(5), 1547-1557. doi:10.1681/ASN.2006080816
- Gibas, A. L., Klatt, R., Johnson, J., et al. (2006). A survey of the pain experienced by males and females with Fabry disease. *Pain Res Manag*, 11. doi:10.1155/2006/828964
- Gorelik, A., Illes, K., Heinz, L. X., et al. (2016). Crystal structure of mammalian acid sphingomyelinase. *Nat Commun*, 7(1), 1-9. doi:10.1038/ncomms12196
- Grewal, R. (1994). Stroke in Fabry's disease. *J Neurol*, 241(3), 153-156. doi:10.1007/BF00868342
- Gribkoff, V. K., Starrett Jr, J. E., & Dworetzky, S. I. (2001). Maxi-K potassium channels: form, function, and modulation of a class of endogenous regulators of intracellular calcium. *Neuroscientist*, 7(2), 166-177. doi:10.1177/107385840100700211

- Grimbacher, B., Aicher, W., Peter, H., & Eibel, H. (1998). TNF- $\alpha$  induces the transcription factor Egr-1, pro-inflammatory cytokines and cell proliferation in human skin fibroblasts and synovial lining cells. *Rheumatol Int*, 17(5), 185-192.
- Guerard, N., Morand, O., & Dingemanse, J. (2017). Lucerastat, an iminosugar with potential as substrate reduction therapy for glycolipid storage disorders: safety, tolerability, and pharmacokinetics in healthy subjects. *Orphanet J Rare Dis*, 12(1), 9. doi:10.1186/s13023-017-0565-9
- Guérard, N., Oder, D., Nordbeck, P., et al. (2018). Lucerastat, an iminosugar for substrate reduction therapy: tolerability, pharmacodynamics, and pharmacokinetics in patients with Fabry disease on enzyme replacement. *Clin Pharmacol Ther*, 103(4), 703-711.
- Hauth, L., Kerstens, J., Yperzeele, L., et al. (2018). Galactosidase alpha p. A143T variant Fabry disease may result in a phenotype with multifocal microvascular cerebral involvement at a young age. *Front Neurol*, 9, 336. doi:10.3389/fneur.2018.00336
- Ho, A. W. Y., Wong, C. K., & Lam, C. W. K. (2008). Tumor necrosis factor- $\alpha$  up-regulates the expression of CCL2 and adhesion molecules of human proximal tubular epithelial cells through MAPK signaling pathways. *Immunobiology*, 213(7), 533-544. doi:10.1016/j.imbio.2008.01.003
- Hoffmann, B., Beck, M., Sunder-Plassmann, G., et al. (2007). Nature and prevalence of pain in Fabry disease and its response to enzyme replacement therapy—a retrospective analysis from the Fabry Outcome Survey. *Clin J Pain*, 23(6), 535-542. doi:10.1097/AJP.0b013e318074c986
- Hofmann, L., Hose, D., Griebshammer, A., et al. (2018). Characterization of small fiber pathology in a mouse model of Fabry disease. *Elife*, 7, e39300. doi:10.7554/eLife.39300.001
- Hopkin, R. J., Bissler, J., Banikazemi, M., et al. (2008). Characterization of Fabry disease in 352 pediatric patients in the Fabry Registry. *Pediatr Res*, 64(5), 550-555. doi:10.1203/PDR.0b013e318183f132
- Hughes, D. A., Nicholls, K., Shankar, S. P., et al. (2017). Oral pharmacological chaperone migalastat compared with enzyme replacement therapy in Fabry disease: 18-month results from the randomised phase III ATTRACT study. *J Med Genet*, 54(4), 288-296. doi:10.1136/jmedgenet-2016-104178
- Hwu, W. L., Chien, Y. H., Lee, N. C., et al. (2009). Newborn screening for Fabry disease in Taiwan reveals a high incidence of the later-onset GLA mutation c. 936+ 919G> A (IVS4+ 919G> A). *Hum Mutat*, 30(10), 1397-1405. doi:10.1002/humu.21074
- Jain, A., Brönneke, S., Kolbe, L., et al. (2011). TRP-channel-specific cutaneous eicosanoid release patterns. *Pain*, 152(12), 2765-2772. doi:10.1016/j.pain.2011.08.025
- Juchniewicz, P., Kloska, A., Tylki-Szymańska, A., et al. (2018). Female Fabry disease patients and X-chromosome inactivation. *Gene*, 641, 259-264. doi:10.1016/j.gene.2017.10.064
- Julius, D., & Basbaum, A. I. (2001). Molecular mechanisms of nociception. *Nature*, 413(6852), 203-210. doi:10.1038/35093019

- Kaneski, C. R., Brady, R. O., Hanover, J. A., & Schueler, U. H. (2016). Development of a model system for neuronal dysfunction in Fabry disease. *Mol Genet Metab*, 119(1-2), 144-150. doi:10.1016/j.ymgme.2016.07.010
- Kessler-Becker, D., Krieg, T., & Eckes, B. (2004). Expression of pro-inflammatory markers by human dermal fibroblasts in a three-dimensional culture model is mediated by an autocrine interleukin-1 loop. *Biochem J*, 379(2), 351-358. doi:10.1042/bj20031371
- Khan, A., Barber, D. L., Huang, J., et al. (2021). Lentivirus-mediated gene therapy for Fabry disease. *Nat Commun*, 12(1), 1-9. doi:10.1038/s41467-021-21371-5
- Kimura, J. (2013). *Electrodiagnosis in diseases of nerve and muscle: principles and practice*: Oxford university press.
- Kishimoto, Y., Hiraiwa, M., & O'brien, J. (1992). Saposins: structure, function, distribution, and molecular genetics. *J Lipid Res*, 33(9), 1255-1267. doi:10.1016/S0022-2275(20)40540-1
- Koltzenburg, M. (2000). Neural mechanisms of cutaneous nociceptive pain. *Clin J Pain*, 16(3), S131-S138. doi:10.1097/00002508-200009001-00004
- Kornreich, R., Desnick, R. J., & Bishop, D. F. (1989). Nucleotide sequence of the human alpha-galactosidase A gene. *Nucleic Acids Res*, 17(8), 3301. doi:10.1093/nar/17.8.3301
- Lachmann, R. H., & Platt, F. M. (2001). Substrate reduction therapy for glycosphingolipid storage disorders. *Expert Opin Investig Drugs*, 10(3), 455-466. doi:10.1517/13543784.10.3.455
- Lakomá, J., Donadio, V., Liguori, R., & Caprini, M. (2016). Characterization of human dermal fibroblasts in Fabry disease. *J Cell Physiol*, 231(1), 192-203. doi:10.1002/jcp.25072
- Lauria, G., Hsieh, S. T., Johansson, O., et al. (2010). European Federation of Neurological Societies/Peripheral Nerve Society Guideline on the use of skin biopsy in the diagnosis of small fiber neuropathy. Report of a joint task force of the European Federation of Neurological Societies and the Peripheral Nerve Society. *Eur J Neurol*, 17(7), 903-e949. doi:10.1111/j.1468-1331.2010.03023.x
- Lenders, M., Weidemann, F., Kurschat, C., et al. (2016). Alpha-Galactosidase A p. A143T, a non-Fabry disease-causing variant. *Orphanet J Rare Dis*, 11(1), 54. doi:10.1186/s13023-016-0441-z
- Lidove, O., Jaussaud, R., & Aractingi, S. (2006). Dermatological and soft-tissue manifestations of Fabry disease: characteristics and response to enzyme replacement therapy. In *Fabry disease: perspectives from 5 years of FOS*: Oxford PharmaGenesis.
- Lieberman, A. P., Pitha, P. M., Shin, H. S., & Shin, M. L. (1989). Production of tumor necrosis factor and other cytokines by astrocytes stimulated with lipopolysaccharide or a neurotropic virus. *PNAS*, 86(16), 6348-6352. doi:10.1073/pnas.86.16.6348
- Lieberman, R. L., Wustman, B. A., Huertas, P., et al. (2007). Structure of acid  $\beta$ -glucosidase with pharmacological chaperone provides insight into Gaucher disease. *Nat Chem Biol*, 3(2), 101-107. doi:10.1038/nchembio850

- Lin, H.-Y., Chong, K.-W., Hsu, J.-H., et al. (2009). High incidence of the cardiac variant of Fabry disease revealed by newborn screening in the Taiwan Chinese population. *Circ Cardiovasc Genet*, 2(5), 450-456. doi:10.1161/CIRCGENETICS.109.862920
- Low, M., Nicholls, K., Tubridy, N., et al. (2007). Neurology of Fabry disease. *Intern Med J*, 37(7), 436-447. doi:10.1111/j.1445-5994.2007.01366.x
- Lu, R., Alioua, A., Kumar, Y., et al. (2006). MaxiK channel partners: physiological impact. *J Physiol*, 570(1), 65-72. doi:10.1113/jphysiol.2005.098913
- Maag, R., Binder, A., Maier, C., et al. (2008). Detection of a characteristic painful neuropathy in Fabry disease: a pilot study. *Pain Med*, 9(8), 1217-1223. doi:10.1111/j.1526-4637.2008.00470.x
- MacDermot, J., & MacDermot, K. D. (2001). Neuropathic pain in Anderson-Fabry disease: pathology and therapeutic options. *Eur J Pharmacol*, 429(1-3), 121-125. doi:10.1016/S0014-2999(01)01312-7
- MacDermot, K., Holmes, A., & Miners, A. (2001). Anderson-Fabry disease: clinical manifestations and impact of disease in a cohort of 98 hemizygous males. *J Med Genet*, 38(11), 750-760. doi:10.1136/jmg.38.11.750
- Magerl, W., Krumova, E. K., Baron, R., et al. (2010). Reference data for quantitative sensory testing (QST): refined stratification for age and a novel method for statistical comparison of group data. *Pain*, 151(3), 598-605. doi:10.1016/j.pain.2010.07.026
- Magg, B., Riegler, C., Wiedmann, S., et al. (2015). Self-administered version of the Fabry-associated pain questionnaire for adult patients. *Orphanet J Rare Dis*, 10(1), 113. doi:10.1186/s13023-015-0325-7
- Mahmoudi, S., Mancini, E., Xu, L., et al. (2019). Heterogeneity in old fibroblasts is linked to variability in reprogramming and wound healing. *Nature*, 574(7779), 553-558. doi:10.1038/s41586-019-1658-5
- Maier, E. M., Osterrieder, S., Whybra, C., et al. (2006). Disease manifestations and X inactivation in heterozygous females with Fabry disease. *Acta Paediatr*, 95, 30-38. doi:10.1111/j.1651-2227.2006.tb02386.x
- Maquat, L. E. (2004). Nonsense-mediated mRNA decay: splicing, translation and mRNP dynamics. *Nat Rev Mol Cell Biol*, 5(2), 89-99. doi:10.1038/nrm1310
- Mark, B. L., Mahuran, D. J., Cherney, M. M., et al. (2003). Crystal structure of human  $\beta$ -hexosaminidase B: understanding the molecular basis of Sandhoff and Tay-Sachs disease. *J Mol Biol*, 327(5), 1093-1109. doi:10.1016/S0022-2836(03)00216-X
- Markham, A. (2016). Migalastat: first global approval. *Drugs*, 76(11), 1147-1152. doi:10.1007/s40265-016-0607-y
- Matsuzawa, F., Aikawa, S.-i., Doi, H., et al. (2005). Fabry disease: correlation between structural changes in  $\alpha$ -galactosidase, and clinical and biochemical phenotypes. *Hum Genet*, 117(4), 317-328. doi:10.1007/s00439-005-1300-5
- McCafferty, E. H., & Scott, L. J. (2019). Migalastat: a review in Fabry disease. *Drugs*, 79(5), 543-554. doi:10.1007/s40265-019-01090-4

- Mehta, A., Clarke, J. T., Giugliani, R., et al. (2009). Natural course of Fabry disease: changing pattern of causes of death in FOS–Fabry Outcome Survey. *J Med Genet*, 46(8), 548-552. doi:10.1136/jmg.2008.065904
- Mehta, A., Ricci, R., Widmer, U., et al. (2004). Fabry disease defined: baseline clinical manifestations of 366 patients in the Fabry Outcome Survey. *Eur J Clin Investig*, 34(3), 236-242. doi:10.1111/j.1365-2362.2004.01309.x
- Mehta, A., West, M. L., Pintos-Morell, G., et al. (2010). Therapeutic goals in the treatment of Fabry disease. *Genet Med*, 12(11), 713-720. doi:10.1097/GIM.0b013e3181f6e676
- Meikle, P. J., Hopwood, J. J., Clague, A. E., & Carey, W. F. (1999). Prevalence of lysosomal storage disorders. *JAMA*, 281(3), 249-254. doi:10.1001/jama.281.3.249
- Millan, M. J. (1999). The induction of pain: an integrative review. *Prog Neurobiol*, 57(1), 1-164. doi:10.1016/S0301-0082(98)00048-3
- Moalem, G., & Tracey, D. J. (2006). Immune and inflammatory mechanisms in neuropathic pain. *Brain Res Rev*, 51(2), 240-264. doi:10.1016/j.brainresrev.2005.11.004
- Møller, A. T., & Jensen, T. S. (2007). Neurological manifestations in Fabry's disease. *Nat Clin Pract Neurol*, 3(2), 95-106. doi:10.1038/ncpneuro0407
- Monsalve, E., Ruiz-García, A., Baladrón, V., et al. (2009). Notch1 upregulates LPS-induced macrophage activation by increasing NF-κB activity. *Eur J Immunol*, 39(9), 2556-2570. doi:10.1002/eji.200838722
- Nagueh, S. F. (2014). Anderson-Fabry disease and other lysosomal storage disorders. *Circulation*, 130(13), 1081-1090. doi:10.1161/CIRCULATIONAHA.114.009789
- Namdar, M., Gebhard, C., Studiger, R., et al. (2012). Globotriaosylsphingosine accumulation and not alpha-galactosidase-A deficiency causes endothelial dysfunction in Fabry disease. *PLoS One*, 7(4), e36373. doi:10.1371/journal.pone.0036373
- Netzker, R. (2012). Zellzyklus und molekulare Genetik. In J. Rassow, K. Hauser, R. Netzker, & R. Deutzmann (Eds.), *Biochemie* (Vol. 3, pp. 466-469). Stuttgart: George Thieme Verlag.
- Niemann, M., Rolfs, A., Giese, A., et al. (2012). Lyso-Gb3 indicates that the alpha-galactosidase A mutation D313Y is not clinically relevant for Fabry disease. In *JIMD Reports-Case and Research Reports*, 2012/4 (pp. 99-102): Springer.
- Niemann, M., Rolfs, A., Störk, S., et al. (2014). Gene mutations versus clinically relevant phenotypes: lyso-Gb3 defines Fabry disease. *Circ Cardiovasc Genet*, 7(1), 8-16. doi:10.1161/CIRCGENETICS.113.000249
- The Nobel Prize in Physiology or Medicine 1991. (n.d.). Retrieved from <https://www.nobelprize.org/prizes/medicine/1991/summary/>.
- Nowak, A., Mechtler, T. P., Desnick, R. J., & Kasper, D. C. (2017). Plasma LysoGb3: A useful biomarker for the diagnosis and treatment of Fabry disease heterozygotes. *Mol Genet Metab*, 120(1-2), 57-61. doi:10.1016/j.ymgme.2016.10.006
- Nowak, A., Mechtler, T. P., Hornemann, T., et al. (2018). Genotype, phenotype and disease severity reflected by serum LysoGb3 levels in patients with



- Fabry disease. *Mol Genet Metab*, 123(2), 148-153.  
doi:10.1016/j.ymgme.2017.07.002
- Oder, D., Liu, D., Hu, K., et al. (2017).  $\alpha$ -Galactosidase A Genotype N215S Induces a specific cardiac variant of fabry disease. *Circ Cardiovasc Genet*, 10(5), e001691. doi:10.1161/CIRCGENETICS.116.001691
- Oder, D., Ueçeyler, N., Liu, D., et al. (2016). Organ manifestations and long-term outcome of Fabry disease in patients with the GLA haplotype D313Y. *BMJ open*, 6(4). doi:10.1136/bmjopen-2015-010422
- Oliván-Viguera, A., Lozano-Gerona, J., López de Frutos, L., et al. (2017). Inhibition of intermediate-conductance calcium-activated k channel (KCa3. 1) and fibroblast mitogenesis by  $\alpha$ -linolenic acid and alterations of channel expression in the lysosomal storage disorders, fabry disease, and niemann pick C. *Front Physiol*, 8, 39. doi:10.3389/fphys.2017.00039
- Opitz, J. M., Stiles, F. C., Wise, D., et al. (1965). The genetics of angiokeratoma corporis diffusum (Fabry's disease) and its linkage relations with the Xg locus. *Am J Hum Genet*, 17(4), 325.
- Orteu, C., Jansen, T., Lidove, O., et al. (2007). Fabry disease and the skin: data from FOS, the Fabry outcome survey. *Br J Dermatol*, 157(2), 331-337. doi:10.1111/j.1365-2133.2007.08002.x
- Park, S., Kim, J. A., Joo, K. Y., et al. (2011). Globotriaosylceramide leads to KCa3. 1 channel dysfunction: A new insight into endothelial dysfunction in Fabry disease. *Cardiovasc Res*, 89(2), 290-299. doi:10.1093/cvr/cvq333
- Park, S. Y., Lee, J. H., Kim, C. D., et al. (2006). Cilostazol suppresses superoxide production and expression of adhesion molecules in human endothelial cells via mediation of cAMP-dependent protein kinase-mediated maxi-K channel activation. *J Pharmacol Exp Ther*, 317(3), 1238-1245. doi:10.1124/jpet.105.098509
- Pastores, G. M., & Lien, Y.-H. H. (2002). Biochemical and molecular genetic basis of Fabry disease. *Clin J Am Soc Nephrol*, 13(suppl 2), S130-S133. doi:10.1097/01.ASN.0000015236.70757.C4
- Pastores, G. M., & Thadhani, R. (2001). Enzyme-replacement therapy for Anderson-Fabry disease. *Lancet*, 358(9282), 601-603. doi:10.1002/14651858.CD006663.pub4
- Politei, J. M., Bouhassira, D., Germain, D. P., et al. (2016). Pain in Fabry disease: practical recommendations for diagnosis and treatment. *CNS Neurosci Ther*, 22(7), 568-576. doi:doi.org/10.1111/cns.12542
- Putko, B. N., Wen, K., Thompson, R. B., et al. (2015). Anderson-Fabry cardiomyopathy: prevalence, pathophysiology, diagnosis and treatment. *Heart Fail Rev*, 20(2), 179-191. doi:10.1007/s10741-014-9452-9
- Rassow, J. (2012). Energiestoffwechsel. In J. Rassow, K. Hauser, R. Netzker, & R. Deutzmann (Eds.), *Biochemie* (Vol. 3, pp. 63-69). Stuttgart: Georg Thieme Verlag.
- Redonnet-Vernhet, I., van Amstel, J. P., Jansen, R., et al. (1996). Uneven X inactivation in a female monozygotic twin pair with Fabry disease and discordant expression of a novel mutation in the alpha-galactosidase A gene. *J Med Genet*, 33(8), 682-688. doi:10.1136/jmg.33.8.682



- Reisin, R., Perrin, A., & García-Pavía, P. (2017). Time delays in the diagnosis and treatment of Fabry disease. *Int J Clin Pract*, 71(1), e12914. doi:10.1111/ijcp.12914
- Replagal. (2018). Retrieved from <https://www.ema.europa.eu/en/medicines/human/EPAR/replagal>
- Riera, C., Lois, S., Domínguez, C., et al. (2015). Molecular damage in Fabry disease: Characterization and prediction of alpha-galactosidase A pathological mutations. *Proteins*, 83(1), 91-104. doi:10.1002/prot.24708
- Rolfs, A., Fazekas, F., Grittner, U., et al. (2013). Acute cerebrovascular disease in the young: the Stroke in Young Fabry Patients study. *Stroke*, 44(2), 340-349. doi:10.1161/STROKEAHA.112.663708
- Rolke, R., Baron, R., Maier, C. a., et al. (2006). Quantitative sensory testing in the German Research Network on Neuropathic Pain (DFNS): standardized protocol and reference values. *Pain*, 123(3), 231-243. doi:10.1016/j.pain.2006.01.041
- Rozenfeld, P., & Feriozzi, S. (2017). Contribution of inflammatory pathways to Fabry disease pathogenesis. *Mol Genet Metab*, 122(3), 19-27. doi:10.1016/j.ymgme.2017.09.004
- Rozenfeld, P. A. (2009). Fabry disease: treatment and diagnosis. *IUBMB life*, 61(11), 1043-1050. doi:10.1002/iub.257
- Rozenfeld, P. A., De, N. F., Borrajo, G., et al. (2009). An easy and sensitive method for determination of globotriaosylceramide (Gb3) from urinary sediment: utility for Fabry disease diagnosis and treatment monitoring. *Clin Chim Acta*, 403(1-2), 194-197. doi:10.1016/j.cca.2009.02.016
- Saalbach, A., Klein, C., Sleeman, J., et al. (2007). Dermal fibroblasts induce maturation of dendritic cells. *J Immunol*, 178(8), 4966-4974. doi:10.4049/jimmunol.178.8.4966
- Sakiri, R., Ramegowda, B., & Tesh, V. L. (1998). Shiga toxin type 1 activates tumor necrosis factor- $\alpha$  gene transcription and nuclear translocation of the transcriptional activators nuclear factor- $\kappa$ B and activator protein-1. *Blood*, 92(2), 558-566. doi:10.1182/blood.V92.2.558
- Sakmann, B., & Neher, E. (1984). Patch clamp techniques for studying ionic channels in excitable membranes. *Annu Rev Physiol*, 46(1), 455-472.
- Sakuraba, H., Togawa, T., Tsukimura, T., & Kato, H. (2018). Plasma lyso-Gb3: a biomarker for monitoring fabry patients during enzyme replacement therapy. *J Clin Exp Nephrol*, 22(4), 843-849. doi:10.1007/s10157-017-1525-3
- Sanchez-Niño, M. D., Carpio, D., Sanz, A. B., et al. (2015). Lyso-Gb3 activates Notch1 in human podocytes. *Hum Mol Genet*, 24(20), 5720-5732. doi:10.1093/hmg/ddv291
- Sanz, A. B., Sanchez-Niño, M. D., Ramos, A. M., et al. (2010). NF- $\kappa$ B in renal inflammation. *Clin J Am Soc Nephrol*, 21(8), 1254-1262. doi:10.1681/ASN.2010020218
- Schaefer, E., Mehta, A., & Gal, A. (2005). Genotype and phenotype in Fabry disease: analysis of the Fabry Outcome Survey. *Acta Paediatr*, 94, 87-92. doi:10.1111/j.1651-2227.2005.tb02119.x

- Schaefer, R. M., Tylki-Szymańska, A., & Hilz, M. J. (2009). Enzyme Replacement Therapy for Fabry Disease. *Drugs*, 69(16), 2179-2205. doi:10.1001/jama.285.21.2743
- Schiffmann, R. (2006). Neuropathy and Fabry disease: pathogenesis and enzyme replacement therapy. *Acta Neurol Belg*, 106(2), 61.
- Schiffmann, R. (2009). Fabry disease. *Pharmacol Ther*, 122(1), 65-77. doi:10.1016/j.pharmthera.2009.01.003
- Schiffmann, R., Floeter, M. K., Dambrosia, J. M., et al. (2003). Enzyme replacement therapy improves peripheral nerve and sweat function in Fabry disease. *Muscle Nerve*, 28(6), 703-710. doi:10.1002/mus.10497
- Schiffmann, R., Kopp, J. B., Austin III, H. A., et al. (2001). Enzyme replacement therapy in Fabry disease: a randomized controlled trial. *JAMA*, 285(21), 2743-2749. doi:10.1001/jama.285.21.2743
- Schiffmann, R., & Scott, L. (2002). Pathophysiology and assessment of neuropathic pain in Fabry disease. *Acta Paediatr*, 91, 48-52. doi:10.1111/j.1651-2227.2002.tb03110.x
- Schiffmann, R., Waldek, S., Benigni, A., & Auray-Blais, C. (2010). Biomarkers of Fabry disease nephropathy. *Clin J Am Soc Nephrol*, 5(2), 360-364. doi:10.2215/CJN.06090809
- Scholzen, T., Armstrong, C., Bunnett, N., et al. (1998). Neuropeptides in the skin: interactions between the neuroendocrine and the skin immune systems. *Exp Dermatol*, 7(2-3), 81-96. doi:10.1111/j.1600-0625.1998.tb00307.x
- Schrodinger, LLC. (2015). The PyMOL Molecular Graphics System, Version 1.8.
- Schuchman, E. (2007). The pathogenesis and treatment of acid sphingomyelinase-deficient Niemann–Pick disease. *J Inherit Metab Dis*, 30(5), 654. doi:10.1007/s10545-007-0632-9
- Serra, W., & Marziliano, N. (2019). Role of cardiac imaging in Anderson-Fabry cardiomyopathy. *J Cardiovasc Ultrasound*, 17(1), 1. doi:10.1186/s12947-019-0151-5
- Shabbeer, J., Yasuda, M., Benson, S. D., & Desnick, R. J. (2006). Fabry disease: Identification of 50 novel  $\alpha$ -galactosidase A mutations causing the classic phenotype and three-dimensional structural analysis of 29 missense mutations. *Hum Genomics*, 2(5), 297. doi:10.1186/1479-7364-2-5-297
- Shah, J. S., Hughes, D. A., Sachdev, B., et al. (2005). Prevalence and clinical significance of cardiac arrhythmia in Anderson-Fabry disease. *Am J Cardiol*, 96(6), 842-846. doi:10.1016/j.amjcard.2005.05.033
- Shen, J.-S., Meng, X.-L., Moore, D. F., et al. (2008). Globotriaosylceramide induces oxidative stress and up-regulates cell adhesion molecule expression in Fabry disease endothelial cells. *Mol Genet Metab*, 95(3), 163-168. doi:10.1016/j.ymgme.2008.06.016
- Sheng, W. S., Hu, S., Kravitz, F. H., et al. (1995). Tumor necrosis factor alpha upregulates human microglial cell production of interleukin-10 in vitro. *Clin Diagn Lab Immunol*, 2(5), 604-608.

- Shin, H. M., Minter, L. M., Cho, O. H., et al. (2006). Notch1 augments NF- $\kappa$ B activity by facilitating its nuclear retention. *EMBO J*, 25(1), 129-138. doi:10.1038/sj.emboj.7600902
- Shin, H. M., Tilahun, M. E., Cho, O. H., et al. (2014). NOTCH1 can initiate NF- $\kappa$ B activation via cytosolic interactions with components of the T cell signalosome. *Front Immunol*, 5, 249. doi:10.3389/fimmu.2014.00249
- Smith, R. S., Smith, T. J., Blieden, T. M., & Phipps, R. P. (1997). Fibroblasts as sentinel cells. Synthesis of chemokines and regulation of inflammation. *Am J Pathol*, 151(2), 317.
- Song, H.-Y., Chiang, H.-C., Tseng, W.-L., et al. (2016). Using CRISPR/Cas9-mediated GLA gene knockout as an in vitro drug screening model for Fabry disease. *Int J Mol Sci*, 17(12), 2089. doi:10.3390/ijms17122089
- Ständer, S., Schneider, S. W., Weishaupt, C., et al. (2009). Putative neuronal mechanisms of sensitive skin. *Exp Dermatol*, 18(5), 417-423. doi:10.1111/j.1600-0625.2009.00861.x
- Stockbridge, L. L., & French, A. S. (1988). Stretch-activated cation channels in human fibroblasts. *Biophys J*, 54(1), 187-190. doi:10.1016/S0006-3495(88)82944-8
- Street, N. J., Michael, S. Y., Bailey, L. A., & Hopkin, R. J. (2006). Comparison of health-related quality of life between heterozygous women with Fabry disease, a healthy control population, and patients with other chronic disease. *Genet Med*, 8(6), 346-353. doi:10.1097/01.gim.0000223545.63012.5a
- Sueoka, H., Aoki, M., Tsukimura, T., et al. (2015). Distributions of globotriaosylceramide isoforms, and globotriaosylsphingosine and its analogues in an  $\alpha$ -galactosidase A knockout mouse, a model of Fabry disease. *PLoS One*, 10(12). doi:10.1371/journal.pone.0144958
- Sun, Y.-Y., Li, L., Liu, X.-H., et al. (2012). The spinal notch signaling pathway plays a pivotal role in the development of neuropathic pain. *Mol Brain*, 5(1), 23. doi:10.1186/1756-6606-5-23
- Tajhya, R. B., Hu, X., Tanner, M. R., et al. (2016). Functional KCa1. 1 channels are crucial for regulating the proliferation, migration and differentiation of human primary skeletal myoblasts. *Cell Death Dis*, 7(10), e2426-e2426. doi:10.1038/cddis.2016.324
- Talagas, M., Lebonvallet, N., Berthod, F., & Misery, L. (2019). Cutaneous nociception: Role of keratinocytes. *Exp Dermatol*, 28(12), 1466-1469. doi:10.1111/exd.13975
- Talbot, A., & Nicholls, K. (2018). Elevated Lyso-Gb3 suggests the R118C GLA mutation is a pathological Fabry variant. In *JIMD Reports, Volume 45* (pp. 95-98): Springer.
- Tian, C., Zhu, R., Zhu, L., et al. (2014). Potassium channels: structures, diseases, and modulators. *Chem Biol Drug Des*, 83(1), 1-26. doi:10.1111/cbdd.12237
- Togawa, T., Kawashima, I., Kodama, T., et al. (2010). Tissue and plasma globotriaosylsphingosine could be a biomarker for assessing enzyme replacement therapy for Fabry disease. *Biochem Biophys Res Commun*, 399(4), 716-720. doi:10.1016/j.bbrc.2010.08.006

- Toro, L., Li, M., Zhang, Z., et al. (2014). MaxiK channel and cell signalling. *Pflugers Arch*, 466(5), 875-886. doi:10.1007/s00424-013-1359-0
- Tsuda, M., Masuda, T., Kitano, J., et al. (2009). IFN- $\gamma$  receptor signaling mediates spinal microglia activation driving neuropathic pain. *PNAS*, 106(19), 8032-8037. doi:10.1073/pnas.0810420106
- Tuttolomondo, A., Pecoraro, R., Simonetta, I., et al. (2013). Anderson-Fabry disease: a multiorgan disease. *Curr Pharm Des*, 19(33), 5974-5996.
- Üçeyler, N., Böttger, J., Henkel, L., et al. (2018). Detection of blood Gb3 deposits as a new tool for diagnosis and therapy monitoring in patients with classic Fabry disease. *J Intern Med*, 284(4), 427-438. doi:10.1111/joim.12801
- Üçeyler, N., Ganendiran, S., Kramer, D., & Sommer, C. (2014). Characterization of pain in Fabry disease. *Clin J Pain*, 30(10), 915-920. doi:10.1097/AJP.0000000000000041
- Üçeyler, N., Kafke, W., Riediger, N., et al. (2010). Elevated proinflammatory cytokine expression in affected skin in small fiber neuropathy. *Neurology*, 74(22), 1806-1813. doi:10.1212/WNL.0b013e3181e0f7b3
- Üçeyler, N., Kahn, A.-K., Kramer, D., et al. (2013a). Impaired small fiber conduction in patients with Fabry disease: a neurophysiological case-control study. *BMC Neurol*, 13(1), 47. doi:10.1186/1471-2377-13-47
- Üçeyler, N., & Sommer, C. (2013b). Morbus Fabry. In *Weiterbildung Schmerzmedizin* (pp. 31-40): Springer.
- Üçeyler, N., Urlaub, D., Mayer, C., et al. (2019). Tumor necrosis factor- $\alpha$  links heat and inflammation with Fabry pain. *Mol Genet Metab*, 127(3), 200-206. doi:10.1016/j.ymgme.2019.05.009
- Van der Tol, L., Smid, B., Poorthuis, B., et al. (2014). A systematic review on screening for Fabry disease: prevalence of individuals with genetic variants of unknown significance. *J Med Genet*, 51(1), 1-9. doi:10.1136/jmedgenet-2013-101857
- Van Steenwinckel, J., Reaux-Le Goazigo, A., Pommier, B., et al. (2011). CCL2 released from neuronal synaptic vesicles in the spinal cord is a major mediator of local inflammation and pain after peripheral nerve injury. *J Neurosci*, 31(15), 5865-5875. doi:10.1523/JNEUROSCI.5986-10.2011
- Vaskar, D. (2015). An Introduction to Pain Pathways and Pain "Targets". In T. J. Price & G. Dussor (Eds.), *Progress in Molecular Biology and Translational Science - Molecular and Cell Biology of Pain* (Vol. 131, pp. 2-30). Waltham, MA, USA: Academic Press.
- Vedder, A., Linthorst, G., Van Breemen, M., et al. (2007). The Dutch Fabry cohort: diversity of clinical manifestations and Gb3 levels. *J Inherit Metab Dis*, 30(1), 68-78. doi:10.1007/s10545-006-0484-8
- Vig, K., Chaudhari, A., Tripathi, S., et al. (2017). Advances in skin regeneration using tissue engineering. *Int J Mol Sci*, 18(4), 789. doi:10.3390/ijms18040789
- Waldek, S., & Feriozzi, S. (2014). Fabry nephropathy: a review—how can we optimize the management of Fabry nephropathy? *BMC Nephrol*, 15(1), 72. doi:10.1186/1471-2369-15-72s
- Waldek, S., Patel, M. R., Banikazemi, M., et al. (2009). Life expectancy and cause of death in males and females with Fabry disease: findings from

- the Fabry Registry. *Genet Med*, 11(11), 790-796.  
doi:10.1097/GIM.0b013e3181bb05bb
- Wang, B., Chen, Q., & Brenner, R. (2009). Ion Channels: Proepileptic Effects of BK Channel Gene Mutations. In *Encyclopedia of Basic Epilepsy Research* (pp. 662-669): Elsevier Inc.
- Wang, R. Y., Lelis, A., Mirocha, J., & Wilcox, W. R. (2007). Heterozygous Fabry women are not just carriers, but have a significant burden of disease and impaired quality of life. *Genet Med*, 9(1), 34-45.  
doi:10.1097/GIM.0b013e31802d8321
- Wang, X.-M., Hamza, M., Wu, T.-X., & Dionne, R. A. (2009). Upregulation of IL-6, IL-8 and CCL2 gene expression after acute inflammation: Correlation to clinical pain. *Pain*, 142(3), 275-283. doi:10.1016/j.pain.2009.02.001
- Wanner, C., Oliveira, J. P., Ortiz, A., et al. (2010). Prognostic indicators of renal disease progression in adults with Fabry disease: natural history data from the Fabry Registry. *Clin J Am Soc Nephrol*, 5(12), 2220-2228.  
doi:10.2215/CJN.04340510
- Waring, D. W., & Turgeon, J. L. (2009). Ca<sup>2+</sup>-activated K<sup>+</sup> channels in gonadotropin-releasing hormone-stimulated mouse gonadotrophs. *Endocrinology*, 150(5), 2264-2272. doi:10.1210/en.2008-1442
- Weidemann, F., Maier, S. K., Störk, S., et al. (2016). Usefulness of an implantable loop recorder to detect clinically relevant arrhythmias in patients with advanced Fabry cardiomyopathy. *Am J Cardiol*, 118(2), 264-274. doi:10.1016/j.amjcard.2016.04.033
- Welford, R., Mühlemann, A., Garzotti, M., et al. (2018). Glucosylceramide synthase inhibition with lucerastat lowers globotriaosylceramide and lysosome staining in cultured fibroblasts from Fabry patients with different mutation types. *Hum Mol Genet*, 27(19), 3392-3403.  
doi:10.1093/hmg/ddy248
- Whybra, C., Kampmann, C., Willers, I., et al. (2001). Anderson–Fabry disease: clinical manifestations of disease in female heterozygotes. *J Inherit Metab Dis*, 24(7), 715-724. doi:10.1023/A:1012993305223
- Wilcox, W. R., Banikazemi, M., Guffon, N., et al. (2004). Long-term safety and efficacy of enzyme replacement therapy for fabry disease. *Am J Hum Genet*, 75(1), 65-74. doi:10.1086/422366
- Winer, J., Jung, C. K. S., Shackel, I., & Williams, P. M. (1999). Development and validation of real-time quantitative reverse transcriptase–polymerase chain reaction for monitoring gene expression in cardiac myocytes in vitro. *Anal Biochem*, 270(1), 41-49. doi:10.1006/abio.1999.4085
- Work, I. G. O. K. H. C. (2018). KDIGO 2018 clinical practice guideline for the prevention, diagnosis, evaluation, and treatment of hepatitis C in chronic kidney disease. *Kidney Int Suppl*, 8(3), 91.  
doi:10.1016/j.kisu.2018.06.001
- Wu, J. C., Ho, C. Y., Skali, H., et al. (2010). Cardiovascular manifestations of Fabry disease: relationships between left ventricular hypertrophy, disease severity, and  $\alpha$ -galactosidase A activity. *Eur Heart J*, 31(9), 1088-1097. doi:10.1093/eurheartj/ehp588
- Zarate, Y. A., & Hopkin, R. J. (2008). Fabry's disease. *Lancet*, 372(9647), 1427-1435. doi:10.1016/S0140-6736(08)61589-5s

Zetterström, M., Sundgren-Andersson, A., Östlund, P., & Bartfai, T. (1998).  
Delineation of the Proinflammatory Cytokine Cascade in Fever Induction  
a. *Ann N Y Acad Sci*, 856(1), 48-52. doi:10.1111/j.1749-  
6632.1998.tb08311.x

## Appendix

### I Abbreviations

|                         |   |
|-------------------------|---|
| 9-AC.....               | 9-Anthracenecarboxylic acid   |
| AAE.....                | Amino acid exchange   |
| $\alpha$ -GalA.....     | $\alpha$ -Galactosidase A   |
| ASMase.....             | Acid shingomyelinase  |
| ASA.....                | Aminosäureaustausch   |
| CCL.....                | Chemokine C-C motif ligand  |
| CNS.....                | Central nervous system  |
| ChTX.....               | Charybdotoxin   |
| CsCl.....               | Caesium chloride  |
| DAPI.....               | 4',6-Diamidin-2-phenylindol   |
| DCPIB.....              | 4,4'-Diisothiocyano-2,2'-stilbenedisulfonic acid                    |
| DNA.....                | deoxyribonucleic acid   |
| ELISA.....              | Enzyme-linked immunosorbent assay                                   |
| FD.....                 | Fabry disease   |
| Gb3.....                | Globotriaosylceramide   |
| GFR.....                | Glomerular filtration rate  |
| HCN.....                | Hyperpolarization-activated cyclic nucleotide-gated channel         |
| ICD.....                | Implantable cardiac device  |
| IENFD.....              | Intraepidermal nerve fiber density                                  |
| IFN $\gamma$ .....      | Interferone- $\gamma$   |
| IL.....                 | Interleukin   |
| LGE.....                | Late gadolinium enhancement   |
| LSD.....                | Lysosomal storage disorder  |
| MRI.....                | Magnetic resonance imaging  |
| NF- $\kappa$ B p65..... | Nuclear factor kappa-light-chain-enhancer of activated B-cells p65  |
| Notch1.....             | Transmembrane receptors notch homolog 1                             |
| NRS.....                | Numeric rating scale  |
| NS 6180....             | 4-[[3-(Trifluoromethyl)phenyl]methyl]-2H-1,4-benzothiazin-3(4H)-one |

PBS.....Phosphate buffered saline  
 p-NF- $\kappa$ B p65.....phosphorylated Nuclear factor kappa-light-chain-enhancer of  
 activated B-cells p65  
 PNS.....Peripheral nervous system  
 QST.....Quantitative sensory testing  
 qRT-PCR.....Quantitative real-time polymerase chain reaction  
 RRT.....Renal replacement therapy  
 SFN.....Small fiber neuropathy  
 SRT.....Substrate reduction therapy  
 TEA.....Tetraethylammonium  
 TGF- $\beta$ 1.....Transforming growth factor- $\beta$ 1  
 TIA.....Transient ischemic attack  
 TNF.....Tumor necrosis factor- $\alpha$   
 TRAM 34.....1-[(2-Chlorophenyl)diphenylmethyl]-1H-pyrazole  
 TTX.....Tetrodotoxin  
 VRAC.....Volume-regulated anion channel



## II List of Figures

|  |      |
|--|------|
| Figure 1. Disease process in classical and non-classical FD phenotype .....                                | 4 -  |
| Figure 2. Diagnostics in FD .....  | 7 -  |
| Figure 3. 3D-structure of $\alpha$ -GalA .....   | 21 - |
| Figure 4. FD patient subgroups and selections .....  | 24 - |
| Figure 5. Subgroups in the study cohort.....   | 36 - |
| Figure 6. Average and maximum pain intensity among FD patients .....                                       | 42 - |
| Figure 7. Pain triggers and pain qualities among FD patients .....   | 43 - |
| Figure 8. Gb3 deposition in dermal fibroblasts .....   | 44 - |
| Figure 9. Median Gb3 load and median number of swollen cells in fibroblasts of different FD subgroups..... | 45 - |
| Figure 10. Median Gb3 load at different ERT-biopsy intervals .....   | 46 - |
| Figure 11. Median Gb3 load in two consecutive biopsies.....  | 47 - |
| Figure 12. Characterization of K <sub>Ca</sub> 1.1. channel in dermal fibroblasts .....                    | 49 - |
| Figure 13. K <sub>Ca</sub> 1.1 function in FD and control fibroblasts .....                                | 50 - |
| Figure 14. K <sub>Ca</sub> 1.1 gene and protein expression in FD and control dermal fibroblasts.....       | 51 - |
| Figure 15. Gene expression of various cytokines and chemokines in FD and control fibroblasts .....         | 53 - |
| Figure 16. Western Blot analysis for NF- $\kappa$ B p65 in dermal fibroblasts.....                         | 54 - |
| Figure 17. Analysis of median pNF- $\kappa$ B/NF- $\kappa$ B p65 in Western Blot .....                     | 55 - |
| Figure 18. AAE location types in the $\alpha$ -GalA 3D-structure.....                                      | 59 - |
| Figure 19. Clinical characterization of male patients younger than 35 years -                              | 62 - |
| Figure 20. Clinical characterization of male patients between 35 and 55 years.....                         | 64 - |
| Figure 21. Clinical characterization of male patients older than 55 years.....                             | 66 - |
| Figure 22. Clinical characterization of all male patients.....   | 68 - |
| Figure 23. Clinical characterization of female patients younger than 35 years.....                         | 70 - |
| Figure 24. Clinical characterization of female patients between 35 and 55 years.....                       | 72 - |

|   |        |
|---|--------|
| Figure 25. Clinical characterization of female patients older than 55 years.....                                      | - 74 - |
| Figure 26. Clinical characterization of all female patients.....  | - 76 - |
| Figure 27. $\alpha$ -GalA activity and lyso-Gb3 levels.....   | - 77 - |
| Figure 28. Potential relations between KCa1.1 gene and protein expression and activity in FD dermal fibroblasts.....  | - 80 - |
| Figure 29. Potential relations between FD mutation, dysfunction in FD dermal fibroblasts and FD-associated pain ..... | - 84 - |

### III List of Tables

|   |        |
|---|--------|
| Table 1. List of typical symptoms and life-threatening events in FD .....   | - 6 -  |
| Table 2. Multi-disciplinary examination in FD .....   | - 8 -  |
| Table 3. FD-specific therapy forms and their current status .....   | - 9 -  |
| Table 4. List of ion channel blockers applied for patch-clamp analysis .....  | - 31 - |
| Table 5. Cardiomyopathy score.....  | - 38 - |
| Table 6. Genetic findings in the FD cohort .....  | - 41 - |
| Table 7. Clinical findings and specific therapy in the FD study cohort.....   | - 42 - |
| Table 8. Percent distribution of classical and non-classical FD mutations in the study cohort, separated by sex.....              | - 56 - |
| Table 9. AAE location type of the individual mutations and their frequency .  | - 58 - |
| Table 10. Percent distribution of classical and non-classical mutations in the study cohort, separated by AAE location type ..... | - 60 - |

## **IV Danksagung**

Zuallererst und ganz besonders möchte ich mich bei meiner Doktormutter Frau Professorin Dr. Nurcan Üçeyler bedanken für ihr beispielloses Engagement, ihre zielsichere Führung und ihre umfassende Betreuung während der gesamten Zeit in ihrer Arbeitsgruppe. Unsere Gespräche, ihre wertvollen Anmerkungen und ihr stetiges Lektorat bei allen schriftlichen Arbeiten haben mich fachlich und persönlich weitergebracht. Darüberhinaus hat mich ihre ansteckende Motivation und Begeisterung auch in anstrengenden und frustrierenden Zeiten stets mit der Arbeit weitermachen lassen. Ich hätte mir keine bessere Betreuung wünschen können. Danke für alles!

Ein ganz herzlicher Dank geht an Herrn Professor Erhard Wischmeyer, der mich nicht nur in das Patch-Clamp Verfahren einführte, sondern vielmehr mit seinen detailgenauen Fachkenntnissen, seiner Hartnäckigkeit sowie mit seiner gelassenen, aber zielstrebigem Art wesentlich zum Erfolg der Arbeit beigetragen hat.

Ebenso möchte ich mich bei Frau Professorin Claudia Sommer bedanken für all Ihre Ideen und Anregungen in Gesprächen, Seminaren und schriftlichen Arbeiten, die stets äußerst wertvoll und gewinnbringend waren.

Ein weiterer herzlicher Dank geht an die Herren Professor Christoph Wanner und Privatdozent Dr. Peter Nordbeck, die ohne Zögern mit großem Engagement und konstruktiven Diskussionen einen entscheidenden Beitrag zum Erfolg der Arbeit und darüberhinaus leisteten. Vielen Dank an Herrn Professor Christoph Wanner auch für die Übernahme der Zweitkorrektur meiner Dissertationsarbeit.

Ein großer Dank geht auch an Frau Privatdozentin Dr. Simone Rost für Ihre ausgezeichnete Anleitung, Unterstützung und Anregungen rund um alle genetischen Fragen. Ich habe sehr viel von ihr gelernt.

Herzlichen Dank auch an alle Mitarbeiter\*innen des FAZiT Würzburg und der Neurologischen Klinik, die den reibungslosen Ablauf der Studie ermöglichten. Besonders hervorheben möchte ich hier Frau Irina Schumacher und Frau Barbara Broll, die meine Arbeit stets maßgeblich erleichterten und mir mit Rat

und Tat zur Seite standen. Ebenso möchte ich den technischen Mitarbeiterinnen der Arbeitsgruppe danken, deren Arbeit unerlässlich war und ist: insbesondere Kathleen Stahl, Hiltrud Klüpfel, Barbara Dekant und Sonja Gommersbach. Bei Daniela Urlaub möchte ich noch einmal besonders bedanken, denn ihre Unterstützung bei vielen Versuchen war Gold wert. Hier möchte ich auch meine Kolleg\*innen der Arbeitsgruppe nennen, die für Fragen stets ein offenes Ohr hatten und mir immer eine Hilfe waren: danke an die gesamte Arbeitsgruppe und insbesondere Frau Dr. Franziska Karl, Herrn Dr. Thomas Klein, Herrn Dr. Lukas Hofmann und Frau Katharina Klug. Vielmals bedanken möchte ich mich auch bei allen Patient\*innen und Kontrollpersonen, die in die Studien einwilligten und diese so überhaupt erst ermöglichten.

Ein weiterer Dank geht an die Mitarbeiter\*innen der Friedrich-Ebert-Stiftung, die mir mehrfach großzügig zusätzliche Förderungszeit gewährten und mir so die Arbeit an meiner Dissertation und ein Studium ohne Zeitdruck möglich machten. Herzlich danken möchte ich auch meinen Kolleginnen im Gesundheitsamt in Karlstadt, die mir in kurzer Zeit sehr ans Herz gewachsen sind und die trotz der schier unermesslichen Mengen an Arbeit immer versuchten, mir das Schreiben meiner Dissertation neben der Arbeit möglich zu machen.

Ein ganz großer Dank geht an meine Freunde und meine Familie für ihren Rückhalt, ihre aufbauenden Worte und die Kraft, die sie mir immer geben - insbesondere an meine beste Freundin Insa, meine Geschwister Verena und Julian sowie meine Schwiegereltern (in spe) Margret und Burkhard.

Und schließlich, zu guter Letzt und vom Grunde meines Herzens, möchte ich jenen Personen danken, für deren immer währende und bedingungslose Unterstützung mir die richtigen Worte fehlen:

...meinen Eltern Romana und Roland: Ihr seid der Inbegriff von Wärme und Güte. Ihr lebt *Familie* mit jeder Faser Eures Körpers. Danke für alles, was Ihr immer, überall und mit grenzenlosem Einsatz für uns macht.

...meinem Partner Martin: Du bist mein Zuhause und mein größter Halt. Deine Ruhe, Deine Geduld und Deine Liebe sind mein größtes Glück. Danke für immer. *You're my lobster.*

## **V      Lebenslauf**

### **Persönliche Daten**

Name:                      Vanessa Christine Hochheimer (geb. Rickert)

## VI Publikationen

Welford, R., Mühlemann, A., Garzotti, M., **Rickert, V.**, Groenen, P., Morand, O., et al. (2018). Glucosylceramide synthase inhibition with lucerastat lowers globotriaosylceramide and lysosome staining in cultured fibroblasts from Fabry patients with different mutation types. *Hum Mol Genet*, 27(19), 3392-3403.

**Rickert, V.**, Kramer, D., Schubert, A.-L., Sommer, C., Wischmeyer, E., Üçeyler, N. (2020). Globotriaosylceramide-induced reduction of Kca1.1 channel activity and activation of Notch1 signaling pathway in skin fibroblasts of male Fabry patients with pain. *Exp Neuro.*, 324, 113-134.

**Rickert, V.**, Wagenhäuser, L., Nordbeck, P., Wanner, C., Sommer, C., Rost, S., Üçeyler, N. (2020). Stratification of Fabry mutations in clinical practice: a closer look at  $\alpha$ -galactosidase A-3D structure. *J Int Med*, 288(5), 593-604.